

Searching for a Self-Contained Work Extraction Procedure

A Semi-Quantum Model of a Szilard Engine

Master's Thesis by Philipp Kammerlander
ETH Zürich

Supervised by:
Lídia del Rio and Prof. Renato Renner
Quantum Information Theory Group
Institute for Theoretical Physics
ETH Zürich

In Collaboration with:
Dr. Johan Åberg
Institute for Physics
University of Freiburg

September 26, 2013

Abstract

A fundamental question of thermodynamics is how much work can be extracted from a physical system in a known state, given access to a thermal bath. In recent years, particular attention has been given to this question with respect to small quantum systems, where the standard theory of thermodynamics is not necessarily applicable.

This thesis is concerned with one particular aspect of work extraction procedures: autonomy. We call a procedure autonomous if the only resources necessary are a heat bath and a system in a well-known state. In particular, the energy-conserving evolution of the involved systems is described by a time-independent Hamiltonian and no external control is needed.

The thesis is divided into two parts. In Part I, we review recent results on self-contained (autonomous) quantum thermal machines and proposed work extraction procedures. We use the gained insights to motivate the search for a self-contained work extraction process that has not yet been found. In Part II, we investigate the work extraction process of a Szilard engine in a semi-quantum model. This is interesting because a Szilard engine, if it works, is self-contained. We analyze numerical simulations of our model and compare it to classical results.

Contents

Introduction	5
I. Part I: Review	8
1. Thermal Machines	9
1.1. Basic Principles – The Carnot Engine	9
1.1.1. Classical Example: Ideal Gas	13
1.2. The Smallest Possible Thermal Machines	15
1.2.1. Small Refrigerator and Heat Pump	15
1.2.2. Small Heat Engine	19
1.3. Efficiency	23
1.4. Discussion	27
2. Maxwell’s Demon and Szilard Engines	30
2.1. Maxwell’s Demon	30
2.2. Szilard’s Engine	32
2.3. Landauer’s Principle	34
2.4. Work Extraction Procedures	38
2.4.1. Semi-Classical Model by Alicki <i>et al.</i> (2004)	39
2.4.2. Quantum Model by Skrzypczyk <i>et al.</i> (2013)	42
2.4.3. Discussion	46
II. Part II: A Semi-Quantum Model of a Szilard Engine	51
3. The Weight Potential	54
4. Classical Statistical Analysis	56
4.1. Single Particle and Piston	56
4.2. Many Particles and Piston	58
4.3. Many Particles and Piston without Upper Bound	59
4.4. Conclusion	61
5. Piston as a Parameter	62
5.1. Calculations	63

5.2.	Discussion	65
5.2.1.	Thermodynamic Quantities and Classical Limit	66
6.	Born-Oppenheimer Approximation	67
6.1.	No Weight	68
6.2.	Linear Potential	70
6.3.	Quadratic Potential	70
6.4.	Other Potentials – Open Questions	74
7.	Thermalization and Time Evolution	75
7.1.	A Semi-Quantum Model	75
7.1.1.	Outline of the Simulation Program	77
7.2.	Boundary Conditions	77
7.3.	Weight Potential	78
8.	Analysis	80
8.1.	Total Energy at $X = L$	80
8.1.1.	Numerical Simulations	80
8.1.2.	Analytical Analysis	83
8.2.	Long-Term Behaviour	85
8.2.1.	Many-Particle Szilard Engine	85
8.2.2.	Single-Particle Szilard Engine	88
9.	Conclusion	90
9.1.	General Concepts	90
9.2.	Our Model and Simulations	91
Bibliography		93
III. Appendices		97
A. Notation		98
B. Calculations for Part I		100
B.1.	Analytical Solution for the Heat Engine	100
B.2.	Optimal Work Extraction with the Protocol by Skrzypczyk <i>et al.</i>	103
C. Calculations for Part II		105
C.1.	Classical Statistical Analysis	105
C.1.1.	Single Particle and Piston	105
C.1.2.	Many Particles and Piston	107
C.1.3.	Many Particles and Piston without Upper Bound	108
C.2.	Static Analysis in the Born-Oppenheimer Approximation	109
C.2.1.	No Weight	109

C.2.2. Quadratic Potential	110
C.3. Analysis of Boundary Conditions	112
C.3.1. Elastic Boundary Conditions	112
C.3.2. Inelastic Boundary Conditions	113
C.3.3. Thermal Boundary Conditions	115
C.3.4. Mixed Boundary Conditions	115
C.3.5. No Boundary Condition at the Right Wall – Open Cylinder	116
C.3.6. Other Ideas	116

Acknowledgements

I would like to express my deep gratitude to Lídia del Rio and Prof. Renato Renner, my supervisors, for their patient guidance and useful critiques as well as for many insightful discussions. I would also like to express my great appreciation to Dr. Johan Åberg, who gave his time so generously, for his valuable and constructive suggestions during the development of this work.

I would like to extend my thanks to Arne Hansen for his help with MATLAB codes and fruitful discussions.

Finally, I wish to thank Ruth and Marzell, my parents, and Jessica, my girlfriend, for their support and encouragement throughout my study.

Introduction

What are the smallest possible thermal machines that still work with maximal efficiency¹? This question has attracted quite some attention in the last few years. Starting with refrigerators, Noah Linden *et al.* showed that a machine consisting of two qubits connected to two heat baths of different temperatures can be used to cool down a third system to an arbitrarily low temperature [1]. Moreover, it has been shown that such a refrigerator approaches Carnot efficiency [2, 3]. At first sight this may seem surprising. It could have been the case that there exists some kind of complementarity between size and efficiency. However, despite the fact that a refrigerator made of only two qubits features a discrete and very small number of states, it can reach the maximum efficiency compatible with the fundamental laws of thermodynamics. Thus, the fundamental limit to the efficiency of thermal engines is independent of their size. An important feature of the proposed machine is that it is self-contained. This means that the only resource necessary is the connection to the heat baths. In particular, the energy-conserving interaction of the subsystems is described by a time-independent Hamiltonian and no external control is needed.

In subsequent papers [4, 5] the same authors have shown that in a similar way it is possible to build not only small refrigerators but also small heat engines (Fig. 1 (a)) and heat pumps. Both types of machines use the same resources as the refrigerator: two heat baths at different temperatures. A heat engine produces work, and a heat pump heats a third system. These machines are reviewed in Section 1 of Part I of this thesis.

There is another type of process that is very interesting from a thermodynamic viewpoint: work extraction procedures (Fig. 1 (b)). As in the heat engine, the goal is to produce work. Work is rather abstractly defined as ordered energy. A classical example of this is a weight m_W at some height h in the gravitational field of the earth g . This would correspond to m_Wgh work. In small quantum systems the definition of work is more difficult. An example could be a quantum harmonic oscillator in an excited energy eigenstate.² The process of work extraction is fundamentally different from the processes happening in thermal machines. Instead of two, one needs only one heat bath. Since it is not possible to drop some waste heat into a cold heat bath in this regime, we need another system which can serve as an entropy sink to meet the Second Law of thermodynamics. This can be a physical system in a well-known state ('information') that is

¹One example of a thermal machine is a heat engine. The general functional principle of a heat engine is depicted in Fig. 1 (a)

²This idea is linked to the idea of an elevated weight. A weight at a higher height corresponds to a higher excited energy eigenstate.

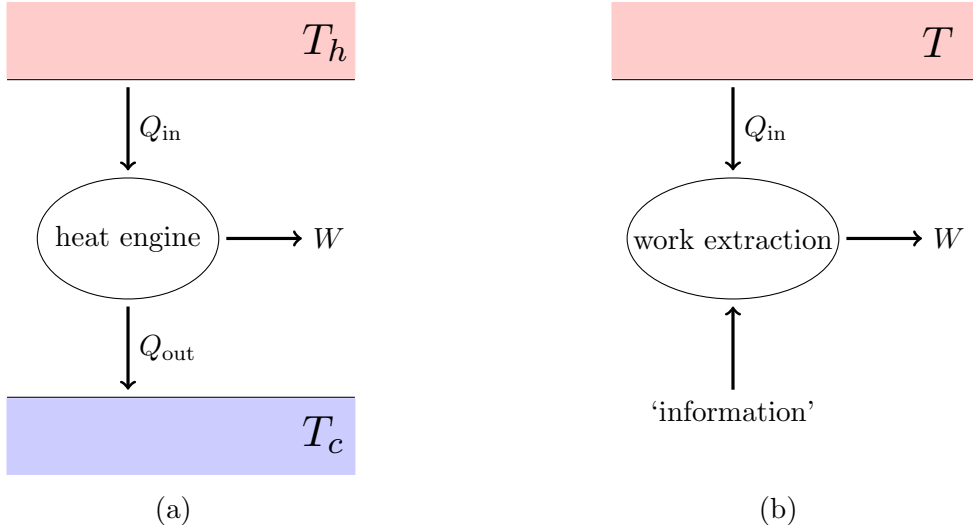


Figure 1.: (a) General heat engine: A heat engine is a physical system that has access to two heat baths at different temperatures and uses these resources to produce work. It takes heat from the warmer bath (at T_h), converts part of it into work, and drops some waste heat into the cold bath (at T_c). It cannot convert all of the heat-like energy extracted from the hot heat bath into work because of the Second Law of thermodynamics. If such a heat engine works reversibly, then one can connect two of them to cool or heat a third system by using the work output of one as a work input for another engine connected to other heat baths. (b) General work extraction procedure: Here, only one thermal bath at some temperature T is needed. The machine extracts heat from this bath and converts all of it into work. In order to fulfil the Second Law of thermodynamics, there must be another system involved with increased entropy after the process. This is depicted as ‘information’. By this we mean a physical system in a known non-equilibrium state that enables us to convert heat into work while raising its entropy. An example of such a system is a qubit in a pure state.

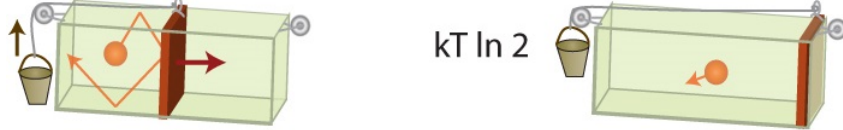


Figure 2.: Classical Szilard engine: A particle in a box interacting with a heat bath and a piston. A weight is attached to the piston such that it has more potential energy if the piston is more to the right. L is the total length of the box, T the temperature of the surrounding heat bath, and m_W the mass of the weight attached to the piston.

returned in a mixed state after the process. In Section 2 we take an approach towards work extraction procedures via Maxwell’s demon. We give examples of proposed work extraction models that use pure qubits as information resources and argue that none of them is self-contained in the above mentioned sense, i.e., their evolution is governed by time-dependent Hamiltonians.

This motivates the second part of the thesis, where we use the idea of a classical Szilard engine and try to find out whether and under what circumstances such a machine can be used to extract work. A macroscopic classical Szilard engine is a box divided into two halves with an ideal gas in one (e.g. the left) half. The location of the gas corresponds to one bit of information (left or right half of the box). If this box is in contact with a heat bath at temperature T one can extract $kT \ln 2$ work from the heat bath by letting the gas expand isothermally. This can be done for instance by attaching a weight to a piston that is lifted during the expansion of the gas.

Leo Szilard miniaturized this idea to a one-particle gas in a box as in Fig. 16. If this system still extracts work from the surrounding heat bath using the information about the initial location of the particle, it is an autonomous work extraction process because it is described by a time-independent Hamiltonian. Furthermore, no external control is needed during the process of work extraction.

We are particularly interested in whether a self-contained work extraction procedure exists for very small (quantum) systems. Therefore, we come up with a semi-quantum model of a Szilard engine and analyze its evolution with the help of numerical simulations. We want to find out whether the work output of such a small system can still be deterministic. Our hope is that a better understanding of the Szilard engine leads to new insights and ideas of how to construct a more general self-contained work extraction process. The ultimate goal would be to implement such a work extraction process in a lab. At the end of the thesis, we raise open questions and discuss important features of our model.

Part I.

Review:

**Quantum Thermal Machines,
Maxwell's Demon and
Work Extraction Procedures**

1. Thermal Machines

A thermal machine is a physical system that has access to two heat baths of different temperatures and uses these resources to heat or cool a body or to perform work. If the goal is to heat, the machine is called a heat pump. If we want to cool down a body, the machine is called a refrigerator. If the system produces ordered energy (i.e., work) it is called a heat engine.

In this section we start by giving classical examples of the three types of thermal machines, where we assume that the reader is familiar with the fundamental laws of thermodynamics. In particular, we are interested in the maximal efficiency that a thermal machine can reach.

After this, we go on and ask ourselves how small such a machine can be and still function in a similar way. We give examples of small thermal machines and investigate the maximal efficiency they can reach.

We conclude the section with an outlook and discuss open questions.

1.1. Basic Principles – The Carnot Engine

We investigate a cyclic process operating between two heat baths of different temperatures, T_c (cold) and T_h (hot), that produces work. The machine uses an arbitrary work medium that can be described by the variables p and V such that produced work by the machine is given by $\delta W = pdV$. This is of course in analogy with the classical example of an ideal gas that is described by pressure p and volume V . In this case work can be defined by the motion of a wall under the expansion of the gas. We come back to this example later in this section. The functional principle of the machine is to take heat from the hot reservoir, transform part of it into work, and drop residual heat into the cold reservoir. A natural question is whether it is possible to transform all of the heat taken from the hot reservoir into work. We will prove below that this is not possible. This is the basic reason why we need two heat baths of different temperatures.

The process we are interested in consists of four steps (see Fig. 3):

- A (1→2):** isothermal expansion,
- B (2→3):** adiabatic expansion,
- C (3→4):** isothermal compression,
- D (4→1):** adiabatic compression.

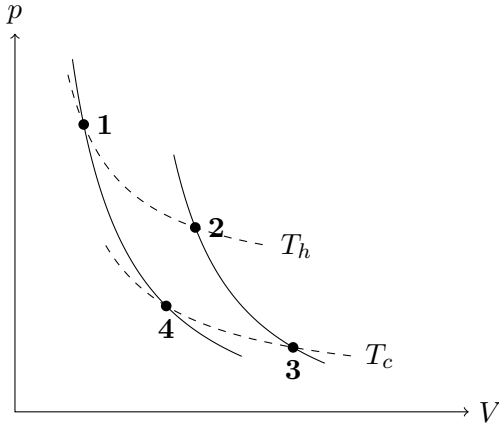


Figure 3.: Schematic Carnot process in a p - V diagram. The diagram must be read as **1**→**2**→**3**→**4**→**1**. The solid lines stand for adiabatic expansion / compression, the dashed lines stand for isothermal expansion / compression. Expansion stands for $dV > 0$, compression for $dV < 0$.

The numbers **1**...**4** denote the states of the medium at the corner points of the cycle. This cycling process is called *Carnot cycle* [6]. In order to describe the process we need the first law of thermodynamics, which states [7, 8]:

$$dU = \delta Q - \delta W, \quad (1.1)$$

where U is the inner energy, Q the heat-like energy coming into the system from a reservoir, and W the produced work going out of the system. In an isothermal process the temperature of the medium is constant ($dT = 0$), whereas in an adiabatic process $\delta Q = 0$. This implies that in steps B and D no heat is exchanged. We denote the heat exchanged in the steps A and C by Q_A^\leftarrow and Q_C^\rightarrow , respectively. The total exchanged quantity of heat is therefore

$$\oint \delta Q = Q_A^\leftarrow - Q_C^\rightarrow. \quad (1.2)$$

The minus sign comes from the fact that we regard Q_A^\leftarrow as heat that is brought to the machine from the hot bath and Q_C^\rightarrow as heat that is extracted from the machine and goes to the colder bath. We will stick to this notation during this section and use arrows to indicate whether the heat (or work) is coming from or going to the machine. Hence, both are positive, and the net heat is the difference between them. Similarly for the total work produced in one cycle:

$$\oint \delta W = \oint pdV = W_A^\rightarrow + W_B^\rightarrow - W_C^\leftarrow - W_D^\leftarrow = W. \quad (1.3)$$

By definition of a cyclic process, the initial and final state of the medium must be the same. In particular, the internal energy after one cycle is the same as it was in the

beginning. Together with the first law this implies

$$W = Q_A^\leftarrow - Q_C^\rightarrow. \quad (1.4)$$

The efficiency factor for the heat engine can then be written as the ratio of the work output and the input heat

$$\eta_{\text{engine}} := \frac{W}{Q_A^\leftarrow} = 1 - \frac{Q_C^\rightarrow}{Q_A^\leftarrow}. \quad (1.5)$$

Now we make use of the Second Law of thermodynamics as stated by Kelvin [9]

“It is impossible, by means of inanimate material agency, to derive mechanical effect from any portion of matter by cooling it below the temperature of the coldest surrounding objects.”

What he means by this is that it is impossible to produce work from a cycling process by cooling one body. In other words, some waste heat must be produced in a cycling process using thermal energy to produce work, i.e., $Q_C^\rightarrow > 0$. In particular, $\eta_{\text{engine}} < 1$.

In the following we consider only reversible Carnot engines, i.e., Carnot engines with no friction, such that the only waste energy comes from the thermodynamical necessity to produce some amount of waste heat. This can be formulated as a statement about entropy, which, in the reversible case, is defined as

$$dS_{\text{rev}} = \frac{\delta Q_{\text{rev}}}{T}, \quad (1.6)$$

where the subscript ‘rev’ stands for ‘reversible’. Reversibility is then equivalent to the statement that the amount of entropy by which the entropy of the hot heat bath is lowered must be equal to the amount of entropy by which the entropy of the cold bath is increased:

$$0 = \oint dS_{\text{rev}} = \oint \frac{\delta Q_{\text{rev}}}{T}. \quad (1.7)$$

We will show that the efficiency of any reversible Carnot engine is the same, regardless of the operating medium. To do so, we first note that the reverse process **1**→**4**→**3**→**2**→**1** mimics a heat pump and a refrigerator at the same time. It takes heat from the colder heat bath and transports it to the hotter bath. During that process the work W must be invested. The coefficient of performance of a heat pump is defined as

$$\eta_{\text{pump}} := \frac{Q_A^\leftarrow}{W} = \frac{1}{1 - \frac{Q_C^\rightarrow}{Q_A^\leftarrow}} = \frac{1}{\eta_{\text{engine}}}, \quad (1.8)$$

where now Q_A is the heat that is pumped to the high-temperature reservoir, and Q_C is the heat taken from the cold-temperature reservoir.¹ By the Second Law $\eta_{\text{pump}} > 1$

¹This is why the arrows change.

always. Suppose now that we have two Carnot engines working with the same heat baths at temperature T_c and T_h . The first Carnot engine shall be acting as a heat engine, the second as a heat pump, as indicated in Fig. 4. The machines are coupled such that the work produced by the first Carnot engine is going directly and without losses to the second one, as a resource to pump the heat back into the hot reservoir. Assume that the efficiency factors are different, w.l.o.g. $\eta_{\text{engine}}^{(1)} > \eta_{\text{engine}}^{(2)}$.² This implies

$$Q_A^{(2)\nearrow} = \frac{W}{\eta_{\text{engine}}^{(2)}} > \frac{W}{\eta_{\text{engine}}^{(1)}} = Q_A^{(1)\nearrow}. \quad (1.9)$$

i.e., the coupled Carnot engines move heat to the hot reservoir. According to the first law of thermodynamics this heat must come from the cold reservoir. In other words, the engine depicted in Fig. 4 generates a net heat current from the cold reservoir at T_c to the hot reservoir at T_h . To see that this is a contradiction to the Second Law of thermodynamics we use its formulation put forward by Clausius [10], which is equivalent to Kelvin's version:

“Heat can never pass from a colder to a warmer body without some other change, connected therewith, occurring at the same time.”

If it was possible that the efficiency of the first Carnot engine is higher than the efficiency of the second, then Clausius' statement would be directly violated. This concludes the proof of the universality of the Carnot efficiency factor under the assumption that the laws of thermodynamics are true for any physical system.

Next we show that the efficiency factor of a reversible Carnot engine is maximal: no other machine producing work by operating with heat baths at temperatures T_h and T_c can be more efficient than a Carnot heat engine. We start by rewriting the Carnot efficiency factor of a reversible Carnot engine. As stated above, reversibility implies $\oint dS_{\text{rev}} = 0$, i.e.,

$$0 = \oint \frac{\delta Q_{\text{rev}}}{T} = \frac{Q_A^{\nearrow}}{T_h} - \frac{Q_C^{\neararrow}}{T_c} \quad (1.10)$$

in the Carnot process from Fig. 3. But this means that the efficiency factor can be rewritten as

$$\eta_{\text{engine}} = 1 - \frac{Q_C^{\neararrow}}{Q_A^{\nearrow}} = 1 - \frac{T_c}{T_h}. \quad (1.11)$$

²If $\eta_{\text{engine}}^{(1)} < \eta_{\text{engine}}^{(2)}$, swap the roles of the two Carnot engines, and we arrive at the same situation. We can do this because by assumption both engines are reversible. So we are free to choose which one works as a heat pump and which as a heat engine.

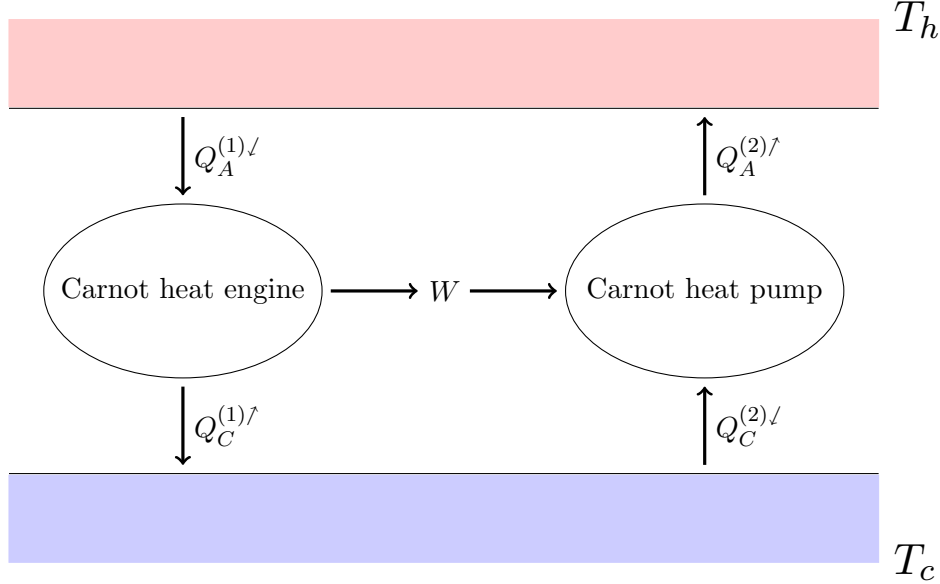


Figure 4.: Two Carnot engines working with the same heat baths at temperatures T_h and T_c . The work produced with the first Carnot engine is used to drive a Carnot heat pump. The assumption that the efficiencies are different leads to a contradiction.

By the mathematical version of Clausius' Second Law of thermodynamics ($\oint \frac{\delta Q}{T} \leq 0$ for cyclic processes) we know that for any cyclic process

$$0 \geq \oint \frac{\delta Q}{T} = \frac{Q_{\text{in}}^{\uparrow}}{T_h} - \frac{Q_{\text{out}}^{\uparrow}}{T_c}, \quad \text{i.e.,} \quad \frac{T_c}{T_h} \leq \frac{Q_{\text{out}}^{\uparrow}}{Q_{\text{in}}^{\uparrow}}, \quad (1.12)$$

which implies that for any other machine operating in a cyclic process with these heat baths the efficiency η' must be smaller:

$$\eta_{\text{engine}} = 1 - \frac{Q_C^{\uparrow}}{Q_A^{\uparrow}} = 1 - \frac{T_c}{T_h} \geq 1 - \frac{Q_{\text{out}}^{\uparrow}}{Q_{\text{in}}^{\uparrow}} = \eta'. \quad (1.13)$$

This concludes the proof.

1.1.1. Classical Example: Ideal Gas

In the last part of this section we give a classical example of a physical system that acts as a Carnot engine. As a medium we consider an ideal gas, described by the equation of state

$$pV = nRT, \quad (1.14)$$

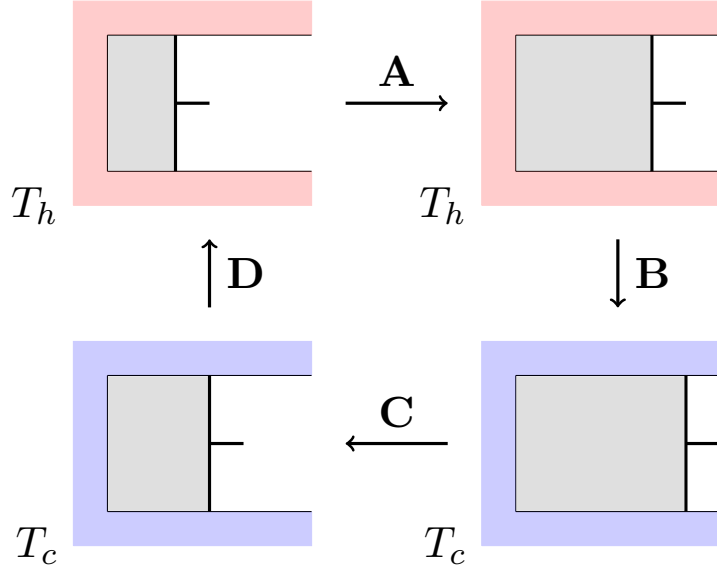


Figure 5.: Carnot process with an ideal gas. **A**: isothermal expansion, **B**: adiabatic expansion, **C**: isothermal compression, **D**: adiabatic compression.

where p is the pressure, V the volume, n the amount of substance (number of moles of gas), T the temperature and R the universal gas constant. The gas is located in a box with a movable wall (the piston), such that the piston performs the work $\delta W = pdV$ when the gas changes its volume by dV at pressure p (see Fig. 5). Using standard thermodynamics one finds the following work and heat exchanges for the steps **A**,..,**D**:

$$\begin{aligned}
 \mathbf{A:} \quad & W_A^\uparrow = nRT_h \ln \frac{V_2}{V_1}, & Q_A^\downarrow = nRT_h \ln \frac{V_2}{V_1}, \\
 \mathbf{B:} \quad & W_B^\uparrow = nC_V(T_h - T_c), & Q_B = 0, \\
 \mathbf{C:} \quad & W_C^\downarrow = nRT_c \ln \frac{V_3}{V_4}, & Q_C^\uparrow = nRT_c \ln \frac{V_3}{V_4}, \\
 \mathbf{D:} \quad & W_D^\downarrow = nC_V(T_h - T_c), & Q_D = 0,
 \end{aligned}$$

where $C_V = \frac{\partial U}{\partial T}|_V$ stands for the heat capacity of the ideal gas for constant volume. The signs were all taken to be positive. The arrows indicate whether work and heat is generated or used during the process. It is straight forward to see that the efficiency of this cyclic process is indeed the Carnot efficiency

$$\eta = \frac{W_A^\uparrow + W_B^\uparrow - W_C^\downarrow - W_D^\downarrow}{Q_A^\downarrow - Q_C^\uparrow} = 1 - \frac{T_c}{T_h}. \quad (1.15)$$

In conclusion, we have introduced the Carnot cycle and showed that its efficiency is universal and maximal for reversible Carnot engines using standard thermodynamics.

We have seen that a Carnot engine can be used as a heat engine, heat pump or refrigerator. Finally, we gave an example of a classical physical system that is in principle able to operate at the Carnot efficiency.

1.2. The Smallest Possible Thermal Machines

We have seen a classical macroscopic heat engine that reaches the Carnot limit. In principle it is possible to build a Carnot engine such that it is self-contained. This is, once we are given the initial states of all involved particles together with the interactions that take place, the evolution is governed by a time-independent Hamiltonian. In other words, the steady state of the system transforms heat into work without using external control or work. However, the theory of thermodynamics can as well be applied to microscopic quantum systems with only few quantum states [11]. Thus the following two questions arise: (1) Does there exist a fundamental limit to the size of a quantum thermal machine? Here, size is measured in terms of the number of different states in the machine. (2) Is there a complementarity between size and efficiency of such a machine?

In this section we review results [1, 3, 4, 5] that show that there is no such fundamental limit to size. This will be done by finding small thermal machines that behave essentially like macroscopic machines. Furthermore, in a subsequent section, we discuss a proof presented in [2] and [3] showing that there is no trade-off between size and efficiency and that the smallest possible refrigerators and heat engines can reach the Carnot limit.

1.2.1. Small Refrigerator and Heat Pump

We start with the task of finding a small thermal machine that allows us to cool a non-degenerate qubit [1]. In the following, by cooling we mean bringing the state of the qubit closer to the lowest energy eigenstate, denoted by $|0\rangle_1$. Consider now two additional qubits. The free Hamiltonian of the three qubits shall be

$$H_0 = E_1|1\rangle\langle 1|_1 + E_2|1\rangle\langle 1|_2 + E_3|1\rangle\langle 1|_3. \quad (1.16)$$

The qubits are in contact with heat baths of temperatures $T_1 = T_c$, $T_2 = T_r$, $T_3 = T_h$, where c , r and h stand for *cold*, *room* and *hot* temperature, respectively and $T_c < T_r < T_h$. The whole system is depicted in Fig. 6. It is convenient to deal with qubits because for any possible diagonal state we can assign a generalized temperature. For instance, a qubit with Hamiltonian $H = E|1\rangle\langle 1|$ in the state $p|0\rangle\langle 0| + (1-p)|1\rangle\langle 1|$ has temperature $T = \frac{E}{k \ln \frac{p}{1-p}}$, where k is the Boltzmann constant. This becomes clear when we compute the Boltzmann state of such a qubit at temperature T which is

$$\tau = \frac{|0\rangle\langle 0| + e^{-\frac{E}{kT}}|1\rangle\langle 1|}{Z}. \quad (1.17)$$

$Z = 1 + e^{-\frac{E}{kT}}$ is the partition sum. In the following we will use the notation τ for Boltzmann states. Notice that the generalized temperature can become infinite (for $p = \frac{1}{2}$) or negative (for $p < \frac{1}{2}$).

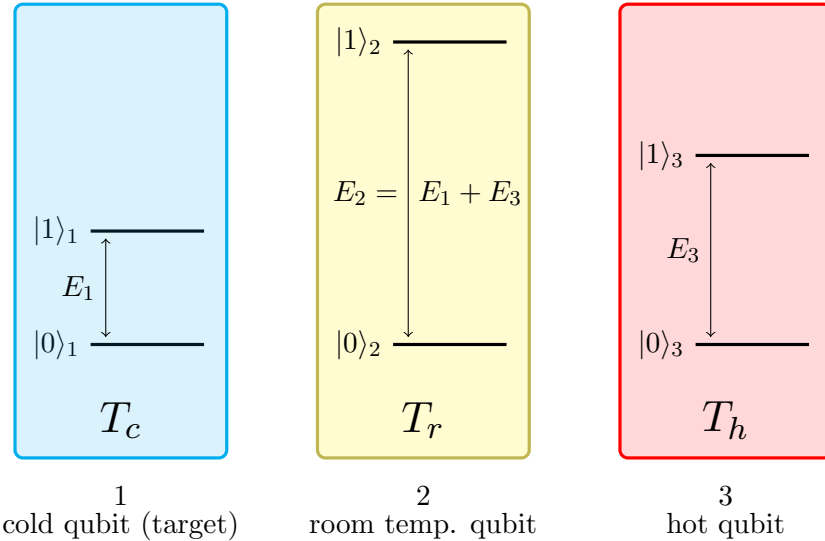


Figure 6.: Setting of the small refrigerator. The three qubits interact with heat baths of different temperatures: T_c *cold*, T_r *room temperature*, and T_h *hot*.

The goal is to find an interaction Hamiltonian that brings the first qubit to a steady state ρ_1^S with temperature $T_1^S < T_c$, corresponding to $\langle 0|\rho_1^S|0\rangle \geq \langle 0|\tau_1|0\rangle$, where ρ_1^S is the reduced state of qubit 1 in the steady state and τ_1 is the thermal state of qubit 1 at temperature $T_1 = T_c$. We will see that this can be achieved by inducing the transition $|101\rangle \leftrightarrow |010\rangle$, where we made use of the notation $|101\rangle$ for $|1\rangle_1|0\rangle_2|1\rangle_3$. We will stick to this notation from now on.

Since we would like to have a self-contained thermal machine, it is not allowed to use external work. In order to fulfil this condition we are only allowed to perform energy-conserving operations. In particular, the energies must satisfy $E_1 + E_3 = E_2$ such that the transition $|101\rangle \leftrightarrow |010\rangle$ satisfies this requirement. For transitions between $|101\rangle$ and $|010\rangle$ to occur we introduce the interaction Hamiltonian

$$H_{\text{int}} = g(|101\rangle\langle 010| + |010\rangle\langle 101|), \quad (1.18)$$

where g is the interaction strength. A short calculation shows that $[H_{\text{int}}, H_0] = 0$, i.e., the interaction is energy preserving, if $E_1 + E_3 = E_2$. Notice that the interaction is via a Hamiltonian and not by discrete unitary transformation steps. This is an important feature of the machine presented here, because a unitary step necessarily implies external control, i.e., a device that allows us to implement the correct timing of the unitary operations.

The next challenge is to model the thermalization of each particle. The simplest way is to imagine that with probability density p_i per unit time each qubit is reset to its

initial thermal state which is

$$\tau_i = \frac{|0\rangle\langle 0|_i + e^{-\frac{E_i}{kT_i}}|1\rangle\langle 1|_i}{\mathcal{Z}_i}. \quad (1.19)$$

The idea is equivalent to saying that in the time interval δt the qubit is exchanged with a new qubit in state τ_i with probability $p_i\delta t$. Mathematically this is correctly described by the trace preserving completely positive map

$$\mathcal{E}_i(\rho) = p_i\tau_i \otimes \text{Tr}_i\rho + (1 - p_i)\rho \quad (1.20)$$

for each $i = 1, 2, 3$. This allows us to derive the master equation. Consider a small time interval δt around a time t_0 . The change of the density matrix ρ is given by³

$$\begin{aligned} \rho(t_0 + \delta t) = & -i\delta t[H_0 + H_{\text{int}}, \rho(t_0)] + (1 - \delta t(p_1 + p_2 + p_3))\rho(t_0) \\ & + \delta t p_1 \tau_1 \otimes \text{Tr}_1\rho(t_0) + \delta t p_2 \tau_2 \otimes \text{Tr}_2\rho(t_0) + \delta t p_3 \tau_3 \otimes \text{Tr}_3\rho(t_0). \end{aligned} \quad (1.21)$$

The first term on the right hand side can easily be derived from basic quantum mechanics. The other terms are due to the non-unitary thermalization process of each qubit. With probability $(1 - \delta t(p_1 + p_2 + p_3))$ the state stays the same, while with probability $\delta t p_i$ qubit i gets decoupled from the other qubits and is reset to the thermal state. Rearranging and using differential notation yields the master equation

$$\begin{aligned} \frac{\partial \rho}{\partial t} = & -i[H_0 + H_{\text{int}}, \rho] + \sum_{i=1}^3 p_i (\tau_i \otimes \text{Tr}_i\rho - \rho) \\ \equiv & -i[H_0 + H_{\text{int}}, \rho] + \sum_{i=1}^3 \mathcal{D}_i(\rho) \end{aligned} \quad (1.22)$$

where we introduced the dissipators of the qubits, denoted by \mathcal{D}_i for $i = 1, 2, 3$. In general the addition of H_{int} with strength g in Eq. 1.22 requires a modification of the dissipation term in order to arrive at a consistent equation. However, if one considers the limit of small g, p_1, p_2 and p_3 corrections of order gp_i and $p_i p_j$ can be neglected and the master equation is consistent.

To analyze the properties of the model in which we are interested, it is sufficient to compute the steady state ρ^S defined by

$$\frac{\partial \rho^S}{\partial t} = 0 \quad \text{i.e.,} \quad 0 = -i[H_0 + H_{\text{int}}, \rho^S] + \sum_{i=1}^3 p_i (\tau_i \otimes \text{Tr}_i\rho^S - \rho^S). \quad (1.23)$$

This can be done analytically or numerically. In the following we will derive the main results for a perfectly insulated qubit analytically, i.e., $p_1 = 0$ and T_1 arbitrary, which

³In this thesis we will set $\hbar = 1$.

simplifies the calculations dramatically. Notice first that the dissipators \mathcal{D}_2 and \mathcal{D}_3 have the following property:

$$\mathcal{D}_2(\rho_{13} \otimes \tau_2) = 0 \quad \text{and} \quad \mathcal{D}_3(\rho_{12} \otimes \tau_3) = 0 \quad (1.24)$$

for all density operators ρ_{12} and ρ_{13} . The idea needed to solve Eq. 1.23 is now straightforward. Start with the ansatz

$$\rho^S = \tau_1^S \otimes \tau_2 \otimes \tau_3 \equiv (r|0\rangle\langle 0|_1 + (1-r)|1\rangle\langle 1|_1) \otimes \tau_2 \otimes \tau_3 \quad (1.25)$$

and use Eq. 1.23 to solve for r . Doing so yields the equation

$$0 = \left(re^{-\frac{E_2}{kT_2}} - (1-r)e^{-\frac{E_3}{kT_3}} \right) (|101\rangle\langle 010| - |010\rangle\langle 101|) \quad (1.26)$$

which has the solution

$$r = \frac{1}{1 + e^{-\frac{E_1}{kT_1^S}}} \quad \text{with} \quad T_1^S = \frac{T_2}{1 + \frac{E_3}{E_1} \left(1 - \frac{T_2}{T_3} \right)}. \quad (1.27)$$

I.e., qubit one has steady state temperature T_1^S . This solution is valid as long as $g, p_2, p_3 \neq 0$. Interestingly, there is no dependence of the steady state upon these parameters if $p_1 = 0$. Besides that, the steady state temperature of qubit 1 is smaller than T_2 if $T_2 < T_3$, which is the case in the above setup where we chose $T_2 = T_r$, $T_3 = T_h$ (remember: r stands for *room temperature*, h stands for *hot temperature*). Furthermore a lower temperature of qubit 1 can be achieved by taking the ratio $\frac{E_3}{E_1}$ to be large. It turns out that exactly the same model can also work as a heat pump. To see this, consider $T_2 = T_h$, $T_3 = T_r$. In this case clearly $T_1^S > T_2 = T_h$, which tells us that heat must flow from qubits 2 and 3 to qubit 1, although qubit 1 has already a higher temperature than both qubits 2 and 3.

The analytic analysis from above was done only for the special case $p_1 = 0$. Nevertheless, numerical results [1] show that also for non-zero p_1 and $T_1 = T_c$ a steady state temperature $T_1^S < T_c$ can be achieved. However, the parameters p_i cannot become arbitrarily large without consequences. Numerical analysis done in [1] shows that increasing p_1 leads to a higher steady state temperatures of qubit 1. Intuitively this makes sense, since this case corresponds to worse isolation of the refrigerator. In contrast to this, higher p_2 and p_3 yield a better performance because then the heat exchanges for qubits 2 and 3 happen faster. For even higher p_2 and p_3 the performance degrades again. The reason is the quantum Zeno effect [12]. Since the dissipators in Eq. 1.22 replace the reduced states with diagonal states τ_i , thermalization acts on the qubits as a measurement. Strong couplings between the qubits and the environment lead to (almost) continuous measurements. In this regime the interaction H_{int} will not have time to act between successive thermalizations and the refrigerator is no longer able to function.

Also in the general case of non-zero p_1 the machine can function as a heat pump when choosing $T_2 = T_h$, $T_3 = T_r$. In this case, qubit 1 can be brought to a steady state with temperature $T_1^S > T_h$. The parameter dependence of the model stays the same.

All in all, this answers question (1) with respect to refrigerators and heat pumps. There is no fundamental limit to the size of such self-contained quantum thermal machines. It was shown that a machine consisting of two qubits, i.e., four different quantum states, is indeed enough to cool or heat a third qubit to a steady state temperature colder or warmer than both temperatures of the heat baths. Whether the ideas presented here can also be used to model a small heat engine will be treated in the following.

1.2.2. Small Heat Engine

Modelling a small heat engine is more subtle than finding systems that act as refrigerators or heat pumps. The reason for this lies in the notion of work one needs to define in order to be able to talk about an engine that produces work. Basically any form of ordered energy can be regarded as work. For instance, a weight of mass m at a certain height h feeling the gravitational acceleration g stores the energy mgh , which is work because we know exactly how we can use this energy to drive a machine or transform it into another form of energy.

As mentioned above, the focus is on self-contained heat engines where there is no external work or control. The only external interaction happens with thermal baths. Here, a definition of work is used that was introduced in [4] and initially put forward by Carnot [6], namely:

“Motive power (work) is the useful effect that a motor is capable of producing. This effect can always be linked to the elevation of a weight to a certain height.”

The engine presented here will produce work in the same way, i.e., by lifting a weight. The weight consists of a system with an infinite number of equidistant energy levels and the work created by the heat engine causes the position of the weight to increase with time. In other words: work is a population of excited states in a quantum system with internal Hamiltonian

$$H_1 = \sum_{n=-\infty}^{\infty} n E_1 |n\rangle\langle n|_1. \quad (1.28)$$

The index 1 suggests that this system will replace qubit 1 from the previous considerations. Defining work like this, it is implicitly assumed that one is able to extract the amount of work E_1 by letting the system decay from the state $|n+1\rangle$ to $|n\rangle$. In this sense, only energy eigenstates can be viewed as work. It is left open in how far superpositions of energy eigenstates should be considered to be work. Questions like these are discussed in [13, 14]. Since we will only encounter mixtures of energy eigenstates in the

treatment here, we will not go further into that.

The functional principle of the heat engine is very similar to the refrigerator and heat pump (Fig. 7). Again, the machine consists of two additional qubits with indices 2 and 3. The Hamiltonian of the system consisting of these three subsystems is therefore

$$H_0 = \sum_{n=-\infty}^{\infty} nE_1|n\rangle\langle n|_1 + E_2|1\rangle\langle 1|_2 + E_3|1\rangle\langle 1|_3, \quad (1.29)$$

where again E_2 and E_3 stand for the energy gaps of qubits 2 and 3. Both qubits are connected to heat baths. Qubit 2 is thermalized by a heat bath of temperature $T_2 = T_h$ and qubit 3 by a heat bath of temperature $T_3 = T_c$. As before, the indices c and h stand for *cold* and *hot*, respectively, which implies $T_c < T_h$. The dissipators are given by

$$\mathcal{D}_i(\rho) = p_i (\tau_i \otimes \text{Tr}_i \rho - \rho) \quad (1.30)$$

for $i = 2, 3$ with τ_i given in Eq. 1.19 and p_i has the interpretation from before. Hence, with respect to the interaction with thermal baths not much has changed except that subsystem 1 is no longer connected to a heat bath. In order to use this system as a heat engine the subsystems must interact. Since we want a self-contained machine, the interaction must be energy conserving. In the spirit of the refrigerator and heat pump we take the interaction Hamiltonian

$$H_{\text{int}} = g \sum_{n=-\infty}^{\infty} \left(|n, 10\rangle\langle n+1, 01| + |n+1, 01\rangle\langle n, 10| \right) \quad (1.31)$$

with the constraint

$$E_1 + E_3 = E_2, \quad (1.32)$$

ensuring that the interaction is energy conserving. This is only a slight modification of Eq. 1.18, where now the swapping term $|n, 10\rangle\langle n+1, 01|$ is taken for all energy eigenstates $|n\rangle$ of the storage system.

The idea behind the interaction is to induce the transition $|n, 10\rangle \leftrightarrow |n+1, 01\rangle$ and bias the direction $|n, 10\rangle \rightarrow |n+1, 01\rangle$, in which the weight is lifted, such that it happens more often than the reverse process. This biasing is done by manipulating the transition probabilities of each process by the interaction with heat baths. Indeed, in the absence of interaction, the probability of finding subsystems 2 and 3 in the state $|01\rangle_{23}$ is $\frac{\exp(-\frac{E_3}{kT_c})}{Z_2 Z_3}$ while the state $|10\rangle_{23}$ is occupied with probability $\frac{\exp(-\frac{E_2}{kT_h})}{Z_2 Z_3}$. Hence, whenever

$$\frac{E_3}{T_c} > \frac{E_2}{T_h}, \quad (1.33)$$

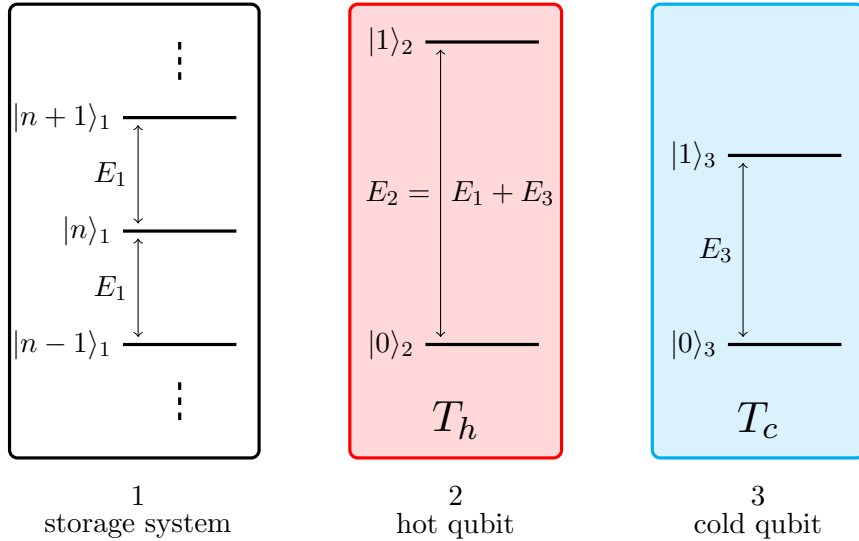


Figure 7.: Setting of the small heat engine presented here. The storage system consists of infinitely many equidistant energy levels. The energy spacings must fulfil $E_2 = E_1 + E_3$ so that the machine is self-contained. Qubits 2 and 3 interact with heat baths whereas the storage system is perfectly isolated from its environment. This means that there are no dissipation processes involving subsystem 1.

the transition that lifts the weight in subsystem 1 is more probable than the transition that lowers it. By the energy conservation constraint on E_1, E_2, E_3 we had $E_1 + E_3 = E_2$. Together with $E_1, E_2, E_3 > 0$ and $T_h > T_c$ this does not automatically give us Eq. 1.33. Hence, this constraint has to be met separately to ensure that the machine works as a heat engine.

Notice that the above calculations of probabilities were done in the case of non-interacting subsystems. Nevertheless, we will see below that Eq. 1.33 must also be fulfilled if the subsystems interact and are coupled to heat baths (for qubits 2 ad 3) to let the machine act as a heat engine.

Now we have everything to set up the master equation

$$\frac{\partial \rho}{\partial t} = -i[H_0 + H_{\text{int}}, \rho] + \sum_{i=2}^3 \mathcal{D}_i(\rho). \quad (1.34)$$

Instead of solving the equation for ρ we take a different path. The figure of interest is $\langle H_1 \rangle = \text{Tr}(H_1 \rho)$, the mean energy of system 1 (the work storage system). H_1 is defined in Eq. 1.28. We would like to show that the mean energy in system 1 increases with time, i.e., that

$$\frac{d}{dt} \langle H_1 \rangle > 0. \quad (1.35)$$

Later in this section we discuss whether this is a good measure. A more precise analysis of what can be regarded as work can be found in [15]. We are only interested in the mean energy after an initial transient period. Thus we relax the requirement and request that Eq. 1.35 be fulfilled only for long times. From Eq. 1.34 we find

$$\frac{d}{dt}\langle H_1 \rangle = -igE_1\Delta(t), \quad (1.36)$$

where $\Delta(t) = \sum_n (\langle n, 10 | \rho | n+1, 01 \rangle - \langle n+1, 01 | \rho | n, 10 \rangle)$. A general solution for $\Delta(t)$ is derived in Appendix B.1 and can be written as

$$\Delta(t) = \sum_{j=1}^3 \delta_j e^{\lambda_j t} + \frac{2igp_2p_3(r_3 - r_2)}{(p_2 + p_3)(2g^2 + p_2p_3)}, \quad (1.37)$$

where δ_j ($j = 1, 2, 3$) are determined by the initial conditions and $r_i^{-1} = \mathcal{Z}_i = 1 + e^{-\frac{E_i}{kT_i}}$ for $i = 2, 3$. The numbers λ_j showing up in the exponent are solutions of the characteristic equation $(\lambda + p_2)(\lambda + p_3)(\lambda + p_2 + p_3) + 2g^2(2\lambda + p_2 + p_3) = 0$. It can be shown as is done in Appendix B.1 that all of them have negative real part, leading to the long time limit

$$\lim_{t \rightarrow \infty} \frac{d}{dt}\langle H_1 \rangle = \frac{2E_1g^2p_2p_3(r_3 - r_2)}{(p_2 + p_3)(2g^2 + p_2p_3)} > 0. \quad (1.38)$$

This expression is positive for $r_3 > r_2$, which is the case if and only if

$$\frac{E_3}{T_c} > \frac{E_2}{T_h}. \quad (1.39)$$

Although Eq. 1.33 was derived assuming no interaction between the subsystems and no connection to a heat bath, it is the correct constraint on the machine parameters in order to function as a heat engine also in the general case. A very important feature of this constraint is that it can be fulfilled for all T_c and T_h if the energies E_2 and E_3 are chosen accordingly.

With this, we have proved that the mean energy in subsystem 1 increases linearly with time for parameters satisfying Eq. 1.33. This corresponds to a weight that is continuously lifted and hence to work production. Thus the machine introduced above functions as a heat engine. However, it must be expected that the spread of the probability distribution of the position of the weight increases with time as well, i.e., that $\frac{d}{dt}\langle (H_1 - \langle H_1 \rangle)^2 \rangle > 0$ for long times. Indeed, this is the case, as is argued in Appendix B.1. More precisely, we find again a linear behaviour in t . Hence, the standard deviation in the energy increases with \sqrt{t} in the long term limit. This behaviour is well-known from biased random walks, where the mean position of the cursor increases linearly with the number of steps n and the standard deviation grows with \sqrt{n} . The above results suggest that the energy increase in the work storage system can be seen a random walk

with bias towards an energy increase.

We have given examples of smallest machines that do the job of a refrigerator, a heat pump and a heat engine. We have shown that the number of states in a physical system does not affect its capability to function as one of these three types of engines. It is possible to construct machines that cool, heat, or produce work, using their connection to two heat baths at different temperatures, even if the machines themselves have only few states available. The second question raised in the introduction to this section is still open: is there a complementarity between size and efficiency of such a thermal machine? We treat this question in the following.

1.3. Efficiency

In this section we show proofs that the engines presented above can reach Carnot efficiency. We start with the heat engine, where we use the analytical solution presented in the previous section. For the refrigerator and the heat pump we take another line of thought, using more fundamental principles of the engines that lead to the Carnot efficiency in a clearer and more intuitive way. The ideas presented in the second part were brought up in [3].

To compute the efficiency of a heat engine we need to be able to talk about heat flows between the qubits and their environment. The rate at which heat flows from the corresponding bath to qubit i is given by the change in energy due to the interaction with the heat bath:

$$\frac{d}{dt}Q_i = p_i \text{Tr}(H_i(\tau_i - \rho_i(t))), \quad (1.40)$$

for $i = 2, 3$. Remember that p_i is a ‘probability per time’, telling us how probable it is that qubit i is reset to the corresponding thermal state during the time δt . The marginal Hamiltonians are $H_i = E_i|1\rangle\langle 1|_i$, and $\rho_i(t)$ is the marginal state of qubit i at time t . We now introduce two new variables that help us finding nicer expressions for the heat flows. Define the ground state populations of $\rho_2(t)$ and $\rho_3(t)$ as

$$\begin{aligned} \Gamma_2(t) &= \sum_n \left(\langle n, 00 | \rho | n, 00 \rangle + \langle n, 01 | \rho | n, 01 \rangle \right), \\ \Gamma_3(t) &= \sum_n \left(\langle n, 00 | \rho | n, 00 \rangle + \langle n, 10 | \rho | n, 10 \rangle \right), \end{aligned} \quad (1.41)$$

respectively. As shown in Appendix B.1 the solution for the ground state populations in the long time limit is

$$\lim_{t \rightarrow \infty} \Gamma_i(t) = \frac{p_2 p_3 (p_2 + p_3) r_i + 2g^2(p_2 r_2 + p_3 r_3)}{(p_2 + p_3)(2g^2 + p_2 p_3)}, \quad (1.42)$$

for $i = 2, 3$. As before, $r_i = \mathcal{Z}_i^{-1}$ is the inverse of the partition sum, which is the same as the ground state probability of the qubit in a thermal state. The quantities Γ_i are very helpful because they allow us to rewrite Eq. 1.40 as

$$\begin{aligned} \frac{d}{dt}Q_i &= p_i E_i \left(\text{Tr}(|1\rangle\langle 1|\tau_i) - \text{Tr}(|1\rangle\langle 1|\rho_i(t)) \right) = p_i E_i (\Gamma_i(t) - r_i) \\ &= (-1)^i \frac{2E_i g^2 p_2 p_3 (r_3 - r_2)}{(p_2 + p_3)(2g^2 + p_2 p_3)}. \end{aligned} \quad (1.43)$$

Since for a heat engine $r_3 > r_2$, we see that the heat is flowing into qubit 2 from the hot reservoir ($\dot{Q}_2 > 0$) and out of qubit 3 into the cold reservoir ($\dot{Q}_3 < 0$), as expected. Together with Eq. 1.38 this allows us to compute the efficiency of the quantum engine

$$\eta = \frac{\frac{d}{dt}\langle H_1 \rangle}{\frac{d}{dt}Q_2} = \frac{E_2 - E_3}{E_2} = 1 - \frac{E_3}{E_2}. \quad (1.44)$$

In addition we know that the heat engine must satisfy $\frac{E_3}{T_c} > \frac{E_2}{T_h} \Leftrightarrow \frac{E_3}{E_2} > \frac{T_c}{T_h}$. Hence, the maximal efficiency is

$$\eta_{\text{engine}}^{\max} = 1 - \frac{T_c}{T_h}. \quad (1.45)$$

Surprisingly, the rather complicated expressions for heat flow and mean energy simplify drastically when considering the efficiency. The obtained efficiency is exactly the Carnot efficiency encountered in Eq. 1.11. We conclude that no additional constraints on the efficiency of a heat engine arise due to size.

As mentioned above we take a different approach to compute the efficiency of the refrigerator. We have seen that the efficiency of the heat engine does not depend on the parameters of the model such as g, p_2, p_3 , but only on the energy gaps of the subsystems E_1, E_2, E_3 . This is an interesting feature. It suggests that the efficiency is more model independent than one could think. And indeed, there is a very elegant way to obtain the efficiency of such thermal machines without knowing anything about the coupling strengths of the qubit interactions and the heat baths.

Let us have a look at the heat flows occurring in the refrigerator presented in section 1.2.1. We are given the constraint $E_1 + E_2 = E_3$ from Eq. 1.32. The qubits exchange energy with the environment (heat bath) as well as with each other. In equilibrium the total energy of a qubit is constant, so the energy it extracts from the environment must be equal to the energy it passes on to the other two qubits. Remember that the interaction Hamiltonian only induces transitions between the degenerate states $|010\rangle$ and $|101\rangle$. Hence, whenever qubit 1 loses energy E_1 , qubit 3 loses energy E_3 and qubit 2 gains energy E_2 . Similarly, if qubit 1 gains energy E_1 , then qubit 3 gains E_3 and qubit 2 loses E_2 . How often such a transition takes place depends on the actual parameters of the model, as well as the heat flows between the qubits. Hence, without these details, we cannot tell what the heat exchange rates are. Nevertheless, we can make statements

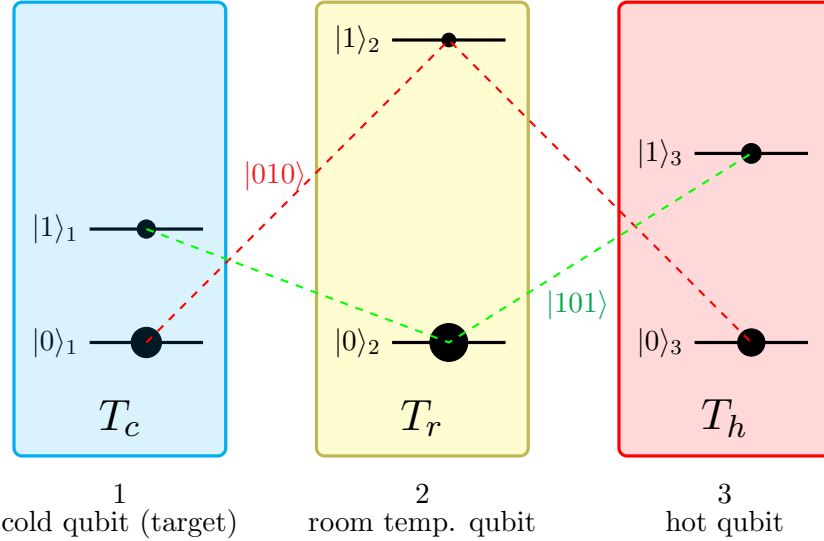


Figure 8.: The setting of the refrigerator revisited. The black dots indicate the probability to find the reduced state of the corresponding qubit in state $|0\rangle$ or $|1\rangle$. The red dashed line connects the states forming $|010\rangle$ and the green dashed line stands for the state $|101\rangle$. To function as a refrigerator the probabilities of the connected states must fulfil $P[101] > P[010]$, which is equivalent to Eq. 1.49.

about the *ratio* of the heat exchange rates because of the constraints of the energy exchanges between the qubits. By the above, the ratios must fulfil [3]

$$Q_1 : Q_2 : Q_3 = E_1 : E_2 : E_3, \quad (1.46)$$

where Q_1 is the energy extracted from qubit 1 (which is the qubit we want to cool), Q_2 is the energy gain of qubit 2 (which is connected to a heat reservoir at room temperature T_c) and Q_3 is the energy extracted from qubit 3 (which is connected to the hot heat bath at T_h). The efficiency of such a refrigerator is then defined as

$$\eta := \frac{Q_1}{Q_3}, \quad (1.47)$$

the ratio of heat that is transported away from the qubit we want to cool and the heat transported away from the qubit that is connected to the hot bath.

As in the case of a thermal heat engine the interaction between the subsystems is such that the transition $|101\rangle \rightarrow |010\rangle$ (which is cooling qubit 1) is enhanced over the transition in the other direction, $|010\rangle \rightarrow |101\rangle$. This is done by arranging the parameters such that the probability to find the system in state $|101\rangle$ in the absence of an interaction is larger than the probability to find it in state $|010\rangle$ (Fig. 8). We can freely choose the

energy gaps of the qubits as long as Eq. 1.32 is satisfied. Hence, we should choose them such that

$$e^{-\frac{E_1}{kT_1}} e^{-\frac{E_3}{kT_3}} > e^{-\frac{E_2}{kT_2}} \quad (1.48)$$

which is equivalent to

$$\frac{E_1}{T_1} + \frac{E_3}{T_3} < \frac{E_2}{T_2}. \quad (1.49)$$

One may wonder why we require this in the absence of an interaction. The reason is fairly simple. Consider a system initially in a thermal state satisfying Eq. 1.48. When we then turn on the interactions, qubit 1 will start to cool, whereas qubit 2 is heated up a little. Hence, it is necessary to request Eq. 1.48 in the absence of an interaction. After some time, qubit 1 has a lower temperature such that the inequality 1.48 is the other way around, in which case qubit 1 starts to heat up again. After a transient period, the qubits will reach a steady state. In this state, the T_i in Eq. 1.48 must be replaced by T_i^S and the steady state temperatures must be such that $T_1^S < T_c, T_2^S > T_r, T_3^S < T_h$, and the qubits neither heat up nor cool down anymore. Eq. 1.48 becomes an equality.

As seen in Section 1.1, the maximal efficiency of a classical machine is reached if the machine works reversibly. This is the same for quantum engines. Here, reversibility means that the transition cooling qubit 3 is infinitesimally close to the reverse transition, which is the case if

$$\frac{E_1}{T_1} + \frac{E_3}{T_3} = \frac{E_2}{T_2}. \quad (1.50)$$

With this we are now in the position to give an expression for the maximal efficiency of a quantum refrigerator. Starting from the definition of η , we use the relation of the ratios of heat flows and energy gaps together with the reversibility condition and the energy conservation condition (Eq. 1.32) to arrive at

$$\eta_{\text{ref}}^{\max} = \frac{Q_1}{Q_3} = \frac{1 - \frac{T_r}{T_h}}{\frac{T_r}{T_c} - 1}, \quad (1.51)$$

which is equal to the optimal efficiency we would obtain in the classical case.

We have seen in section 1.2.1 already that heat pump and refrigerator are essentially the same machine doing slightly different jobs. Hence, the complete analysis done here for refrigerators can also be used for heat pumps. Thus, heat pumps can heat up a qubit at Carnot efficiency as well. So we answered the second question from the introduction of Section 1.2 in the negative in general. It is possible to construct maximally efficient thermal machines of all three types even if the machines have only few degrees of freedom.

1.4. Discussion

In this last section on quantum thermal machines we raise and discuss questions concerning the models presented in the previous sections. We do this with a focus on feasibility in an experimental setting and try to evaluate how physical certain assumptions of the model are.

Hamiltonians In doing so we have to take into account the Hamiltonians as well as the dissipators because these are the ingredients that make the system behave as it does. The free Hamiltonians of the qubits (Eq. 1.16) are standard. We do not discuss it further and just assume that a physical system with such a Hamiltonian can be found in nature to arbitrary accuracy (e.g. in trapped ions or flux qubits). Things are different with the Hamiltonian of the work storage system that stores the work produced with a quantum heat engine (Eq. 1.28). It is somewhat unphysical in that it has no ground state. Brunner *et al.* show in [5] that also for finite systems, i.e. for systems with free Hamiltonian as in Eq. 1.28 but with a finite sum over energy eigenstates, it is possible to raise the population to higher energy levels with an exponential decay of the population probability for lower energy levels. In this sense, the Hamiltonian presented in Eq. 1.28 is not physical, but we can replace it by a physical one and still have a heat engine.

Now to the interaction Hamiltonian (Eq. 1.18): it is an interaction inducing a transition involving three parties at the same time. This is arguably not physical on a basic level. Physical processes are usually described by Hamiltonians containing only two-body terms. Terms with more parties come only into play as higher order effects. It is therefore questionable whether this Hamiltonian can be regarded as a physical Hamiltonian. In [1] the authors present a refrigerator made up of a qubit and a qutrit that interact with each other according to an interaction Hamiltonian that contains only two-body terms. Hence, although the presented model does not have this feature, it is in principle possible to cool or heat a qubit with physical interactions. Furthermore, in [16] Thomas Lawson argues that almost any Hamiltonian that induces inter-qubit interactions allows us to cool, heat or produce work. We refer to his thesis for further explanations.

To sum up: the Hamiltonians presented in this review may not be physical, but physical Hamiltonians that do the same job exist and have been proposed.

Dissipators The derivation of the dissipators that were introduced in Eq. 1.22 was very intuitive. We went out from an abstract probabilistic process that resets each qubit to its thermal state with some probability p and leaves its state unchanged otherwise. However, a physical process that does this has not been proposed. This is also the case in the above cited papers: the authors say nothing about a physical system that has this property. Nevertheless, the simplicity of the approach leading to the dissipators suggests that it is possible to find a system in nature that behaves essentially like this. For instance, it is possible to prepare thermal states of qubits (actually any state) in trapped ions with very high accuracy. Hence for an implementation of one of the above thermal

machines in ion traps we can think of the thermalization process as just resetting the qubits from time to time (according to the probability p) to the thermalized state. This would not necessarily be energy neutral, but it would mimic the thermalization process used in these models.

Quantum Effects Another question is how quantum the small refrigerator is. After all, when describing its functional principle we did never refer to any quantum feature such as a coherent superposition of energy eigenstates or entanglement between the involved qubits. So in principle it could be that we only used a quantum framework to describe the thermal machines, but nothing quantum is going on when they do their job.

Regarding this an interesting result was presented in [17]. The authors show that a quantum fridge can outperform a classical one for parameter settings that lead to an efficiency away from the Carnot limit. Furthermore, in the settings where the efficiency of the quantum fridge was higher, more entanglement between the qubits could be observed in the steady state. This strongly suggests a functional relationship between the enhancement of the efficiency and entanglement between the qubits. Even if the existence of such a relation is not proved, the results show that the qubits in the quantum fridge are entangled, which is a quantum feature that a classical refrigerator can never have. For the heat engine a similar statement is likely to be true. In how far entanglement is present in the heat engine must be investigated in further research.

Autonomy What is particularly nice for the models presented is that they are self-contained. This means that, once the Hamiltonians, dissipation processes and initial states are set up and the necessary constraints are met, one can let the system evolve without controlling it anymore, and the system cools, heats or produces work, as desired. Basically this is due to the fact that only time-independent Hamiltonians and dissipators show up. In a potential implementation in trapped ions this means that all one has to do is to turn on the lasers (mimicking the heat baths and driving the energy-conserving interactions) and wait until the machine does its job. We will see later when we deal with work extraction procedures that external control can play an important role in such processes, and that it is not always straight forward to get rid of control without corrupting the efficiency of the process.

Quality of Extracted Work Finally we make a few comments about the notion of work used in the explanation of the heat engine. We regarded work as an excited population of states in an ‘energy ladder’ and mentioned that the spread of the population grows as \sqrt{t} (t the time). However, we argued that the mean energy in the storage system grows as t which is faster than the spread. In a classical engine such as the one presented in Section 1.1 this is not the case. The work one can extract is deterministic, there is nothing like an uncertainty about the actual state in the system that stores the energy (e.g. a weight

attached to the piston that is lifted when the gas expands). Naturally this raises the question whether it possible to produce ‘noise-free’ energy with small quantum thermal machines. As a measure we use the spread $\langle(H_1 - \langle H_1 \rangle)^2\rangle$ in the storage system. But this is just one possible measure. Investigating this question more deeply would require the development of a measure of ordered energy (which we call work here). We refer to [15] for a more detailed discussion on the difference between work and heat in terms of thermal machines and work extraction procedures.

2. Maxwell's Demon and Szilard Engines

In 1871 the Scottish physicist James Clerk Maxwell suggested a creature small enough to see and handle individual molecules that might be exempt from the Second Law of thermodynamics [18]. It might be able to create and sustain differences in temperature without doing any work. In this section we expose the main idea of what this creature, called Maxwell's demon, does and why it kicked off a still ongoing discussion on the relation between information and thermodynamics. Moreover, it led to a new interpretation of Landauer's Principle, which will also be discussed here. After introducing the concepts we move on to processes that use this connection between information and thermodynamics to extract work from (quantum) systems. In this context, we present recently proposed semi-classical and quantum models that use one bit of information to gain $kT \ln 2$ work. The section is concluded with a discussion of advancements and weaknesses of the presented models. Thereby we motivate further research in this direction, which led to the ideas investigated in Part II of this thesis.

2.1. Maxwell's Demon

In his 'Theory of Heat' Maxwell wrote [18]:

"...if we conceive a being whose faculties are so sharpened that he can follow every molecule in its course, such a being, whose attributes are still as essentially finite as our own, would be able to do what is at present impossible to us. For we have seen that the molecules in a vessel full of air at uniform temperature are moving with velocities by no means uniform.... Now let us suppose that such a vessel is divided into two portions, A and B, by a division in which there is a small hole, and that a being, who can see the individual molecules, opens and closes this hole, so as to allow only the swifter molecules to pass from A to B, and only the slower ones to pass from B to A. He will thus, without expenditure of work, raise the temperature of B and lower that of A, in contradiction to the Second Law of thermodynamics."

Numerous versions of Maxwell's demon have been proposed ever since. One of them produces a pressure difference¹ between two halves of a box by letting particles pass from one side to the other (right to left) but not the other way around (see Fig. 9). The demon opens a shutter each time he sees a particle coming from the right, as in Fig. 9 (a). By doing this until all the particles are on the left side, the demon could in principle

¹Rather than a temperature difference, as Maxwell himself proposed.

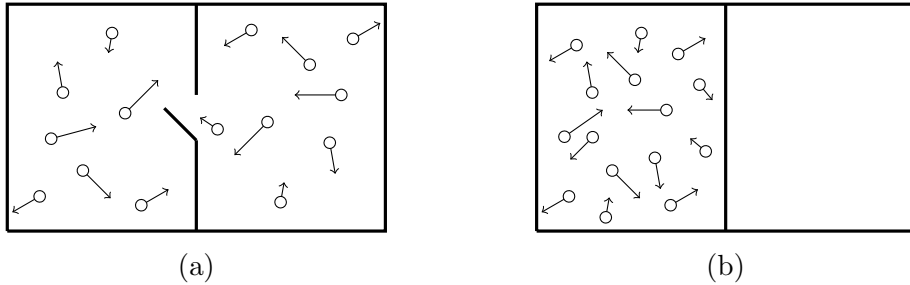


Figure 9.: Functional principle of a modified version of Maxwell’s demon. (a) A box surrounded by a heat bath at temperature T is filled uniformly with a gas. The demon inserts a wall in the middle with a shutter that he can open and close with no net energy cost. He opens the shutter whenever a particle moves through it from the right to the left half of the box. (b) After a while, all particles are in the left half, leading to an increased pressure. This pressure difference from left to right half allows us to extract the work $kT \ln 2$ by letting the gas expand. If a creature exists that is able to do this job, the process can in principle be done in a cycle **1**→**2**→**1**→... where **1**: ‘gather particles on one side’, and **2**: ‘let the gas expand and extract work’.

produce a perfect vacuum on the right side of the wall, as in Fig. 9 (b). Then, one can let the gas expand and extract $kT \ln 2$ work during the expansion process, where k is the Boltzmann constant and T the temperature of the surrounding heat bath. This can now be repeated in a cyclic process that has a net work output under the assumption that the opening and closing of the shutter does not cost work.² Because of energy conservation, the work produced in such a cycle must come from the environment, i.e., from the heat bath surrounding the box of gas. But a cyclic process extracting work from one heat bath without dropping waste heat into another would violate the Second Law of thermodynamics (as stated by Kelvin) and is thus impossible in reality. So where is the flaw?

In 1912 Marian Smoluchowski, an Austro-Polish physicist, tried to model the demon as an independent spring-loaded shutter [20] as shown in Fig. 10. Hence, in this model, there is no demon but just the spring-loaded shutter. Intuitively one could think that this shutter, if the spring constant is properly adjusted, lets particle pass from right to left but not in the other way. Smoluchowski correctly pointed out that such a construction could not be seen as a demon because the shutter being struck by the particles will

²This assumption can be justified by thinking of a shutter attached to a weight. When the demon opens the shutter, he has to invest work to lift the weight. But by closing the shutter again, he can regain this work, which exactly compensates the invested work from before. A more detailed discussion of different versions of Maxwell’s demon can be found in [19].

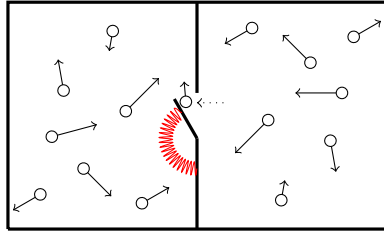


Figure 10.: A spring-loaded shutter mimicking the demon. It lets particles pass from right to left, but not from left to right. In order for particles to push the shutter aside such that they can pass, the spring must be weak. This is, the energy of the compressed spring must be of the order of the kinetic energy of a particle. But the construction does not work as a demon. After a while, the shutter will have a random motion due to thermalization. This happens because of the collisions with the particles. Hence, if we want this shutter to be closed for particles coming from the left, we would have to cool it with a heat bath at very low temperature in order to prevent it from opening randomly.

acquire its own thermal kinetic energy leading to a random motion. This kinetic energy will be of the order of the kinetic energy of one particle because the spring constant must be such that the particles coming from the right can pass in the first place. A random motion of the shutter leads to a higher probability that particles from the left can also pass it to get back to the right half of the box. Moreover, it can happen that a particle about to move from right to left is hit by the shutter such that it gets pushed back into the right half. Smoluchowski showed that in the steady state of such a system there are as many particles on the left as on the right side of the wall [20]. Hence, the spring-loaded shutter is essentially the same as a hole in the wall and does not lead to an imbalance in pressure.

Although a simple mechanical demon cannot work, an intelligent one can. Among others, Smoluchowski came to the conclusion that intelligence was the critical property allowing the demon to operate. In a 1914 paper he writes [21]:

“As far as we know today, there is no automatic permanently effective perpetual-motion machine, in spite of the molecular fluctuations, but such a device might, perhaps, function regularly if it were appropriately operated by intelligent beings.”

2.2. Szilard's Engine

In 1929, Leo Szilard tried to conduct a quantitative analysis of this question [22]. Although the title ‘On the Decrease of Entropy in a Thermodynamic System by the Intervention of Intelligent Beings’ may sound as if an intelligent being could violate the Second Law of thermodynamics, Szilard refuted this notion and argued that no being,

intelligent or not, can do so. He saw the critical point in the measurement process, which, according to Szilard, cannot be done without dissipating work-like energy and therefore causing an entropy increase in the environment. Szilard claimed that this increase of entropy was sufficient to prevent a violation of the Second Law. To support this, he came up with his own version of the demon, the so called *Szilard engine*. A Szilard engine is a box containing one particle. The box is immersed into a heat bath that thermalizes the particle to some temperature T . Szilard proposed the following cyclic process³ (see Fig. 11):

- A:** Insert a partition (the piston), trapping the particle on one side.
- B:** Measure on which side of the wall the particle is.
- C:** Depending on the outcome, attach a weight on the left or on the right side of the piston.
- D:** Let the particle expand isothermally. The particle pushes the piston while lifting the weight.

In the expansion step (**D**) the work $kT \ln 2$ can be extracted, Szilard claimed. Having in mind the classical picture of a many-particle gas, this is justified.⁴ The particle thermalizes when it bounces into the walls, and gives this energy to the piston dragging the weight. Hence, thermal energy is transformed into work, which is the same process as would happen for instance in a car engine, where a pressurized gas expands while driving the engine. Furthermore, he argued that the work needed to insert the partition can be made arbitrarily small. According to Szilard, the crucial step is **B**, where the measurement is done. However, he was vague about how this entropy increase actually takes place. In the following years other physicists, among them Leon Brillouin and Dennis Gabor, modelled the measurement process with a photon gas [23, 24, 25, 26].⁵ They argued that a demon cannot observe the particle without some kind of light source. Therefore every time a measurement is performed the demon must dissipate at least the energy of one photon. This energy must be larger than some threshold determined by the temperature of the environment. They assumed that this energy was lost, and thus turned into heat-like energy, causing an entropy increase in the environment. Although this argument was not completely rigorous, it seemed to provide a good answer to the problem of Maxwell's demon.

As a new field of research on reversibility of computations [19] came up in the 60's, the question of whether a measurement process must have a fundamental work cost was reconsidered. Charles Bennett proposed a slightly modified version of a Szilard engine. In his model, he found a thermodynamically reversible measurement process that allows us to determine the side (left or right) on which the particle is without

³In the original paper [22] he proposes a slightly different setting. However, the functional principle of the engine is the same as the one presented here.

⁴The question of whether this is actually true will be discussed in detail in subsequent sections.

⁵All of these publications are reprinted in [27].

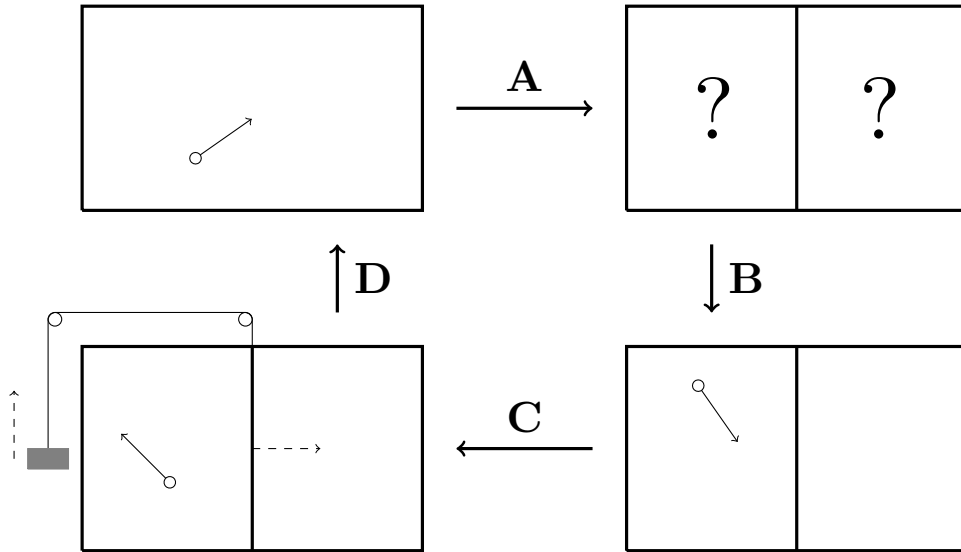


Figure 11.: One cycle of a Szilard engine. **A:** The partition is inserted. **B:** Measurement of the position of the particle, finding the particle, e.g., on the left side of the piston. **C:** Attaching the weight to the piston according to the outcome of the measurement such that the isothermal expansion of the one-particle gas in **D** allows us to lift it.

doing appreciable work [28]. This rules out a fundamental entropy increase during the measurement process and thus also eliminates Brillouin's and Gabor's explanation. So are we back at the beginning of our journey trying to exorcise Maxwell's demon? Not quite.

2.3. Landauer's Principle

Szilard's measurement apparatus included a memory device with three possible states: a blank state, corresponding to no measurement, 'L', saying that the particle has been observed on the left side and 'R', signifying that the particle is on the right side of the partition. During the measurement, the state of the memory changes from blank to 'L' or 'R', depending on the position of the particle. Consequently, after step **D** the memory must be reset to the blank state. If this was not done, the process could not be called cyclic, since the demon would then not have the same state before and after one complete cycle. As Bennett points out in [28] there is one passage in Szilard's 1929 paper [22] where he makes an accounting of entropy changes during the cycle and finds, without explicitly commenting on it, that the increase in entropy takes place during the resetting of the memory. Bennett shows in a paper from 1982 [29] that this is the crucial point in the Szilard cycle. The resetting of the information on the particle's position has a fundamental work cost that accounts for the entropy decrease when measuring the

position of the particle. The theoretical work leading to this perception has been done approximately 20 years earlier, in 1961 by Rolf Landauer [30]. Landauer's Principle states the following:

The work cost of erasure of one bit of information has a fundamental lower bound of $kT \ln 2$.

Erasure is understood as resetting an unknown bit of information to a reference state, e.g. 0. By work we mean any form of ordered energy that we have access to. We have discussed the difficulties of what should be considered as work previously in Section 1.4. In his seminal paper from 1961, Landauer starts with the premise that distinct logical states of a computer must be represented by distinct physical states of the device. To illustrate this he makes two examples. We give the idea of the first example here. It is a bistable potential well as in Fig. 12 (a), where x is a generalized coordinate, e.g. position or magnetic moment. If we know that the system is, e.g., in state 1 and we would like to reset it to state 0, we can apply a generalized force bringing it to the local maximum of the potential well in a controlled way. This costs work. But from there one could in principle let the system equilibrate to the 0 state while regaining the energy spent on bringing x to the local maximum. Hence this process is reversible and has no net work cost. However, the situation changes if we do not know in which state the system initially is. In this case, we must apply a force as well, but due to thermal fluctuations this force must have some minimal strength. If it is weaker, we cannot be sure that the system will end up in state 0. Moreover, we do not know exactly when to apply the retarding force in order to regain the invested energy spent while bringing the system to the local maximum. This means that some of the energy is lost. In a detailed analysis, Landauer shows that in order to bring the system to the reference state 0 from an unknown initial state one has to spend at least $kT \ln 2$ work, if the physical system is in contact with a heat bath at temperature T . In a computer this heat bath is the environment.

Another example, closely related to the Szilard engine, would be a particle in a box (Fig. 12 (b)). The bit of information would be the position of the particle (in the left or in the right half of the box), and erasing would correspond to compressing the one-particle gas by pushing a wall from the right side of the box to the middle, forcing the particle to the left half. Doing so has a work cost of $kT \ln 2$ because one has to push against the particle that thermalizes every time it bounces into the surrounding walls of the box. If it gained energy in the collision with the wall, it will give part of it to the environmental heat bath while thermalizing. Hence, the invested work is transformed into heat.

These are just two example systems that show the behaviour predicted by Landauer's Principle, but it is not a proof of the Principle. Landauer himself argues that, due to the entropy decrease in the memory, there must be an entropy increase in the degrees of freedom of the device that do not encode information in order to fulfil the Second Law

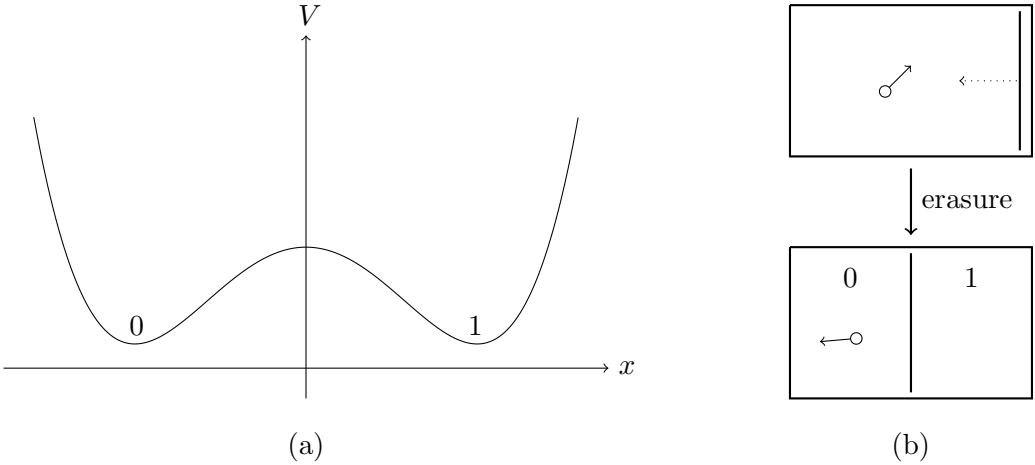


Figure 12.: (a) Bistable potential from Landauer’s example given in [30]. The distinct physical states of the physical system are denoted by 0 and 1. (b) Particle in a box used to store one bit of information. Initially in a state where we have no information about the particle’s position, we bring it to the left half by pushing a movable wall from the right end to the middle of the box. According to Landauer this is an erasure process.

of thermodynamics ($dS \geq 0$). Using this argument, Landauer’s Principle is a logical consequence of the Second Law. However, it has been disputed whether it is necessary to assume the validity of the Second Law in order to derive Landauer’s Principle or, conversely, whether the Second Law itself is actually a consequence of the Principle [31, 32, 33]. In a more recent publication David Reeb and Michael Wolf derive a more general principle which implies Landauer’s Principle from basic quantum mechanical assumptions [34]. Furthermore, a quantitative version of Landauer’s Principle has been proved in a resource theory framework by Philippe Faist *et al.* in [35]. We will not go further into this discussion. Instead we focus on important implications of Landauer’s Principle.

First, we show how exactly Landauer’s Principle can be used to resolve the problem with Maxwell’s demon. As said in the beginning of this section, it is the erasure process that costs at least $kT \ln 2$ work. This is exactly the work one can extract within one cycle of the Szilard engine from Fig. 11. One could now think that there might be a loophole, namely that the demon does not necessarily have to erase at every step but could always use a new memory instead. But this is not the case. As Maxwell himself already mentioned, the demon must be a finite being. This means that it cannot have access to any kind of infinite resource such as an infinitely large memory. If it was possible to access an infinite ‘resource of order’ it would be fairly easy to violate the Second Law and to build a perpetual motion machine of the second kind. But with a finite memory there comes a point when the demon has to erase what it has written in his

memory if it wants to continue the cyclic work extraction process. This is the solution to Maxwell’s demon: even if a measurement can be done without work cost, due to the finite memory of the demon, the net work output must be zero or below.

As a second implication we investigate how Landauer’s Principle affects the way we think about computational processes in a computer. Charles Bennett used Landauer’s result to make a significant statement about the heat generation of any computation. He argued that every irreversible computation is equivalent to a reversible computation followed by erasure [19]. A reversible computation (e.g. a NOT gate: $x \rightarrow \neg x$, where x is an arbitrary input bit) can be done without the dissipation of energy. But, as Bennett showed, irreversible computations must have a fundamental work cost. In the case of a XOR gate this can be well illustrated. A XOR gate takes input bits x and y and outputs the sum modulo 2, i.e., it outputs $x \oplus y$ (see Fig. 13 (a)). Since there are two input bits and only one output bit, this gate must be irreversible. Following Bennett’s idea we can decompose this gate into a reversible XOR gate that takes x and y as inputs and outputs x and $x \oplus y$ followed by the erasure of the bit stored in x . Before the erasure, the gate was reversible because by applying the same gate again one could get back the inputs x and $x \oplus (x \oplus y) = y$. However, after resetting the bit x to a reference state, the total gate becomes irreversible. This erasure has $kT \ln 2$ work cost. Hence, the original XOR gate must have at least this work cost.

Using Bennett’s argument it becomes clear that the heat generation of computers is not only due to imperfections in the computing devices, but also due to a fundamental principle.⁶ This could be circumvented if computers were reversible machines, i.e., if they never had to erase. In 1973, Bennett showed that reversible computers can in principle be built [19]. The idea is to exchange in a first step all irreversible logical gates with their reversible counterparts. Then the computer saves all intermediate results and after reading the output, it retraces the steps of the first stage in backward order, thereby restoring the machine to its original condition.

So far we have shown how to ‘exorcise’ Maxwell’s demon using Landauer’s Principle. Furthermore we mentioned the deeper reason for heat generation in computing devices which is due to the Principle as well. But Szilard’s idea of using the information about the position of a particle in a box as a resource to extract work from a heat bath is still very interesting. In the following we investigate whether this relation between information and thermodynamics can be generalized to other types of information and extraction processes. Special attention will be given to whether something changes if we go to a quantum regime instead of using a classical system.

⁶However, commercial technology is still orders of magnitude away from Landauer’s bound. Hence, the main part of the heat generated in a computing process is due to other factors.

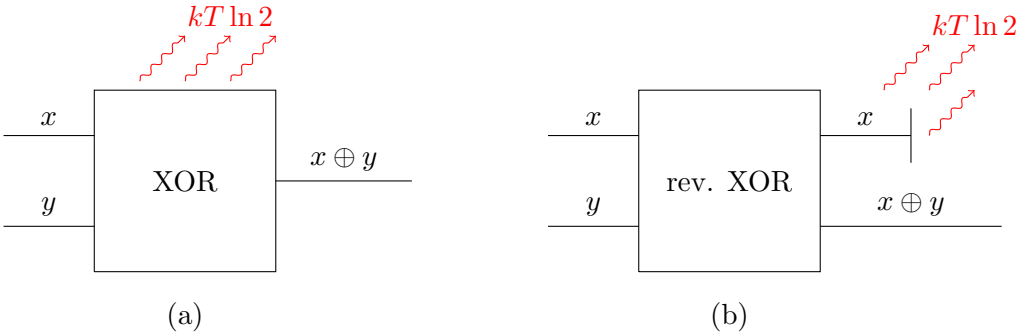


Figure 13.: (a) Irreversible XOR gate. It is clear that this gate is irreversible because there are two input and only one output bits. (b) Reversible XOR gate followed by erasure (vertical line) of the bit x . While in the irreversible case the heat generation happened during the actual gate, here the heat is produced when erasing the bit x .

2.4. Work Extraction Procedures

When Szilard proposed his thought experiment with only one particle driving a piston, he clearly had the classical example of a macroscopic ideal gas in mind. In the classical case, standard thermodynamics tells us that an isothermal expansion of an ideal gas from volume V to $2V$ allows us to extract the work $kT \ln 2$. This example captures a very important feature: throughout the process, the internal energy of the gas does not change. This is because an ideal gas has internal energy $U = \frac{3}{2}NkT$, independently of the volume. Since the process is supposed to happen isothermally, U must stay constant. Hence the work-like energy $kT \ln 2$ extracted during the process must come completely from the heat-like energy provided by the surrounding heat bath at temperature T . With the same argumentation one could see the reverse process as erasure. There we compress an ideal gas from $2V$ to V and have to invest $kT \ln 2$ work to do so (the analogue of Fig. 12 (b) for many particles). This energy will be dissipated into the environment during the process.

We now use this very illustrative example to motivate interest in work extraction procedures. Given the above, we can interpret a work extraction process as the reverse process of erasure. It is therefore interesting to ask whether such a process is actually feasible and how it may be possible to extract the work $kT \ln 2$ from one bit of information in practice. Furthermore, since we would like to have a microscopic process, we have to describe such a process in terms of quantum mechanics rather than classical mechanics and classical thermodynamics. In fact, this must be done already with Szilard's work extraction process because, if one was able to put exactly one particle (i.e. one molecule) in a box, this particle's evolution would clearly be quantum. Part of this has been done in [36] by Sang Wook Kim *et al.* There, the authors compute the work balance of the process suggested by Szilard in a quantum regime. However,

they only look at the initial and final configurations of a quantum Szilard engine and compute the work balance. They do not say anything about the Hamiltonian evolution the system undergoes while extracting the work. Here, we want to focus on the process of work extraction decoupled from the picture of a Szilard engine. Therefore we follow a different line of thought.

In the following we give two examples of processes that (in theory) allow us to extract work from information, a semi-classical and a quantum process. We focus on the assumptions made for the proposed models and explain how the processes extract work. Afterwards we compare and discuss them. Particular attention is paid to experimental feasibility.

2.4.1. Semi-Classical Model by Alicki et al. (2004)

In [37] Alicki *et al.* come up with a model that extracts $kT \ln 2$ work from a pure qubit, i.e., from a qubit that is initially in a pure state. A less general formulation of this model that is still precise, correct, and easier to read can be found in Section 4 of [38]. We call this model semi-classical because work-like energy will not explicitly be stored in a quantum system. The model is such that the initial and the final Hamiltonian of the qubit is the same degenerate Hamiltonian

$$H_{\text{in}} = H_{\text{fin}} = E_0, \quad (2.1)$$

where E_0 is some arbitrary zero-point energy. The initial state of the two level system is pure, and we denote it by $|0\rangle$. The state orthogonal to $|0\rangle$ is denoted by $|1\rangle$. We make the following assumptions:

- (i) The Hamiltonian of the system can be chosen freely by the experimenter. In particular, any time-dependent Hamiltonian $H = H(t)$ can be modelled.
- (ii) Raising or lowering an unpopulated energy level (e.g. $|1\rangle$ in the initial configuration) has no net work cost. This is, work that is invested to raise or lower an unpopulated energy level can be extracted again.
- (iii) Raising or lowering populated energy levels by the energy dE has the work cost or gives the work dE , respectively.
- (iv) Connecting the system to a heat bath at temperature T imposes a Gibbs state on the system. This is, if coupled to the reservoir the state of the system changes to

$$\frac{e^{-\frac{H}{kT}}}{\text{Tr} \left(e^{-\frac{H}{kT}} \right)}, \quad (2.2)$$

where H is the current Hamiltonian of the qubit.

An energy level $|l\rangle$, $l = 0, 1$, is populated with probability q if $\langle l|\rho|l\rangle = q$, where ρ is the state of the system.

A physical two-level system that allows us to shift energy levels is for instance a spin in a magnetic field. To first order, the Hamiltonian of such a system is

$$H = -\boldsymbol{\mu} \cdot \mathbf{B} = g\mu_B B_z \sigma_z, \quad (2.3)$$

where g is the corresponding g -factor, μ_B is the Bohr magneton, σ_z is the Pauli z -matrix in the $|0\rangle$, $|1\rangle$ basis, and we set $\hbar = 1$. For simplicity we chose $\mathbf{B} \parallel \hat{\mathbf{z}}$. In this system it is possible to increase or decrease the energy gap between the energy eigenstates $|0\rangle$ and $|1\rangle$ by tuning the magnetic field B_z . Although one has to put energy into the system to tune the magnetic field, this energy can in principle be extracted again afterwards, when changing the Hamiltonian back to its initial configuration.

The actual thermalization procedure is not specified. The authors give no physical system that has the above thermalization properties. However, knowing that connecting the system to a heat bath thermalizes its state is enough to understand what the model does. Moreover, the assumption that the thermalization works as described above is a reasonable assumption.

We will see now that changing the energy of certain energy eigenstates is all we need to be able to do. The procedure that follows is depicted in Fig. 14. As said before, we start in a pure state $|0\rangle$. In a first step (a) we change the Hamiltonian continuously to

$$H = E_1|1\rangle\langle 1| + E_0|0\rangle\langle 0|, \quad (2.4)$$

while isolating the system. Due to the isolation the state of the system stays $|0\rangle$. Since $|1\rangle$ is unpopulated by definition, this step will not have a net work cost in the end. Thus we arrive at (b). Now we couple the system to a heat bath at temperature T . We then slowly decrease the energy gap between $|0\rangle$ and $|1\rangle$ while thermalizing the system at all times (see (c)) until we reach the degenerate configuration with Hamiltonian $H_{\text{fin}} = H_{\text{in}} = E_0$ again (see (d)). By assumption we extract work when we go from (c) to (d). At energy E the state $|1\rangle$ is populated with probability

$$p = p(E) = \frac{e^{-\frac{E-E_0}{kT}}}{1 + e^{-\frac{E-E_0}{kT}}} = \frac{1}{1 + e^{\frac{E-E_0}{kT}}}, \quad (2.5)$$

according to the Gibbs distribution. Hence, by doing this process very slowly and many times we will on average extract the work

$$\langle W \rangle = \int_{E_0}^{E_1} dE p(E). \quad (2.6)$$

This follows from the assumption that lowering a populated energy level by dE allows us to extract the work dE from the system. Furthermore the final state is fully mixed,

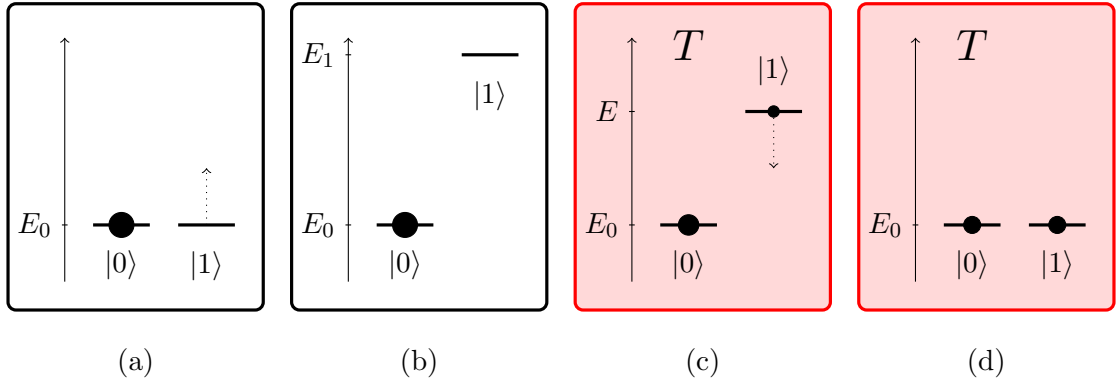


Figure 14.: The four steps in the work extraction procedure proposed in [37]. We work with a two-level quantum system with initially degenerate Hamiltonian. (a) The initial state is pure and denoted by $|0\rangle$. The orthogonal state to this shall be denoted by $|1\rangle$. (b) The energy of state $|1\rangle$ is raised to E_1 without changing the state of the system. This operation has no net work cost by assumption. (c) While coupling the system to a heat bath at temperature T the energy of state $|1\rangle$ is lowered again to E_0 . In this step work can be extracted by assumption (iii) because the lowered state $|1\rangle$ is populated with non-zero probability $p(E) = [1 + \exp(\Delta E/kT)]^{-1}$, where $\Delta E = E - E_0$. (d) Finally, we end up with the initial degenerate Hamiltonian for the system. The thermal state of this configuration is a fully mixed state, which corresponds to having no information about the state of the system.

i.e. the final state of the system is $\frac{1}{2}|0\rangle\langle 0| + \frac{1}{2}|1\rangle\langle 1| = \frac{1}{2}$. This follows from Eq. 2.5 with $E = E_0$. In a work extraction procedure this is what one wants. It is the analogue to a particle in a box if the piston is moved completely to the right wall. In this case, the particle could be anywhere and we have no information about its position. Hence, no subsequent work extraction process could extract work from the qubit in this final state.

Now we focus on Eq. 2.6. The integral can be computed to

$$\begin{aligned}\langle W \rangle &= \int_{E_0}^{E_1} dE p(E) \\ &= \int_0^{E_1 - E_0} dE \frac{e^{-\frac{E}{kT}}}{1 + e^{-\frac{E}{kT}}} \\ &= kT \int_0^{\frac{E_1 - E_0}{kT}} dE \frac{e^{-x}}{1 + e^{-x}} \\ &= kT \int_1^{\exp(-\frac{E_1 - E_0}{kT})} du \frac{1}{1 + u} \\ &= kT \left[\ln 2 - \ln \left(1 + e^{-\frac{E_1 - E_0}{kT}} \right) \right].\end{aligned}\tag{2.7}$$

In particular, for $E_1 \rightarrow \infty$ we are able to extract the work

$$\langle W \rangle \xrightarrow{E_1 \rightarrow \infty} kT \ln 2\tag{2.8}$$

on average. In other words, with this model it is possible to extract an amount of work arbitrarily close to $kT \ln 2$ from a pure qubit that is left in the fully mixed state after the procedure. However, it is important to notice that the maximal amount of work can only be extracted if we accept an infinitely slow process. This is a feature that shows up in other proposals again, as we will see below.

Instead of discussing the assumptions here we postpone the discussion to a subsequent section (Section 2.4.3) and proceed by presenting another model by Skrzypczyk *et al.*

2.4.2. Quantum Model by Skrzypczyk et al. (2013)

As in the model from Alicki *et al.* also here we start with an initially pure qubit $\rho_S = |0\rangle\langle 0|$. Moreover, the qubit is degenerate with Hamiltonian $H_S = 0$. Throughout this section subscript S (as in ‘Szilard’) is used for this qubit. The goal is to find a procedure that extracts $kT \ln 2$ work and leaves qubit S in the fully mixed state.⁷ In the following, we present a simpler version of a model initially brought up in [14]. We refer to this paper for a more general treatment with arbitrary initial states and more general Hamiltonians of qubit S .

First, we consider the assumptions necessary for this model:

⁷The notion of work used in this context has to be defined first. This is done on assumption (ii) below.

- (i) In order to produce work we need a resource. In the model by Alicki *et al.* presented in the previous section this was ensured by assumption (iv), which allowed us to couple the qubit to a thermal bath at temperature T . Here, we assume that we have an unlimited supply of two-dimensional systems (qubits) with any desired Hamiltonian in their thermal state at temperature T . This is, there is an unlimited supply of qubits with arbitrary Hamiltonians H_B in the Gibbs state

$$\tau_B = \frac{e^{-\frac{H_B}{kT}}}{\text{Tr} \left(e^{-\frac{H_B}{kT}} \right)}. \quad (2.9)$$

- (ii) Next we need to define what work is in this context. We introduce an additional system, a work storage system (subscript W), whose purpose is to provide and store work for thermodynamic transformations. This system can be viewed as a suspended weight, which is raised or lowered when work is done on or by it. In particular, we will consider a quantum system whose height is given by the position operator \hat{x} with Hamiltonian $H_W = \hat{x}$. This is in analogy with the classical notion of a weight in the gravitational field, where we set $mg = 1 \text{ J/m}$ for simplicity.⁸ The energy eigenstates of this system are denoted by $|E\rangle_W$, where E stands for the energy (height) of the weight. Hence, the states $|E\rangle_W$ are such that

$$H_W|E\rangle_W = \hat{x}|E\rangle_W = E|E\rangle_W. \quad (2.10)$$

Notice that the notion of work introduced here is the same used for thermal heat engines. Here, as well as there, work is regarded as an excited population in some energy ladder. Back in Section 1.2.2 this ladder was discrete, now it is continuous. The reason why the storage system is chosen to be continuous here is only for simplicity. It makes it easier to talk about bath qubits with energy gaps that are not equal to the energy difference of two energy levels in a discrete storage system.

- (iii) The third ingredient is a set of allowed operations. Before, this was an arbitrary change of the qubit's Hamiltonian. Here, we use a different framework in which the individual Hamiltonians of the subsystems are fixed. Namely, we allow any energy-conserving unitary transformation. This contains in particular any unitary operation that commutes with the total (non-interacting) Hamiltonian of the global system.

Regarding the work storage system, some additional constraints are formulated to ensure that this system cannot be abused as an entropy sink. This is done by requesting that the average amount of work extracted in an allowed protocol must be independent of the initial state of the weight. Furthermore, the system of the weight should have a

⁸It is not necessary to assume that the height of the weight is a continuous degree of freedom. This is shown in Appendix G of [14]. However, we will use the continuous version here. A treatment of a very similar work extraction process with a discrete energy ladder can be found in [13].

translational symmetry. This ensures that only displacements in the weight's height are important and not its absolute height. In this context we introduce translation operators

$$\Gamma_E = \int dE' |E' + E\rangle\langle E'|_W \quad (2.11)$$

that fulfil $\Gamma_E|E'\rangle_W = |E' + E\rangle_W$. Using these additional assumptions we can start in the state $|0\rangle_W$ without loss of generality for any allowed work extraction protocol.

Consider now a global system containing the qubit S , a bath qubit with Hamiltonian $H_B = E_B|1\rangle\langle 1|_B$ in the corresponding thermal state, and the work storage system introduced above (as depicted in Fig. 15). The unitary swap operation

$$U = |01\rangle\langle 10|_{SB} \otimes \Gamma_{-E_B} + |10\rangle\langle 01|_{SB} \otimes \Gamma_{E_B} + (|00\rangle\langle 00|_{SB} + |11\rangle\langle 11|_{SB}) \otimes \mathbb{1}_W \quad (2.12)$$

is then an allowed unitary operation in our framework because it commutes with the global non-interacting Hamiltonian $H = H_S + H_B + H_W = 0 + E_B|1\rangle\langle 1|_B + \hat{x}$. It swaps the states $|0\rangle_S|1\rangle_B|E\rangle_W \longleftrightarrow |1\rangle_S|0\rangle_B|E + E_B\rangle_W$ for all E , whilst leaving all orthogonal states unchanged. Depending on the initial states of the qubits this either raises or lowers the energy stored in W . Due to the initially pure state of qubit S it is possible to make the energy increase in W more probable than the energy decrease. This is basically the only energy-conserving unitary operation we will use in the following.

The basic idea is to apply the unitary introduced in Eq. 2.12 repeatedly to the global system with different thermal qubits of different energy gaps E_B . By using many different thermal qubits it is possible to make only small changes in the states of the thermal qubits and qubit S in each step. This allows us to achieve a higher efficiency. In [39] it was shown that by applying the unitary once one can optimally extract $\approx 0.40 kT \ln 2$ work. But for a higher number of thermal qubits with different energy gaps we can come arbitrarily close to $kT \ln 2$. Therefore, fix an integer $N \gg 1$, and consider N thermal qubits with Hamiltonians

$$H_{B_i} = kT \ln \left(\frac{1 - r_i}{r_i} \right) |1\rangle\langle 1|_{B_i} \quad (2.13)$$

for $i = 1, \dots, N$, such that the thermal state of the i^{th} bath qubit is

$$\tau_{B_i} = (1 - r_i)|0\rangle\langle 0|_{B_i} + r_i|1\rangle\langle 1|_{B_i}, \quad \text{where } r_i = \frac{i}{2N}. \quad (2.14)$$

These bath qubits have excitation probabilities r_i that vary linearly from that of the initial state of the system ($\rho_S = |0\rangle\langle 0|_S$, hence initially zero excitation probability) to $\frac{1}{2}$, which is describing the fully mixed state, in steps of $\frac{1}{2N}$. We now apply, in turn, the sequence of unitary transformations $\{U_i\}_{i=1,\dots,N}$ where U_i acts on qubit S , the work storage system and bath qubit i , and swaps the states

$$|0\rangle_S|1\rangle_{B_i}|E\rangle_W \longleftrightarrow |1\rangle_S|0\rangle_{B_i}|E + E_i\rangle_W, \quad (2.15)$$

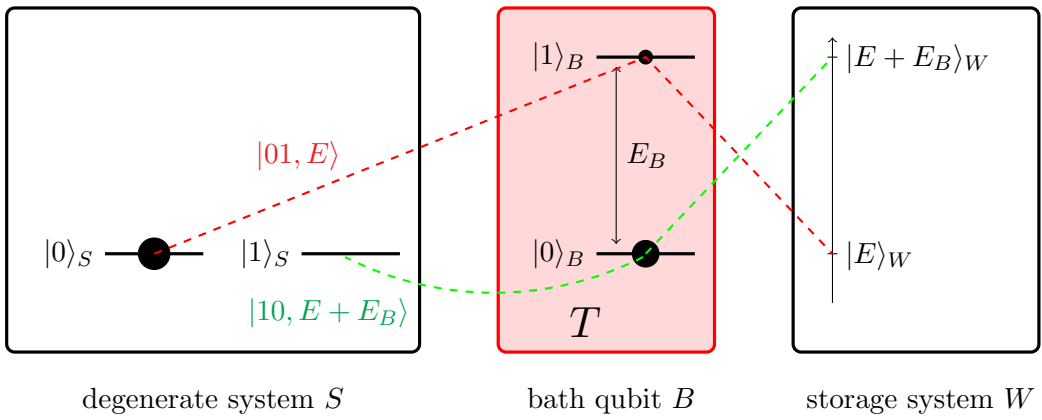


Figure 15.: Configuration of the system with one bath qubit. Qubit S is initially in a pure state, the bath qubit is in the thermal state at temperature T and the continuous storage system is in some arbitrary pure state $|E\rangle_W$, which we will choose to be $|0\rangle_W$ for simplicity. We can do this without loss of generality because of the additional assumptions made for the storage system mentioned above. Only the bath qubit is connected to the thermal reservoir at temperature T . The other two subsystems are perfectly isolated. The unitary U from Eq. 2.12 swaps the state indicated by the red dashed line $|0\rangle_S|1\rangle_B|E\rangle_W$ with the state indicated by the green dashed line $|1\rangle_S|0\rangle_B|E + E_B\rangle_W$.

where the E_i are determined by the Hamiltonians H_{B_i} . The states orthogonal to the states showing up in Eq. 2.15 are left unchanged. Assuming that the weight starts in the state $|0\rangle_W$, it is the final state of the weight that is of interest. We now look at the final average energy $\langle E \rangle_W$ of the weight. As it is shown in Appendix B.2, the final average energy in system W tends to $kT \ln 2$ for $N \rightarrow \infty$:

$$\langle E \rangle_W \xrightarrow{N \rightarrow \infty} kT \ln 2. \quad (2.16)$$

Accordingly, the final state of qubit S is the fully mixed state $\frac{\mathbb{I}_S}{2}$.

Altogether, this model does the same as Alicki's model: it uses a pure qubit that will be returned in the fully mixed state to extract $kT \ln 2$ work from a heat bath. However, the setting is very different. In particular, the notion of work is a different one.

Before we discuss the similarities and differences of the two models in detail we give an example of a potential platform of implementation. As Bettina Meyer showed in [40], ion traps as they exist today are in principle capable of implementing one step of this protocol. This is, it is possible to implement one unitary transformation U as in Eq. 2.12. In this work, she decomposed the unitary U into six unitary operations that can be executed in ion traps. The Szilard qubit and the bath qubit were encoded in internal degrees of two different ions and the storage system was encoded in the normal mode of the motional degree of freedom of the ions. State preparation could be achieved by optical pumping (for internal degrees of freedom) and sympathetic cooling (for motional degrees of freedom). In this case, the storage system was discrete because the relative motion of two ions in an ion trap is to very good approximation described by a quantum harmonic oscillator. Since only one step of the protocol is executed, this is not a problem. One may wonder whether it is possible to mimic a degenerate qubit in an ion trap. Indeed, it is not so easy to do so.⁹ Fortunately, as Skrzypczyk *et al.* show, the protocol also works with almost as high efficiency if qubit S is not fully degenerate, but has a small energy gap E_S .

The proof of principle that one step of this protocol can be implemented in an ion trap suggests that, if it becomes possible to trap many ions at the same time, an implementation of the protocol with N bath qubits is not far away.

2.4.3. Discussion

In this section we discuss the two models presented in the previous sections. We start by analyzing and comparing the assumptions. In the following we refer to the model by Alicki *et al.* as the *shifting model* and to the model by Skrzypczyk *et al.* as the *unitary model*.

⁹In [40], Bettina Meyer discusses the possibility of using the X -basis of a non-degenerate qubit as a degenerate computational basis.

Time Evolution and Operations The assumption of the shifting model that any time-dependent Hamiltonian can be modelled, is similar to the assumption from the unitary model that any energy-conserving unitary transformation can be applied. It seems to be necessary to make an assumption that allows us to perform a rather large class of operations on the system in order to be able to extract the optimal amount of work. However, the assumption made for the unitary model is closer to current technology standards. In ion traps it is possible to simulate a large class of unitary transformations on internal and motional degrees of freedom of ions [41].¹⁰ In contrast to this, the opportunities of manipulating Hamiltonians of individual quantum particles are limited. The example we gave for the shifting model with a spin in a magnetic field already suggests this. It is very difficult to produce strong magnetic fields. Hence, in practice there are limitations on how large the maximal energy gap of the two qubit states can become. However, this limits not only the efficiency of the shifting model, but also the one of the unitary model. There as well, the optimal amount of work can only be extracted if we have access to qubits with arbitrarily large energy gaps.

Connection to the Heat Bath Both models assume access to a heat bath at temperature T . In the shifting model it is in addition assumed that one can turn on and off the interaction of our system with the heat bath arbitrarily, whereas the unitary model does not assume this. However, it is compensated in the unitary model by assuming an infinite supply of thermalized qubits with arbitrary Hamiltonians.

Notion of Work The notion of work used in the shifting model is rather abstract, whereas in the unitary model it seems to be clear what work is. It is left open what one should understand by the second and third assumption of the shifting model: they state that we can raise unpopulated energy levels arbitrarily without a net work cost and that we can extract work by lowering a populated energy level. The example of the spin in a magnetic field might give an idea of a physical model that could have these properties. But if macroscopic magnetic fields are needed to model work, the work extraction procedure is no longer small in the sense that only systems with few degrees of freedom are involved.

The notion of work used in the unitary model was discussed already in Section 1.4. Although the energy ladder was discrete there, the main properties are the same. Furthermore, as Skrzypczyk *et al.* show, their protocol also works with a discrete energy ladder. An example has been given by a quantum harmonic oscillator. A potential platform of implementation would then be the normal motional mode of two ions in a trap.

In both models the work output is not deterministic. This means, that there are fluctuations in the energy that the systems outputs as work. We did not treat this feature of the models in detail because we considered only the mean work output. However, if

¹⁰In fact, trapped ion technology is in principle capable of doing universal quantum computation.

these fluctuations are of the order of the energy output, then the energy can no longer be considered to be work. In this case, it would be heat-like energy, because it is unordered in the sense that one can not predict what the (approximate) output is going to be in a single run of the protocol.

Autonomy Another point of interest is external control. In the picture of discrete unitary steps it is clear that very precise external control must be available. In order to apply a unitary transformation one needs to be able to turn on and off interactions and change Hamiltonians at precise time intervals with very high accuracy. In the shifting model precise external control is also needed. The change of Hamiltonians as requested in the shifting model needs to be executed slowly and in a controlled way in order to maintain the validity of the formulas derived. Hence, at least in the unitary model, it might be necessary to add an external clock to the assumptions in order to be consistent with the resource framework the models use.

The problem with external control is not that it is impossible to control quantum systems with high accuracy. Significant progress has been made in this regard [41, 42, 43]. For instance, current ion traps are in principle capable of executing one step of the unitary model [40]. The problem is that in the spirit of the Szilard engine, we would like to be able to say that all one has to put in the system is one bit of information (quantum or classical) and this allows us to extract the work $kT \ln 2$. External control can be viewed as additional information and thus a self-contained work extraction procedure should not make use of it. The models cannot rule out that additional information, and hence free energy, is needed in order to extract the optimal amount of work. In this sense, they are not autonomous.

One may argue that the problem of external control vanishes in the limit of large systems. When doing the same procedure with many input bits at the same time, the additional information per input bit that is needed vanishes. The idea behind that is to parallelize the change of the Hamiltonians or the unitary steps, respectively. Although this is true, it is not a satisfactory answer. It solves the problem of external control if one has many pure qubits in the beginning, but one important point of both models is that they also work when only one pure qubit is accessible (i.e. in the case of small systems). This feature would be lost if additional information is needed to perform the work extraction process.

Quasi-Static Processes A feature both models have in common is the time they take to be executed. In the shifting model, an optimal work extraction requires an infinitely high energy gap in Fig. 14 (b): $E_1 \rightarrow \infty$. Hence, also an infinite amount of time because the change of the energy gap is supposed to happen smoothly. Something similar happens in the unitary model, where the maximal amount of work can be extracted only for infinitely many steps. Clearly this would require an infinitely long running time as well. The fact that optimal work extraction processes are slow already showed up in the classical example of a macroscopic gas. The expansion of the gas must happen quasi-

static such that it is always in thermal equilibrium with the environment at temperature T . If this is not the case, the process is no longer isothermal and the extractable work decreases. From what we saw so far it seems that any optimal process extracting work has this feature.

Quantum Effects Finally we address the question how quantum the models are. An important feature that can give an insight to this question is how the models deal with coherent states. What happens if the input state is a superposition, e.g. $\frac{1}{\sqrt{2}}(|0\rangle + |1\rangle)$? We argue that in both models, as they are presented here, this question is circumvented. In the shifting model we only assumed that the initial state is pure. Since we are free to choose the Hamiltonian of the system, we can choose it such that the states $\{|\bar{0}\rangle = \frac{1}{\sqrt{2}}(|0\rangle + |1\rangle), |\bar{1}\rangle = \frac{1}{\sqrt{2}}(|0\rangle - |1\rangle)\}$ are the orthogonal energy eigenstates. In doing so we do not have to deal with coherent states anymore since we just redefined the states we are referring to as the computational basis.

In the unitary model the reasoning is similar. By assumption, the qubit containing the information is degenerate and we can perform any energy-conserving unitary. Hence, if we are given a qubit in the state $\alpha|0\rangle + \beta|1\rangle$ we can rotate it to the state $|0\rangle$. This is certainly a unitary transformation, and since the qubit is degenerate, it is also energy-conserving. This way, the question what happens with coherent superpositions need not be answered. However, if the qubit is not exactly degenerate, but has a small energy gap E_S , this is not allowed anymore, because the unitary transformation would no longer be energy-conserving. In the case of non-degenerate quantum systems, the protocol proposed by Skrzypczyk *et al.* can only extract the optimal work from diagonal states in the energy eigenbasis. In [14], the authors show that for non-classical states, where coherences between energy levels exist, collective actions are necessary as long as no external sources of coherence are present. Thus, the model loses its feature of being able to extract the optimal amount of work from only one copy of a quantum system if confronted with non-degenerate coherent states.

Hence, in this regard, both models are classical. They either circumvent the problem of work extraction from coherent states or are not able to give a satisfactory answer. However, as Johan Åberg shows in [13], a source of coherence is enough to achieve optimality again also for single copies of quantum systems in the framework of the unitary model. Furthermore, this resource of coherence is not diminished by using it. In this sense, coherence is a catalyst.

In this section, we started with a classical example of a Szilard like process involving a macroscopic ideal gas. We went on to two models that involve a quantum formalism and use pure qubits with degenerate Hamiltonian as an information resource. Under the assumptions made for each model, both processes turned out to extract the maximal amount of work from a pure qubit, namely $kT \ln 2$. However, it is debatable in how far the models can be regarded as quantum models. Both cannot deal with coherence in the energy eigenbasis in a satisfactory way. The shifting model because it circumvents

this problem, the unitary model because it loses its capability of extracting the optimal amount of work when dealing only with single copies of the information resource.

Part II.

A Semi-Quantum Model of a Szilard Engine

The second part of this thesis is concerned with the question whether the work extraction step in Szilard's protocol does indeed allow to extract $kT \ln 2$ work. Therefore we try to describe how a more physical version of a Szilard engine could look like. In the following, the term 'Szilard engine' is used only for the work extraction step in Szilard's protocol presented in Section 2.2.

We try to model Szilard's idea of one particle in contact with a thermal bath and interacting with a piston quantum mechanically. The idea is simple: We consider a box of length L that is surrounded by a heat bath at temperature T and contains a particle and a piston. Both particle and piston are modelled as particles with masses m and M , respectively, where $M \gg m$. These particles interact repulsively. Furthermore, the piston feels a *weight* potential V_{weight} . This potential can be e.g. a linear potential in the piston's position, in analogy to the classical Szilard engine, where a weight is attached to the piston that models work. Also in our model, work is regarded as potential energy of the piston with respect to the weight potential. This concept of work that is linked to the elevation of a weight was already encountered in the small heat engine. We then let the piston start in the middle of the box and the particle in the left half and simulate the evolution of the system. The question is whether the model yields a work gain. The information in this work extraction process is the particle's initial position. If we do not know whether it is in the right or in the left half, we cannot extract the work because we would not know what weight potential we should apply.¹¹ In the following, we always assume that we know that the particle is initially in the left half of the box. This corresponds to one bit of information that will be lost after an optimal work extraction process, because then the particle can be anywhere in the box.

After an introduction with general remarks to the work extraction of a classical Szilard engine and the optimality of such a process (Section 3), we recapitulate a classical analysis done by Johan Åberg [44]. In the following section we have a look at the free energy of a quantum particle in a box of a certain length and compare it with the free energy of such a particle in a box with double size (Section 5). In Section 6 we have a closer look at a system containing a quantum particle and a quantum piston. Since the Schrödinger equation of such a system is too difficult to solve analytically, we make use of the Born-Oppenheimer approximation. This is an approximation from molecular physics used to describe electrons and a much heavier nucleus quantum mechanically without solving the total Schrödinger equation. We do this analysis for different weight potentials that the piston feels and compute the wave functions of the piston in the ground state and the first excited states. This analysis is static, in the sense that we only solve the time-independent Schrödinger equation, but do not talk about thermalization processes or time evolution of the interacting systems. The latter questions are addressed in Section 7, where we introduce a semi-classical model to find out whether our idea of a quantum particle interacting with a piston and a thermal bath really has the properties we would expect from a Szilard engine. We do simulations of the semi-classical model of

¹¹We would not know whether the weight potential should increase to the left or to the right.

the system and analyze the mean energy gain with different parameter settings. Finally, some concerns about the approximations used in the semi-classical model are expressed. The thesis is completed with a short discussion of the results.

3. The Weight Potential

Consider the classical Szilard engine with a weight attached to the piston (as in Fig. 16). Let L be the length of the box, m_W the mass that is attached to the piston, and T the temperature of the surrounding heat bath. At first sight it may seem that the mass of the weight is a parameter of the model that we can chose freely. But since we would like to extract the work $kT \ln 2$ of the system (k again the Boltzmann constant) which is in this case equivalent to raising the weight by the height $\frac{L}{2}$, we must choose the mass such that

$$gm_W \frac{L}{2} = kT \ln 2, \quad (3.1)$$

where g is the gravitational constant. What we learn form this is that the parameters of any model that tries to describe a Szilard engine must be chosen such that the extracted work can fulfil Eq. 3.1. In the more general case of a piston that feels a weight potential V_{weight} , the equation will be

$$V_{\text{weight}}(L) - V_{\text{weight}}(L/2) = kT \ln 2. \quad (3.2)$$

Another question is the shape of the potential. In Fig. 16 the potential is linear. But we could as well think of a spring instead of a mass in the gravitational field attached to the piston (see Fig. 17 (b)). So the shape of the potential is something we should be able to choose (almost) freely.

Nevertheless, if we want an optimal Szilard engine in the sense of maximal extracted work, the force of the weight potential should equal the force the particle exerts on the

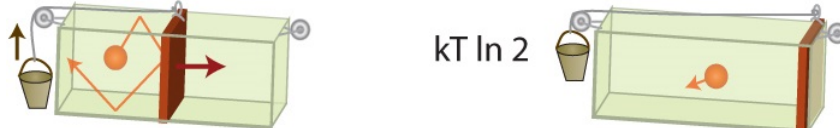


Figure 16.: A classical Szilard engine: A particle in a box interacting with a heat bath and a piston. A weight is attached to the piston such that it has more potential energy if the piston is more to the right. L is the total length of the box, T the temperature of the surrounding heat bath, and m_W the mass of the weight attached to the piston.

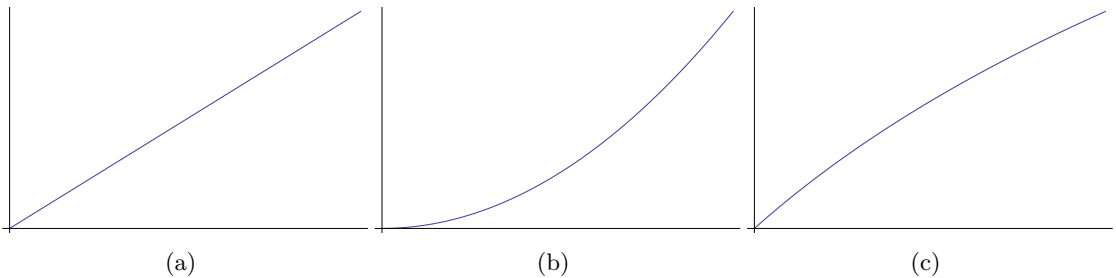


Figure 17.: Different shapes of weight potentials that the piston could feel. Not all of them have a straight forward physical example. (a) Linear potential, e.g., mass in gravitational field. (b) Quadratic potential, e.g., spring. (c) A logarithmic potential. This would be the natural choice if we think of an ideal gas because there the pressure is inversely proportional to the current volume of the gas, and hence also to the current position of the piston, leading to an integrated potential of logarithmic form.

piston in the interaction. Only then, the ‘expansion’ of the one-particle gas is quasi-static and we can hope for an optimal work extraction.¹

Fig. 17 shows a linear, a quadratic and a logarithmic potential. The logarithmic potential can be motivated by thinking of a macroscopic Szilard engine: an ideal gas pushing a piston. The pressure that the piston feels from the gas is inversely proportional to the volume of the gas.² Hence, if the gas pushed the piston already towards L , its pressure is decreased. This leads to a force proportional to $1/X$. Integrating this force yields a logarithmic potential. Therefore, we should use this potential for our simulations later on.

¹Notice that the feature that any optimal process seems to be quasi-static has been observed in the previous section already.

²For an ideal gas: $pV = nRT$. Hence, in an isothermal process: $p \propto V^{-1}$. The force that the piston feels from the gas is proportional to the pressure of the gas.

4. Classical Statistical Analysis

4.1. Single Particle and Piston

Consider two particles with masses m and M and position degree of freedom x and X . Let p and P be the corresponding conjugate momenta. In the following we want to understand how a system consisting of these particles behaves when it is confined to a one-dimensional box of length L and is thermalized at a temperature T . Therefore we postulate a classical Hamiltonian of the form

$$H(x, X, p, P) = \frac{p^2}{2m} + \frac{P^2}{2M} + V(x, X), \quad (4.1)$$

where V is some potential modelling a repulsive interaction between the particles as well as the boundaries given by the box of length L . Furthermore, V will also contain the weight potential term that the piston (the heavier of the particles) feels:

$$V(x, X) = V_{\text{int}}(x, X) + V_{\text{box}}(x, X) + V_{\text{weight}}(X). \quad (4.2)$$

The analysis done here is taken from [44].

We now study what happens when the whole system is thermalized using the canonical ensemble. The probability density of the canonical ensemble is

$$f_\beta(x, X, p, P) = \frac{e^{\beta H(x, X, p, P)}}{\mathcal{Z}(\beta)}, \quad (4.3)$$

where $\beta = \frac{1}{kT}$ the inverse temperature and $\mathcal{Z}(\beta)$ the partition function,

$$\mathcal{Z}(\beta) = \int dx \int dX \int dp \int dP e^{-\beta H(x, X, p, P)}. \quad (4.4)$$

The detailed calculations for the following results are carried out in Appendix C.1. It turns out that the partition functions for the two momentum degrees of freedom and the positions degrees of freedom separate.¹ Hence, we can look at the marginal distributions of the momenta independently. The momenta are normal distributed with standard deviation

$$\sigma_p = \sqrt{\frac{m}{\beta}} \quad \text{and} \quad \sigma_P = \sqrt{\frac{M}{\beta}}. \quad (4.5)$$

¹This is always the case when the Hamiltonian splits up in a sum: $H(x, p) = H(x) + H(p)$.

Increasing temperature or mass broaden these distributions. In terms of velocities $v = p/m$ and $V = P/M$ the standard deviations are

$$\sigma_v = \sqrt{\frac{1}{\beta m}} \quad \text{and} \quad \sigma_V = \sqrt{\frac{1}{\beta M}}, \quad (4.6)$$

respectively. The larger the masses, the narrower the velocity distribution will become. For increasing temperature we can still observe a broadening in the velocity distribution. This will be useful later on, when we consider classical and quantum simulations of different models of a Szilard engine.

For the rest of this section we will be interested in the probability distribution in position space. Consider the potential

$$V(x, X) = \begin{cases} \alpha X & \text{if } 0 < x \leq X \leq L, \\ +\infty & \text{otherwise.} \end{cases} \quad (4.7)$$

The potential is a box potential for the piston that is infinitely high outside the interval $[0, L]$. The piston feels a linear weight potential of strength α . Here, α is a parameter replacing m_W from the previous section. It determines the strength of the force that the piston drags to the left. The particle also feels a box potential. However, the walls of the box are determined by 0 and X , the varying position of the piston. Hence, the particle is always on the left side of the piston. Also here, the box walls are infinitely high. This X -dependent box potential for the particle mimics a repulsive interaction between particle and piston. With this potential, the partition function becomes

$$\mathcal{Z}_{\text{pos}}(\beta) = \int_0^L dX X e^{-\beta \alpha X} \quad (4.8)$$

and hence the marginal distribution of the piston is

$$f_\beta(X) = \frac{X e^{-\beta \alpha X}}{\int_0^L dX X e^{-\beta \alpha X}} = \frac{\tilde{X} e^{-c \tilde{X}}}{\int_0^1 d\tilde{X} \tilde{X} e^{-c \tilde{X}}}, \quad \text{for } 0 \leq \tilde{X} = \frac{X}{L} \leq 1, \quad (4.9)$$

where we introduced the normalized position $\tilde{X} = X/L$ and the dimensionless parameter

$$c = \beta \alpha L = \frac{\alpha L}{kT}. \quad (4.10)$$

Using the *lower incomplete gamma function* $\gamma(s, r) = \int_0^r dt t^{s-1} e^{-t}$, the marginal probability density can be written as

$$f_\beta(\tilde{X}) = \frac{c^2}{\gamma(2, c)} \tilde{X} e^{-c \tilde{X}}, \quad (4.11)$$

where we used

$$\int_0^1 d\tilde{X} \tilde{X} e^{-c \tilde{X}} \stackrel{[y=c\tilde{X}]}{=} \frac{1}{c^2} \int_0^c dy y e^{-y} = \frac{\gamma(2, c)}{c^2}. \quad (4.12)$$

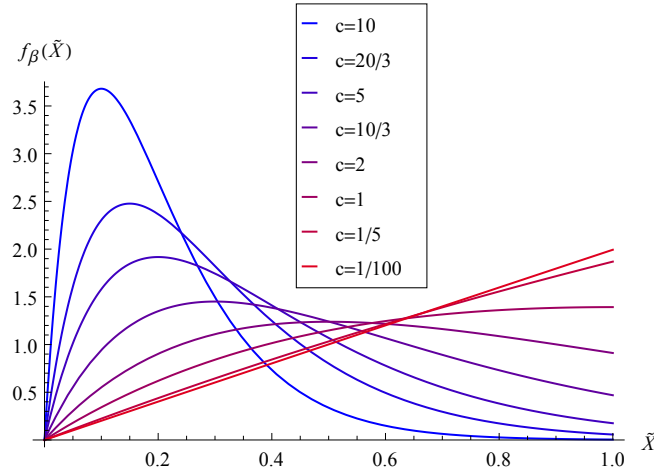


Figure 18.: Probability density from Eq. 4.11 of the normalized position of the piston \tilde{X} for a single particle and representative values of c . The more red a curve is, the higher is the temperature and the smaller is c . The decrease of c corresponds to an increase of temperature relative to the maximal potential energy. Only for very small c the piston has higher probability to be close to the right wall. But not even then it is localized.

Fig. 18 shows a plot of the marginal probability distribution for representative values of c . We see that that only for very small values of c the probability to find the piston close to the right wall increases. But even for $c \approx 0$ the piston is not localized to a small region close to the right wall. In this case, $e^{-c\tilde{X}} \approx 1$ on the interval $[0, 1]$ and thus $f_\beta(\tilde{X}) \approx 2\tilde{X}$. This case corresponds to small α , i.e. a weak force dragging the piston to the left, or to a very high temperature T .

4.2. Many Particles and Piston

Consider now N non-interacting particles of mass m and a piston of mass M described by the Hamiltonian

$$H(x_1, \dots, x_N, X, p_1, \dots, p_N, P) = \sum_{i=1}^N \frac{p_i^2}{2m} + \frac{P^2}{2M} + V(x_1, \dots, x_N, X). \quad (4.13)$$

Suppose the position coordinates are confined to $x_1, \dots, x_N, X \in [0, \infty)$ and the potential is given by

$$V(x_1, \dots, x_N, X) = \begin{cases} \alpha X & \text{if } \max(x_1, \dots, x_N) \leq X \leq L, \\ +\infty & \text{otherwise.} \end{cases} \quad (4.14)$$

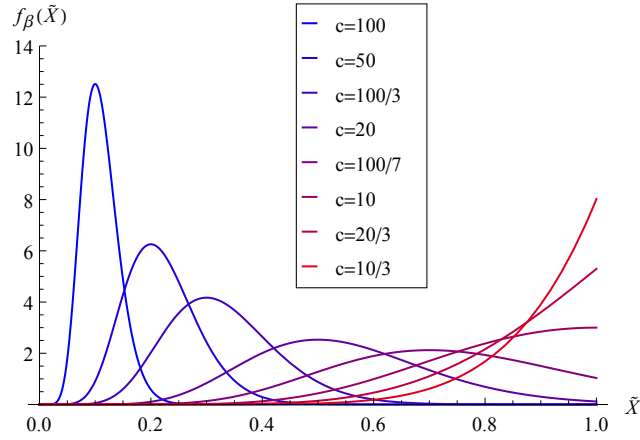


Figure 19.: Probability density from Eq. 4.15 of the normalized position of the piston \tilde{X} for $N = 10$ particles and representative values of c . The more red a curve is, the higher is the temperature and the smaller is c . The decrease of c corresponds to an increase of temperature relative to the maximal potential energy. Again, only for very small c the piston has higher probability to be close to the right wall.

This potential is analogous the the potential in Eq. 4.7 above. The only difference is that now N particles interact with the piston instead of one. Again, the exact calculations are done in Appendix C.1. Using again the normalized position $\tilde{X} = X/L$ and the lower incomplete gamma function, the marginal distribution of the piston can be expressed as

$$f_\beta(\tilde{X}) = \frac{c^{N+1}}{\gamma(N+1, c)} \tilde{X}^N e^{-c\tilde{X}}. \quad (4.15)$$

For $c \approx 0$, i.e. for high temperature (compared to the maximal potential energy of the piston) we find $f_\beta(\tilde{X}) \approx (N+1)\tilde{X}^N$. Fig. 19 shows the marginal distribution of the piston's normalized position for $N = 10$ particles and representative values of c . Again we can observe that only for very small c , i.e. only for high temperature or low strengths of the potential, the piston is localized around $X = L$. However, compared to the one-particle case the piston distribution is more localized.

The distributions of momenta still follow a normal distribution with the standard deviations from above.

4.3. Many Particles and Piston without Upper Bound

So far we have investigated the behaviour of one or many particles and a piston in a box of length L . Here, we consider an open box. This is, the piston's position is no longer upper bounded by L . There is still an (infinitely high) wall at $X = 0$. For the

position coordinates $x_1, \dots, x_N, X \in [0, \infty)$ of N particles and the piston the potential then changes to

$$V(x_1, \dots, x_N, X) = \begin{cases} \alpha X & \text{if } \max(x_1, \dots, x_N) \leq X, \\ +\infty & \text{otherwise.} \end{cases} \quad (4.16)$$

In Appendix C.1 we show that the position part of the partition function is then

$$\mathcal{Z}_{\text{pos}}(\beta) = \frac{N!}{(\beta\alpha)^{N+1}}. \quad (4.17)$$

The marginal distribution of the piston's position is described by the *gamma distribution* $g(x; l, \theta) = \frac{x^{l-1} e^{-x/\theta}}{\theta^l \Gamma(l)}$, where in our case $\theta = \frac{1}{\beta\alpha}$ and $l = N + 1$:

$$f_\beta(X) = \frac{(\beta\alpha)^{N+1}}{N!} X^N e^{-\beta\alpha X}. \quad (4.18)$$

The scale parameter $\frac{1}{\beta\alpha} = \frac{kT}{\alpha}$ has unit of length and it stands for the distance by which the average thermal energy kT can lift the position of the piston against the force α . Since we deal with a gamma distribution we can use existing formulas to compute the mean position and standard deviation of the position of the piston [45]

$$\begin{aligned} \langle X \rangle &= l\theta = (N + 1) \frac{kT}{\alpha}, \\ \sqrt{\langle (X - \langle X \rangle)^2 \rangle} &= \sqrt{l\theta^2} = \sqrt{N + 1} \frac{kT}{\alpha}. \end{aligned} \quad (4.19)$$

Thus, taking the standard deviation divided by the mean position as a measure of relative fluctuations,

$$\frac{\sqrt{\langle (X - \langle X \rangle)^2 \rangle}}{\langle X \rangle} = \frac{1}{\sqrt{N + 1}}, \quad (4.20)$$

we see the ‘typical’ $\frac{1}{\sqrt{N}}$ suppression of fluctuations in the limit of infinitely many particles. Moreover, the more particles interact with the piston, the more its mean position moves to higher potential energies. Interestingly, the relation between N and $\langle X \rangle$ is linear, as is the relation between T and $\langle X \rangle$.

However, in the one-particle case the fluctuations are of the order of the mean energy gain. Hence, the piston's potential energy is in this sense unordered, i.e. unpredictable, energy and can therefore not be regarded as work. A very similar problem of the notion of work was discussed in the discussion of Section 1 on heat engines, where we also had the problem that the spread in the work storage system could be too large. We refer to Section 1 for a more detailed discussion.

4.4. Conclusion

The parameter c quantifies how large the maximal potential energy is compared to the typical thermal energy in the system. Taking Eq. 3.2 into account, c would be determined by $2 \ln 2 \approx 1.38$. For this value of c the piston's distribution is almost flat for the one-particle Szilard engine. However, this is not exactly the regime of a Szilard engine where the initial configuration of the piston is in the middle of the box of length L . In a Szilard engine the piston is not thermalized immediately but only through the interaction with the particle and, maybe (depending on the model), when it hits the right wall. Here, both particle and piston are thermalized, and no evolution is simulated.

The above results state that in the case where particle and piston are thermalized there is not much hope for the one-particle Szilard engine. Only for many particles the distribution of the piston's position starts to become localized close to the right wall. However, the model is not necessarily a good indicator of whether a one-particle Szilard engine can work or not. For instance, the probability distributions for the positions are insensitive to the masses m and M of the involved bodies. This is counterintuitive. One may think that a smaller particle mass should lead to more but less intensive collisions between particle and piston. Hence, the piston's behaviour is affected by the particle mass. Since the model is static, it does not take this into account. Therefore, we should look for a different model, preferably accounting for the quantum nature of a system containing only few particles.

5. Piston as a Parameter

In this section we conduct a semi-quantum static analysis of a single particle and a piston. We call it semi-quantum because the piston acts via a classical potential on a quantum particle. More precisely, the particle is in a one-dimensional box with walls at 0 and X , where X is again the position of the piston, which is now a parameter. The particle is described by the position and conjugate momentum (x, p) .¹ The resulting potential for the particle is given by

$$v_X(x) = \begin{cases} 0 & \text{if } 0 < x < X, \\ +\infty & \text{otherwise,} \end{cases} \quad (5.1)$$

for $0 \leq X$. This corresponds to a box potential that the particle feels as encountered in Section 4. The walls of the box are at 0 (fix) and X , the variable position of the piston. The Hamiltonian describing the evolution of the particle is hence

$$h(X) = \frac{p^2}{2m} + v_X(x). \quad (5.2)$$

In the following, we calculate the free energy of such a particle depending on the piston's position. Since we only treat the particle as a physical body and use the piston as a parameter the thermalization at temperature T acts only on the particle in this model. This is in contrast to the classical model from the last section, where both the particle and the piston were thermalized. We proceed as follows:

1. Calculate eigenstates and eigenenergies of $h(X)$.
2. Calculate the partition sum $\mathcal{Z}(h(X))$ and the free energy $F(h(X)) = -kT \ln \mathcal{Z}(h(X))$ using the piston's position as a parameter.
3. Compare $F(h(X = L/2))$ and $F(h(X = L))$, i.e., what is the difference in the free energy of the particle if the piston is in the middle or at the right end of a box of length L ?

In general, the partition sum of such a system is given by

$$\mathcal{Z}(h) = \text{Tr} \left(e^{-\beta h} \right), \quad \text{with } \beta = \frac{1}{kT}. \quad (5.3)$$

¹For the rest of the thesis we will use the same letters for parameters of particle and piston, where the majuscule stands for the corresponding parameter of the piston and the lowercase stands for the corresponding parameter of the particle.

The idea behind this approach is to find out whether the free energy of a particle in a box does behave as Szilard argued. If Szilard's argument is correct, the free energy of particle in a box of length $L/2$ should be larger by $kT \ln 2$ compared to the free energy of a particle in a box of length L . It will be discussed in Section 5.2 under which conditions this is actually the case.

5.1. Calculations

The time-independent Schrödinger equation reads

$$e\psi(x) = -\frac{\hbar^2}{2m}\psi''(x) \quad \text{for } x \in [0, X]. \quad (5.4)$$

With the plane wave ansatz $\psi(x) = Ae^{ikx}$ this leads to the energy $e = \frac{\hbar^2 k^2}{2m}$. Together with the boundary conditions $\psi(0) = 0 = \psi(X)$ one arrives at the following orthonormal system of eigenfunctions with eigenenergies:

$$\begin{aligned} \text{For } n = 1, 2, \dots \text{ we have eigenstates } \psi_n(x) &= \sqrt{\frac{2}{X}} \sin\left(\frac{\pi n x}{X}\right) \\ \text{with eigenenergies } e_n &= \frac{\hbar^2 \pi^2}{2mX^2} n^2. \end{aligned} \quad (5.5)$$

Now we can write the Hamiltonian in terms of the energy eigenstates $|\psi_n\rangle$ as $h = \sum_{n=1}^{\infty} e_n |\psi_n\rangle \langle \psi_n|$.² This allows to compute

$$\mathcal{Z}(h(X)) = \text{Tr}\left(e^{-\beta h(X)}\right) = \sum_{n=1}^{\infty} e^{-\beta e_n(X)} = \sum_{n=1}^{\infty} \exp\left[-\beta \frac{\hbar^2 \pi^2}{2mX^2} n^2\right] \quad (5.6)$$

and

$$F(h(X)) = -kT \ln \mathcal{Z}(h(X)) = -kT \ln \left(\sum_{n=1}^{\infty} \exp\left[-\beta \frac{\hbar^2 \pi^2}{2mX^2} n^2\right] \right). \quad (5.7)$$

For readability we introduce the parameter $c = \beta \frac{\hbar^2 \pi^2}{2mL^2}$ and the normalized position of the piston $\tilde{X} = X/L$. Similar to the treatment from Section 4, the smaller c is, the higher is T . In addition we introduce the *elliptic theta function*

$$\vartheta_3(u, q) = 1 + 2 \sum_{n=1}^{\infty} q^{n^2} \cos(2nu) \quad (5.8)$$

which allows us to write the results in a more compact way:

$$\mathcal{Z}(h(X)) = \frac{1}{2} \left(\vartheta_3(0, e^{-c/\tilde{X}^2}) - 1 \right) \quad (5.9)$$

²Here we imply $h = h(X)$ and $e_n = e_n(X)$.

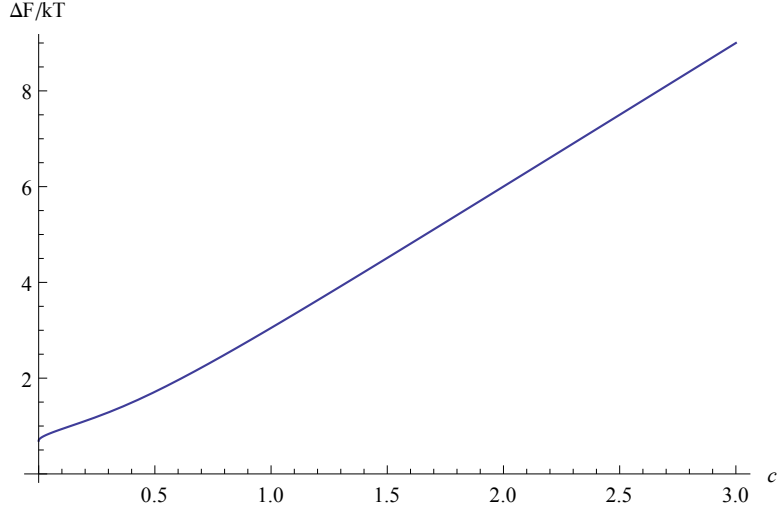


Figure 20.: Behaviour of ΔF w.r.t. $c = \beta \frac{\hbar^2 \pi^2}{2mL^2}$. The plot suggests that $\Delta F/kT$ is higher for small temperatures when the other parameters are fixed. Doing the analysis shows that ΔF approaches a linear behaviour w.r.t. c for $c \rightarrow \infty$.

and

$$F(h(X)) = -kT \ln \left(\frac{1}{2} \left(\vartheta_3(0, e^{-c/\bar{X}^2}) - 1 \right) \right). \quad (5.10)$$

Next we compare $F(h(L/2))$ with $F(h(L))$, i.e., we compute

$$\Delta F := F(h(L/2)) - F(h(L)). \quad (5.11)$$

Analytically this is

$$\frac{\Delta F}{kT} = \ln \left(\frac{\vartheta_3(0, e^{-c}) - 1}{\vartheta_3(0, e^{-4c}) - 1} \right). \quad (5.12)$$

Notice that these calculations do not contain one of the most important features of a work extraction procedure like the one proposed by Szilard. Here, we explicitly investigate the statistical properties in the canonical ensemble of such a system. But in a Szilard engine the dynamics are very important. In this sense it would be wrong to expect an outcome similar to the one expected in a Szilard engine. However, in certain limits the change in free energy is indeed $kT \ln 2$, as is shown in the following plots.

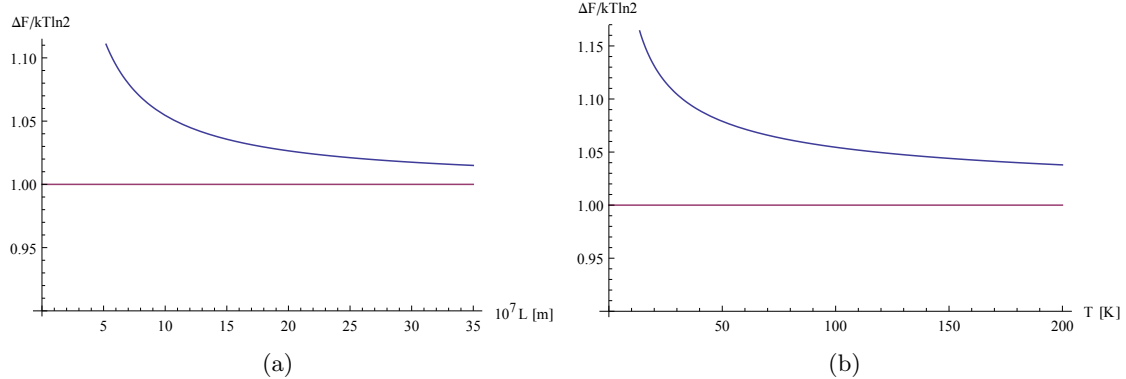


Figure 21.: Behaviour of ΔF w.r.t. L and T . As in Fig. 20 we see that the difference in free energy approaches $kT \ln 2$ for $L \rightarrow \infty$ and for $T \rightarrow \infty$. For this plot we chose $m = 10^{-30} \text{ kg}$.

5.2. Discussion

Fig. 20 shows ΔF for varying c . A more precise analysis with Mathematica confirms the first impression that

$$\lim_{c \rightarrow 0} \frac{\Delta F}{kT} = \ln 2. \quad (5.13)$$

In particular, it shows that a quantum particle in a box with length $\frac{L}{2}$ has a higher free energy than a particle in a box of length L . This is what we expect. We believe that the limit $c \rightarrow 0$ stands for the limit of negligible change in the Hamiltonian and that this is the reason why we get $kT \ln 2$ for the difference in free energy in this limit.

Fig. 21 depicts the behaviour of ΔF with respect to varying L . For $L \rightarrow \infty$ we find the expected change in free energy of $kT \ln 2$. A closer look at $c = \beta \frac{\hbar^2 \pi^2}{2mL^2}$ (together with Fig. 20) shows that the same is true for $T \rightarrow \infty$. For $T \rightarrow \infty$ we could interpret the behaviour as follows: A high temperature makes the actual Hamiltonian less important. This is, with a very hot temperature, high-energy quantum states have non-zero occupation probability regardless of what the actual form of the Hamiltonian is. In addition, the energy of the ground state does no longer have a direct influence on the behaviour of the system. But if the change in the Hamiltonian is negligible, then also the inner energy does not change significantly. The free energy of a system is defined as

$$F = F(T, V) = U - TS, \quad (5.14)$$

where U is the inner energy, T the temperature and S the thermodynamic entropy of the system. Hence, in the limit of $T \rightarrow \infty$, the change in free energy corresponds to the change in entropy of the system. Doubling the size of the volume where the particle can be leads to an increase in entropy by $k \ln(\frac{2V}{V}) = k \ln 2$. This is why one finds $\Delta F \approx kT \ln 2$ in this case.

5.2.1. Thermodynamic Quantities and Classical Limit

In the following we compare statistical quantities with thermodynamic quantities. As we have seen, the thermodynamic free energy of a system is defined as $F = U - TS$, where U is the inner energy, T the temperature and S the thermodynamic entropy of the system. We consider now another classical limit: $X \rightarrow \infty$. The statistical free energy calculated in the above model of a quantum particle in a box with walls at 0 and X should approach the classical expression for the free energy of an ideal gas in this limit.

For a classical ideal gas the inner energy and entropy are given by [46]

$$U(T, V) = \frac{3}{2} N k T, \quad S(T, V) = N \left[C_V \ln(T/T_0) + k \ln \left(\frac{V/V_0}{N} \right) \right], \quad (5.15)$$

where T_0 and V_0 are reference temperature and volume and N is the number of particles. In our case the temperature is constant throughout the process. Furthermore, the volume V changes linearly with X , the position of the piston. Therefore we find a behaviour

$$F(X) = -NkT \ln(\tilde{X}) + \text{const.}, \quad (5.16)$$

where we used again the notation $\tilde{X} = \frac{X}{L}$. The constant term can depend on N and T , but not on X . The goal of this section is to show that the statistical free energy $F(h(X))$ from Eq. 5.10 also shows a logarithmic behaviour for $\tilde{X} \rightarrow \infty$. Expanding the case of one quantum particle in a box to many independent non-interacting quantum particles yields a factor of N for the free energy

$$F(h(X)) = -NkT \ln \left(\frac{1}{2} \left(\vartheta_3(0, e^{-c/\tilde{X}^2}) - 1 \right) \right). \quad (5.17)$$

Hence, we only need to show that to leading order

$$\vartheta_3(0, e^{-c/\tilde{X}^2}) - 1 \sim \tilde{X} \quad \text{for } \tilde{X} \rightarrow \infty \quad (5.18)$$

because in that case

$$F(h(X)) \approx -NkT \ln(\tilde{X}) + \text{const.} \quad \text{for } \tilde{X} \rightarrow \infty. \quad (5.19)$$

This can be done by showing that the limit

$$\lim_{x \rightarrow \infty} \frac{\vartheta_3(0, e^{-x^{-2}}) - 1}{x} \quad (5.20)$$

exists and is non-zero. And indeed, a calculation with Mathematica shows that

$$\lim_{x \rightarrow \infty} \frac{\vartheta_3(0, e^{-x^{-2}}) - 1}{x} = \sqrt{\pi}. \quad (5.21)$$

Hence, for $X \rightarrow \infty$ the free energy of N quantum particles in a box of length X corresponds to the free energy of a classical ideal gas.

6. Born-Oppenheimer Approximation

Now we include the piston as a heavy (quantum) particle of mass M into our considerations. The idea is to use the Born-Oppenheimer approximation, an approximation used in molecular physics. It separates the movement of the electrons (here: our particle) from the movement of the nuclei (here: the piston) of a molecule in two steps:

1. Solve the Schrödinger equation of the particle, neglecting the kinetic term of the piston. This yields eigenstates and eigenenergies of the particle that contain X (the position of the piston) as a parameter (as in Section 5).
2. Solve the Schrödinger equation of the piston for each eigenstate of the particle (numbered by the integer n) where the particle's energy is taken as a potential term in the Schrödinger equation of the piston.

The underlying assumption is that the mass of the particle is much smaller than the mass of the piston. In the classical Szilard engine this assumption is always implicitly included in the setting of one small particle and a piston. The Born-Oppenheimer approximation yields good results for the ground states of molecules, especially if the nuclei are heavy [47]. The hope is that this is also true for the particle-piston system treated here.

Notice that although we claim to treat the Szilard engine quantum mechanically, the interactions between particle and piston are classical. First, we went out from the assumption that the particle feels the piston only through a potential (Eq. 5.1). This is an approximation we came up with. Second, because of the Born-Oppenheimer approximation, the piston feels the particle through a potential as well. Here, the potential is given by the eigenenergies of the particle that contain the position of the piston as a parameter.

In Section 5 we already did the first step. There we found expressions for the eigenstates and eigenenergies of a particle in a box of length X . Suppose now the particle is in the n^{th} eigenstate of the Hamiltonian $h(X)$ from Eq. 5.2. According to the Born-Oppenheimer approximation the Hamiltonian describing the evolution of the piston is in this case

$$H_n = \frac{P^2}{2M} + V(X) + e_n(X), \quad (6.1)$$

where $e_n(X) = \frac{\hbar^2\pi^2n^2}{2mX^2}$ and

$$V(X) = V_{\text{weight}}(X) + V_{\text{box}}(X) = V_{\text{weight}}(X) + \begin{cases} 0 & \text{if } 0 < X < L, \\ +\infty & \text{otherwise.} \end{cases} \quad (6.2)$$

The potential $V(X)$ contains the weight potential as well as the box potential for the piston, where L is the length of the box. In molecular physics $V(X) + e_n(X)$ is called *potential energy surface*. Each potential energy surface corresponds to an eigenstate of the small particle.

6.1. No Weight

Consider first the case of $V_{\text{weight}} = 0$. The Schrödinger equation of the piston is

$$E_{n,k} \Psi_{n,k}(X) = -\frac{\hbar^2}{2M} \Psi''_{n,k}(X) + \frac{\hbar^2 \pi^2 n^2}{2m X^2} \Psi_{n,k}(X), \quad (6.3)$$

with boundary conditions $\Psi(0) = 0 = \Psi(L)$. The integer k stands for the eigenstate of the piston whereas n is (as before) the number of the eigenstate of the particle. A detailed calculation of the eigenenergies and eigenfunctions for this Schrödinger equation can be found in Appendix C.2. The general solution for $n = 1, 2, \dots$ to this boundary value problem is:

$$\begin{aligned} \text{For } k = 1, 2, \dots \text{ we have eigenstates } \quad & \Psi_{n,k}(X) = C_{n,k} \sqrt{X} J_{\nu_n} \left(z_{n,k} \tilde{X} \right) \\ \text{with eigenenergies } \quad & E_{n,k} = \frac{\hbar^2 z_{n,k}^2}{2ML^2}, \end{aligned} \quad (6.4)$$

where we use the notation $\nu_n = \frac{1}{2} \sqrt{1 + 4 \frac{M}{m} \pi^2 n^2}$ for readability. J_ν is the *Bessel function of the first kind* and $C_{n,k}$ is a constant that normalizes the wave function. $\tilde{X} = \frac{X}{L}$ is the normalized position and $z_{n,k}$ denotes the k^{th} zero of the Bessel function J_{ν_n} .¹

In the following we plot the probability of finding the piston at normalized position \tilde{X} for different settings of $\frac{M}{m}$ and n (Fig. 22). We observe that a larger ratio of $\frac{M}{m}$ leads to a more localized wave function of the piston. This makes sense, since the limit $\frac{M}{m}$ large corresponds to the limit of a classical piston. Furthermore, the higher the energy of the eigenstate of the particle, the higher is the probability to find the piston closer to $X = L$. This is again what we would expect from our model. It also makes sense that the probability of finding the piston more to the left in higher energy states increases. So far the only form of energy that the piston can have is kinetic energy and potential energy with respect to the potential term coming from the eigenenergy of the particle. This potential term is proportional to $\frac{1}{X^2}$. Hence, if the energy of the piston is increased, we expect it to be more to the left. This is observable in Fig. 22.

¹The $z_{n,k}$ come into play here because of the second boundary condition $\Psi(L) = 0$. How this work exactly can be found in Appendix C.2.

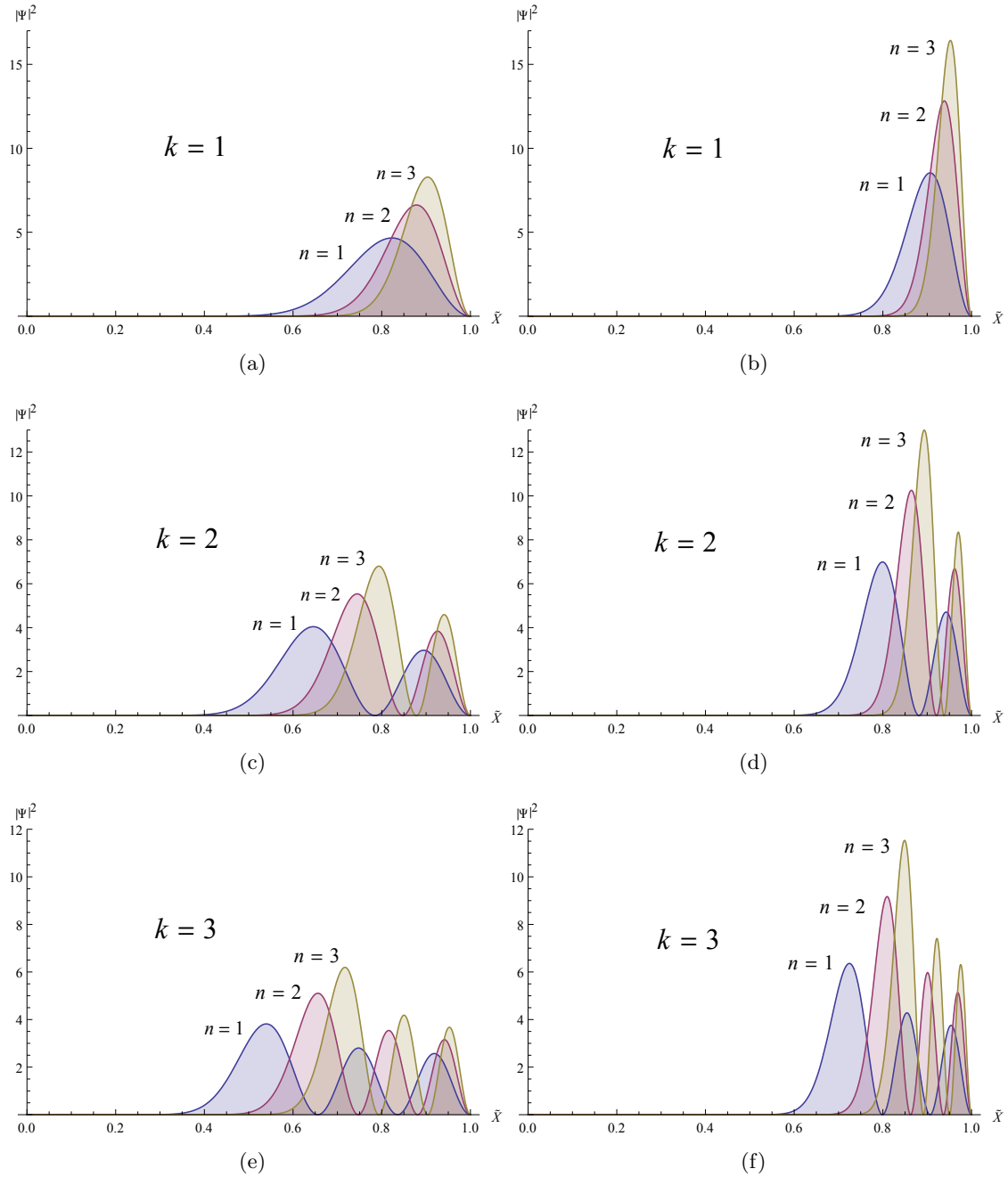


Figure 22.: Plot of $|\Psi_{n,k}|^2$ w.r.t. the normalized position $\tilde{X} = \frac{X}{L}$ for $m = 10^{-30}\text{kg}$, $L = 10^{-7}\text{m}$ and different values of n, k . In the left column (figures (a), (c), (e)): $\frac{M}{m} = 10$ and in the right column (figures (b), (d), (f)): $\frac{M}{m} = 100$. Here, n is the integer describing the energy eigenstate of the particle, k the integer denoting the energy eigenstate of the piston (for given n).

6.2. Linear Potential

Next we have a look at the case $V_{\text{weight}}(X) = \alpha X$ for some $\alpha > 0$. The Schrödinger equation is then

$$E_{n,k}\Psi_{n,k}(X) = -\frac{\hbar^2}{2M}\Psi''_{n,k}(X) + \left(\frac{\hbar^2\pi^2n^2}{2mX^2} + \alpha X\right)\Psi_{n,k}(X), \quad (6.5)$$

still subject to the same boundary conditions $\Psi(0) = 0 = \Psi(L)$. This case corresponds to the picture of the original Szilard engine where a weight is attached to the piston such that the potential energy of the piston (actually: of the weight) is higher if the position is closer to L .

Unfortunately the solution to this equation is not as straight forward as for Eq. 6.3; Mathematica is not able to solve it anymore. This changes if we use a different, quadratic potential.

6.3. Quadratic Potential

Let us now consider the potential $V_{\text{weight}}(X) = \alpha X^2$ leading to the Schrödinger equation for the piston

$$E_{n,k}\Psi_{n,k}(X) = -\frac{\hbar^2}{2M}\Psi''_{n,k}(X) + \left(\frac{\hbar^2\pi^2n^2}{2mX^2} + \alpha X^2\right)\Psi_{n,k}(X). \quad (6.6)$$

The analogy with the Szilard engine, where the piston's potential energy is implemented by a weight that is attached to it, is lost. But that was an arbitrary choice of weight potential anyway. It could as well be that the extracted work is stored in a system whose energy grows as X^2 . An example of this is a spring with spring constant k attached to the piston leading to the energy $\frac{1}{2}kX^2$.

Detailed calculations of the results of this section can be found in Appendix C.2. For each $n = 1, 2, \dots$ the eigenstates and eigenenergies are the following:

$$\begin{aligned} \text{For } k = 1, 2, \dots \text{ we have eigenstates } \quad & \Psi_{n,k}(X) = C_{n,k}X^{\frac{1}{2}+\nu_n}e^{-\frac{1}{2}gX^2}L_{b_{n,k}}^{(\nu_n)}(gX^2) \\ \text{with eigenenergies } \quad & E_{n,k} = \frac{2g\hbar^2}{M} \left[b_{n,k} + \frac{1}{2}(1 + \nu_n) \right]. \end{aligned} \quad (6.7)$$

$L_b^{(a)}$ is the *associated Laguerre polynomial*.² Again, we used $\nu_n = \frac{1}{2}\sqrt{1 + 4\frac{M}{m}\pi^2n^2}$. Additionally we introduced the parameter $g = \sqrt{\frac{2M\alpha}{\hbar^2}}$ and positive coefficients $b_{n,k}$. These coefficients follow from the boundary condition $\Psi(L) = 0$ and are such that

²Note that the associated Laguerre polynomial is no polynomial in the case of non-integer b , but it is still well-defined.

$L_{b_{n,k}}^{(\nu_n)}(gL^2) = 0$ (see detailed analysis in Appendix C.2.) They can be determined numerically with Mathematica.

Again we plot the squared wave function for different $\frac{M}{m}$ and n to illustrate how the parameters influence the behaviour of the piston w.r.t. normalized position \tilde{X} (see Fig. 23). This time we leave away the $k = 3$ plot because it is almost the same as for $k = 2$. As before a larger ratio of $\frac{M}{m}$ leads to a more localized probability distribution of the piston's position. Moreover, the higher the energy of the particle is (n) the higher is the probability of finding the piston closer to $X = L$. In particular, the piston's state seems to react more sensitively on n for higher mass ratios. For $\frac{M}{m} = 100$ the wave functions share less support than for $\frac{M}{m} = 10$. This phenomenon is very interesting and will also show up in a semi-classical analysis done in subsequent sections. It says that the smaller the particle's mass, the more the piston is localized in a region close to the right wall of the box at L .

For the lowest energy eigenstates the energy of the piston comes almost completely from the potential as can be seen in the above figures. This changes for highly excited states as depicted in Fig. 24. For fixed n (i.e., fixed eigenstate of the particle) the mean position of the piston does not change with k . Instead the increase of the piston's energy goes almost completely into kinetic energy. We can tell that from Fig. 24 because the wave function for fixed $n = 2$ and fixed $\frac{M}{m}$ stays within an enveloping curve but oscillates more wildly for higher k .

This is an interesting feature. If we let such a system evolve in time and couple the particle to a heat bath of temperature T then eventually the piston will be thermalized as well. Hence, it will have non-zero probability of being in an excited state as shown in Fig. 24. There, we can see that being in an excited state corresponds to having more kinetic energy. Therefore, in a quantum Szilard engine, the energy that the piston will have is not purely potential, but also kinetic energy. We will see in Section 8 that something similar happens if we take a more classical approach. The kinetic energy of the piston grows more or less in the same way as its mean potential energy does. Thinking of the equipartition theorem from classical statistical mechanics it makes sense that the energy gain of the piston is comparable in its kinetic and potential degree of freedom. But when we think of a classical Szilard engine we only talk about potential energy of the piston and neglect its kinetic energy because we implicitly assume a quasi-static evolution.

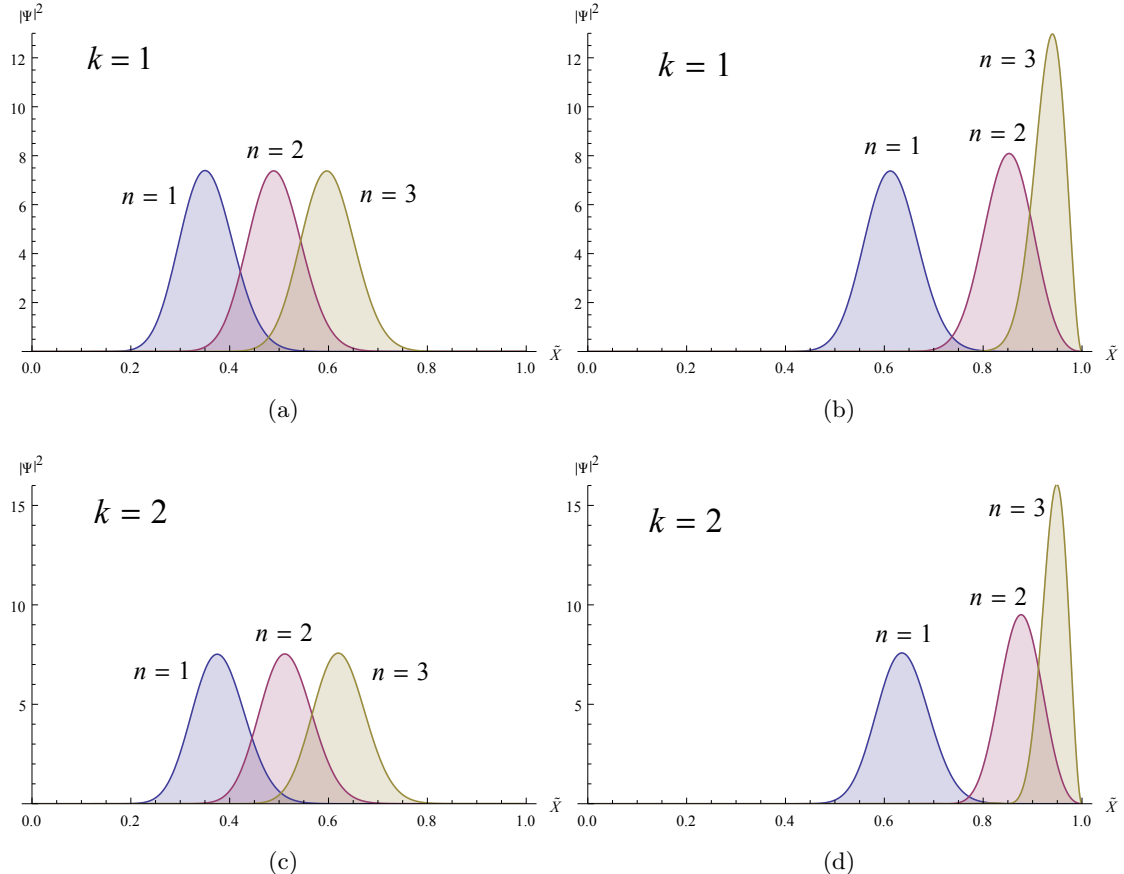


Figure 23.: Plot of $|\Psi_{n,k}|^2$ w.r.t. the normalized position $\tilde{X} = \frac{X}{L}$ for $\alpha = 4 \cdot 10^{-9} \frac{\text{J}}{\text{m}^2}$, $m = 10^{-30} \text{kg}$, $L = 10^{-7} \text{m}$ and different values of n, k . In the left column (figures (a), (c), (e)): $\frac{M}{m} = 10$ and in the right column (figures (b), (d), (f)): $\frac{M}{m} = 100$. Here, n is the integer describing the energy eigenstate of the particle, k the integer denoting the energy eigenstate of the piston (for given n).

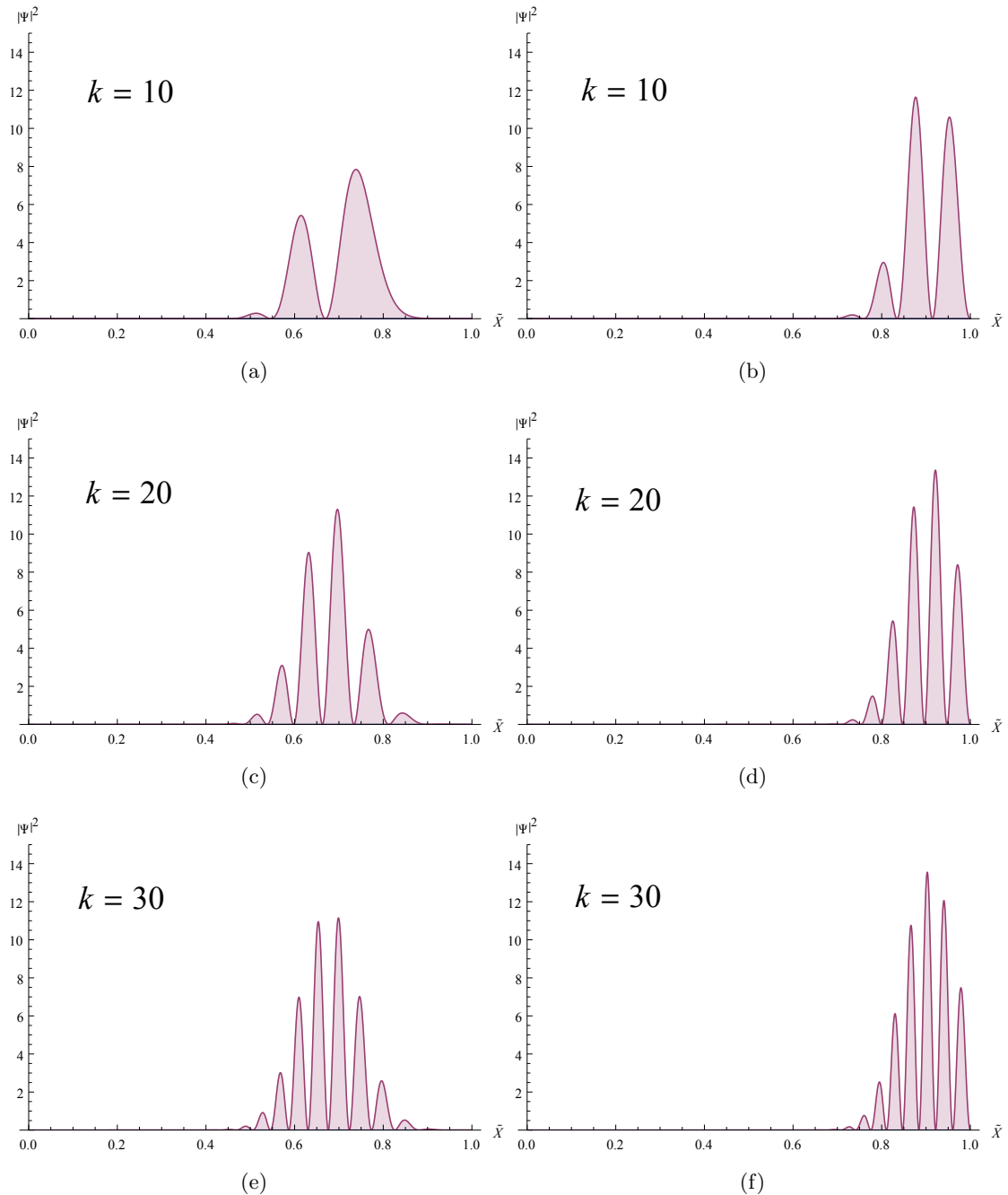


Figure 24.: Plot of $|\Psi_{2,k}|^2$ for different k 's and ratios of masses w.r.t. the normalized position $\tilde{X} = \frac{X}{L}$. In the left column (figures (a), (c), (e)): $\frac{M}{m} = 10$ and in the right column (figures (b), (d), (f)): $\frac{M}{m} = 100$. Here, k is the integer describing the energy eigenstate of the piston given $n = 2$.

6.4. Other Potentials – Open Questions

As mentioned in Section 3 it would be very interesting to find out more about the quantum behaviour of such a system if the piston feels a different, maybe more optimal potential. Unfortunately the Schrödinger equation for, e.g., a logarithmic potential is very hard to solve analytically. For now we will not put more effort in the analytical analysis of the Born-Oppenheimer approximation in the quantum regime.

Another point is that the static analysis of the time-independent Schrödinger equation does not tell us anything about the time evolution of a quantum Szilard engine. But the time evolution and the steady state that the total system may reach are the interesting points. Moreover, we have not said anything about the thermalization process that makes sure that the particle is connected to a heat bath at temperature T . We give ideas of how to treat these questions in the next section. Furthermore , we do a numerical analysis of a classical piston interacting with a quantum particle in the Born-Oppenheimer approximation.

7. Thermalization and Time Evolution

So far we have used the Born-Oppenheimer approximation to find the approximate behaviour of a small particle and a heavy piston in a box potential. We calculated eigenstates, eigenenergies, and plotted the results. However, the idea of a Szilard engine is that the particle transfers energy between the thermal bath and the piston. This implies that we must provide a reasonable procedure that thermalizes the particle.

Here, we come up with a model. In the classical Szilard engine the particle can only interact with the thermal bath when it is close to the walls of the box.¹ Otherwise it is to a good approximation a free particle. This can be modelled in a first step by letting the system evolve in discrete time steps. For instance, we can start with a state of particle and piston such that the piston is in the middle of the box at $X = L/2$ and the particle is in an eigenstate. Then we let the piston evolve according to the Hamiltonian H_n from Eq. 6.1 during the time interval Δt . In this step, n remains unchanged. The second step would then be to choose $n \in \{1, 2, \dots\}$ randomly according to the Gibbs distribution at temperature T , where n denotes the ‘new thermalized’ state of the particle. Then we go back to step one and start again.

7.1. A Semi-Quantum Model

In the following, we regard the piston as a purely classical particle that evolves on the potential energy surfaces according to classical mechanics. To do so, we use the canonical coordinates (X, P) , describing the position and its canonical conjugate, the momentum, of the piston. The (now classical) Hamiltonian of the piston is

$$H_n = \frac{P^2}{2M} + V(X) + e_n(X) \quad (7.1)$$

with $e_n = \frac{\hbar^2 \pi^2}{2mX^2} n^2$ from Eq. 5.5, n numbering the current state of the particle and V being the total potential consisting of box and weight potential. The classical equations of motion are

$$\dot{X} = \frac{\partial H_n}{\partial P} \quad \text{and} \quad \dot{P} = -\frac{\partial H_n}{\partial X}. \quad (7.2)$$

The procedure is now the following. At each time step:

¹For now we neglect electromagnetic radiation, which could in principle also lead to a thermalization of the particle if it is not close to the wall.

1. Start with position and momentum of the piston (X, P) and choose the particle's state n randomly according to the Gibbs distribution of the states ψ_n from Eq. 5.5. Let n be the number of the state of the particle. (X, P) does not change in this step.
2. Let (X, P) evolve for a small time step Δt under H_n ending up in the state (X', P') . This is, the piston feels the interaction with a particle in state n for the time Δt and evolves. In this step, n does not change.
3. Repeat these steps N times (N large) for $(X, P) = (X', P')$ and store the trajectory of the piston.

In step 1 the probabilities for the Gibbs distribution for the states ψ_n are given by

$$p(n; X) = \frac{e^{-\frac{e_n(X)}{kT}}}{\sum_{n=1}^{\infty} e^{-\frac{e_n(X)}{kT}}} \equiv \frac{\exp\left(-\frac{\hbar^2\pi^2n^2}{2mX^2kT}\right)}{\mathcal{Z}(h(X))}, \quad (7.3)$$

where $\mathcal{Z}(h(X))$ is the partition sum from Section 5. This probability distribution depends on the piston's current position because the eigenenergies of the particle do so as well. In step 2 (X', P') are determined by

$$X' = X + \Delta t \left(\frac{\partial H_n}{\partial P} \right) = X + \Delta t \frac{P}{M} \quad (7.4)$$

and

$$P' = P - \Delta t \left(\frac{\partial H_n}{\partial X} \right) = P - \Delta t \left(\frac{dV}{dX}(X) - \frac{\hbar^2\pi^2n^2}{mX^3} \right). \quad (7.5)$$

In the quantum approach of Section 6 we introduced the potential V as

$$V(X) = V_{\text{weight}}(X) + V_{\text{box}}(X) \quad \text{with} \quad V_{\text{box}}(X) = \begin{cases} 0 & \text{if } 0 < X < L, \\ +\infty & \text{otherwise.} \end{cases} \quad (7.6)$$

In this semi-classical treatment, the infinitely high box potential no longer makes sense. Instead we could think of it as a finitely high potential that is nevertheless high enough to keep the piston inside the region $[0, L]$. But that does not solve the problem that it is possible to find the piston at $X > L$ or $X < 0$ when we run the simulation discretely. Due to our discrete steps it can happen that, e.g., $X = L - \varepsilon$ (for some small $\varepsilon > 0$) and $P > \frac{M}{\Delta t}\varepsilon$. In this case, $X' > L$, which should be impossible in a box with solid walls. Another problem is that we have to take the derivative of such a box potential (see Eq. 7.5). This will lead to Dirac delta functions for any height of the box potential. Distributions like a Dirac delta function are not easy to treat in a numerical simulation. Therefore, we want to circumvent the problem of treating a distributional potential. One way of doing so is setting the box potential to zero, $V_{\text{box}} \equiv 0$, and using boundary

conditions instead. Hence, for our semi-classical model we use $V(X) = V_{\text{weight}}(X)$ which leads to the discretized steps

$$X' = X + \Delta t \frac{P}{M} \quad \text{and} \quad P' = P - \Delta t \left(\frac{dV_{\text{weight}}}{dX}(X) - \frac{\hbar^2 \pi^2 n^2}{m X^3} \right), \quad (7.7)$$

and enforce the boundary conditions, as discussed in Section 7.2. This solves the problem of distributions in the numerical simulations. Furthermore, it opens new possibilities of introducing friction in our model.

7.1.1. Outline of the Simulation Program

A program computing position and momentum of the piston could now look as follows (in pseudo code):

```

1 Input: (X,P), N, dt, m, M, L, T % initial position and momentum,
2                               % number of steps, time interval,
3                               % mass param.s, box length, temp.
4 Output: (X',P')                % trajectory of the piston
5
6 for l=1 to N do
7   choose n randomly from 1,2,... according to Gibbs distribution
8   % define a function to do so
9
10  X <- X'(X,P,n,dt,m,M)      % previously defined functions
11  P <- P'(X,P,n,dt,m,M)      % for X' and P'
12
13 % insert the block with boundary conditions here
14
15 store (X,P)
16 end

```

Here, we used the short notation $X'(X, P)$ and $P'(X, P)$ for the expressions in Eq. 7.7. With such a program we can simulate the time evolution of the piston. For instance, we can let the piston start in the middle at $X = L/2$ with zero momentum and let the simulation run until a steady state is reached (if a steady state is reached at all). With the data from this steady state we can then do statistical analysis, i.e., we can compute time averages of the position and the energy of the piston. Before going into the analysis of the model we discuss settings for the boundary conditions and the weight potential.

7.2. Boundary Conditions

A detailed discussion of possible choices for boundary conditions is given in Appendix C.3. We discuss elastic, inelastic and thermal boundary conditions as well as mixtures of them. The boundary conditions come into play when the piston bounces into the walls

of the box.² For the simulations presented in the next section we chose to use thermal boundary conditions. The reason for this choice is that the numerical simulations are not stable for simulations with elastic boundary conditions (as is discussed in detail in Appendix C.3). There are two alternatives for elastic boundary conditions: inelastic or thermal boundary conditions. The problem with inelastic boundary conditions is that they introduce friction. Friction suggests the involvement of another heat bath of zero (or at least very small) temperature. Thermal boundary conditions introduce friction as well, but one can argue that the assumption of a friction process that involves the present heat bath at temperature T is a physical assumption. Since we want to model a Szialrd engine, it is very important that we have only access to one heat bath. This is a very important feature of a work extraction process that distinguishes it from thermal machines such as refrigerators or heat engines. These machines explicitly need access to two heat baths in order to function.

With thermal boundary conditions the piston's momentum is reset to a random momentum chosen according to the Gibbs distribution if the piston reaches a wall. For the right wall (at $X = L$) the (unnormalized) probability density function describing the Gibbs distribution is

$$f(P) = \begin{cases} \exp\left(-\frac{P^2}{2MkT}\right), & \text{for } P < 0, \\ 0, & \text{otherwise.} \end{cases} \quad (7.8)$$

For the left wall the probability density function is the same with P replaced by $-P$. This approach brings a much faster thermalization of the piston with it. In this sense, it contradicts the idea (suggested in Section 4) that it could be helpful to prevent the piston from thermalizing and to extract the work before that happens. Nevertheless, we use these boundary conditions in Section 8.

7.3. Weight Potential

As discussed in Section 3, there are different possibilities for the weight potential. We did simulations with linear, quadratic and logarithmic potentials (as suggested in Fig. 17 of Section 3) in our model with thermal boundary conditions. It turned out that for strengths of the potential that are close to the constraint

$$V_{\text{weight}}(L) - V_{\text{weight}}(L/2) = kT \ln 2, \quad (7.9)$$

the differences in the properties of the steady state were only small. This means that the mean position as well as the mean energy and the fluctuations were almost the same for the different potential shapes. Therefore we chose to use the logarithmic potential for our simulations:

$$V_{\text{weight}}(X) = A \ln\left(\frac{X}{L}\right), \quad (7.10)$$

²I.e., when it leaves the box in time step l and must be reset for the next time step $l + 1$ so that the simulation can continue with the piston at a position in $[0, L]$.

where A is a parameter determining the magnitude of the potential. The reason for this choice is mentioned in Section 3 already: in the case of a classical macroscopic Szilard engine, a logarithmic potential would lead to a quasi-static work extraction process, which is optimal. According to the constraint for an optimal work extraction in a Szilard engine introduced in Section 3, A should then approximately fulfil

$$kT \ln 2 \stackrel{!}{=} V_{\text{weight}}(L) - V_{\text{weight}}(L/2) = A \left(\ln 1 - \ln \frac{1}{2} \right) = A \ln 2. \quad (7.11)$$

Hence, A should be of the order of kT .

8. Analysis

To analyze the behaviour of this system evolving in discrete steps we implemented the program outlined above in MATLAB. We then used this program to investigate two main questions:

1. Suppose the piston starts in the middle of the box at $X = L/2$ with the particle in the left half and evolves according to the model introduced in Section 7. We stop the simulation when the piston reaches the right wall (at $X = L$) for the first time and compute its total energy at this point. How does this energy relate to the parameters of the model? How does it change if the starting position is $X = X_0$?
2. Instead of stopping the piston we let it evolve for a long time. Does the piston reach a steady state after some time? If so, what are the properties of this steady state? And if not, why not?

Question 1 is treated in Section 8.1, question 2 in Section 8.2.

8.1. Total Energy at $X = L$

In this section we use our model to do the following simulations: we let the piston start at position X_0 (e.g. in the middle of the box at $L/2$) and let it evolve until it reaches the right wall for the first time. Then we consider its energy at this point. This can be done with different weight potentials (and different weight strengths of potentials). Note that in this case we need not specify boundary conditions because we stop the simulation at the point where they become important.

8.1.1. Numerical Simulations

It turns out that the final energy of the piston is almost deterministic, in the sense that it does not vary much if we compare the outputs of many runs with the same parameters.¹ Nevertheless, we let the simulation run five times to make sure that the data is representative.

Kinetic Energy – No Weight Potential Our numerical results suggest that the kinetic energy the piston has when it reaches the right wall for the first time is equal to the change in free energy of the quantum particle:

$$E_{\text{kin}} = \Delta F \equiv F(h(L/2)) - F(h(L)). \quad (8.1)$$

¹Although there is a random process involved, namely choosing n (the energy eigenstate of the particle) after each time step.

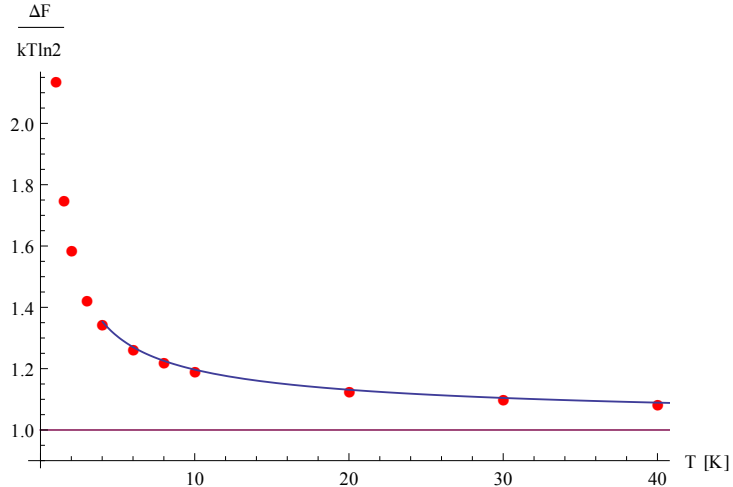


Figure 25.: Kinetic energy (red dots) and difference in free energy of a quantum particle in a box of length L and of length $L/2$ (blue line, both normalized w.r.t. $kT \ln 2$) vs. temperature T . The other parameters are fixed to $L = 10^{-7}\text{m}$, $m = 10^{-30}\text{kg}$, $M = 100m$. The constant red line stands for the energy $kT \ln 2$. We see that the kinetic energy of the piston when it reaches $X = L$ for the first time and the difference in free energy ΔF coincide to very good approximation.

As in Section 5, $h(X)$ is the Hamiltonian of the quantum particle in a box of length X , $F(h(X))$ is the free energy of such a particle at temperature T and L is the length of the box in which the particle and the piston are.

We saw this for instance in simulations for different temperatures, as is shown in Fig. 25. Both the free energy and the kinetic energy of the piston approaches $kT \ln 2$ for high temperatures. Simulations with other parameter settings showed the same characteristics to high precision. This is a nice result. It shows that the difference in free energy of a quantum particle in boxes of different lengths (e.g., L and $L/2$) has an operational meaning.

There are other ways of approaching the classical limit besides letting $T \rightarrow \infty$. For instance, it would be interesting how this kinetic energy changes with increasing L and constant temperature to compare it to Fig. 21 from Section 5. Unfortunately, a longer box requires a longer computation time. Furthermore, the time steps must be chosen smaller because otherwise the simulation is unstable.² However, the few cases we tested strongly suggest that also in this case ΔF and E_{kin} coincide. Analytical analysis done in Section 8.1.2 supports that.

²We have no explanation for that. But in the simulations we could observe that for larger boxes the time steps must be chosen even smaller.

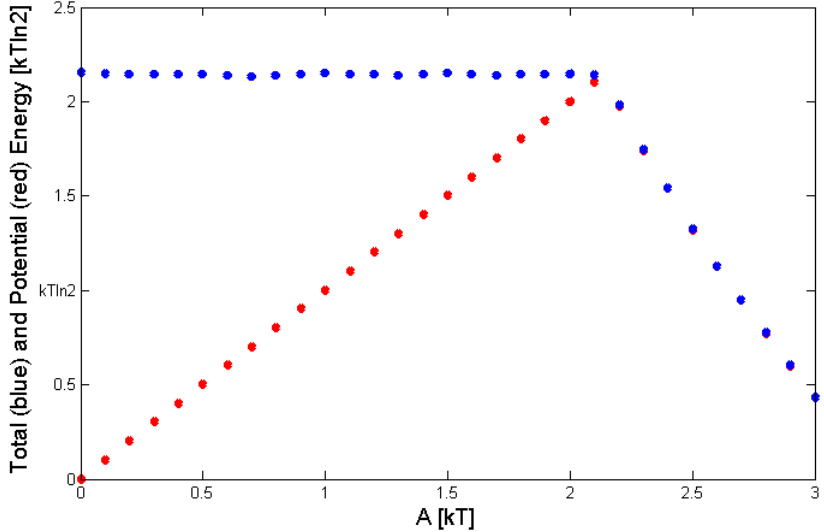


Figure 26.: Total energy (blue dots) and potential energy (red dots, both normalized w.r.t. $kT \ln 2$) vs. strength of potential A . The other parameters are fixed to $L = 10^{-7}\text{m}$, $m = 10^{-30}\text{kg}$, $M = 100m$, $T = 1\text{K}$. For $A \gtrsim 2.14 kT$ the red and blue dots coincide, which is due to the fact that the turning point of the piston is smaller than $X = L$, hence the kinetic energy at the point we are interested in is zero. The value of $2.14 kT$ comes from the difference in free energy with the above parameter setting, which is $\Delta F = 2.14 kT \ln 2$. This corresponds to the red point at $T = 1\text{K}$ in Fig. 25.

Another check to support our claim is to let L and T constant, but change the starting position of the piston X_0 . Also there the kinetic energy at $X = L$ coincides in a great measure with the difference in free energy $F(h(X_0)) - F(h(L))$.

We conclude that the difference in free energy $\Delta F = F(h(X_0)) - F(h(L))$ and the kinetic energy of the piston when it reaches $X = L$ for the first time are equal in our model. Hence, the kinetic energy approaches $kT \ln 2$ for high temperatures ($L = \text{const.}$) or large boxes ($T = \text{const.}$).

Kinetic and Potential Energy It is interesting to see what changes if we introduce a weight potential. To do so, we take the logarithmic potential $V_{\text{weight}}(X) = A \ln(X/L)$ and do the same simulations as before. When the piston reaches the right wall for the first time, we consider the total energy and the part of it that is potential energy. This is plotted in Fig. 26. In general, the total energy of the piston has the same characteristics here as the kinetic energy had in the case of no weight potential: it is equal to the difference in free energy of the quantum particle. The strength of the weight potential

determines only the portion of the total energy that goes into kinetic energy. This is even true in the case where the potential is too strong so that the piston turns around before reaching the right wall. The output of the simulations was then the potential energy of the piston at the turning point (because at the turning point $E_{\text{kin}} = 0$). This turning point comes into play exactly when the strength of the potential is such that the potential energy gain of the piston at $X = L$ is equal to the difference in free energy of the quantum particle (at $A \gtrsim 2.14 kT = \frac{\Delta F}{\ln 2}$).³

We did the same analysis for more than one particle, for other weight potentials and other settings of parameters. In all cases, the total energy of the piston at the right wall was equal to the change in free energy of the quantum particle. In the following section we show an analysis indicating why this must be the case.

8.1.2. Analytical Analysis

In the simulations we thermalize the particle after each time step Δt . The time steps are very small in order simulate a continuous evolution of the piston's position and momentum. Hence, one has to do many steps already before the piston reaches $X = L$ for the first time. The fact that we sample many times from the Gibbs distribution suggests that instead of thermalizing the particle after each time step, we could work with an average *effective* force coming from the interaction with the particle in the equation of motion of the piston. This is, instead of choosing n according to the Gibbs distribution before each time step and letting the piston evolve with the Hamiltonian H_n from Eq. 7.1 we define an average force $\bar{\mathcal{F}}(X)$ for the piston's evolution which leads to the equations of motion

$$\dot{X} = \frac{P}{M} \quad \text{and} \quad \dot{P} = -\frac{dV_{\text{weight}}}{dX}(X) - \bar{\mathcal{F}}(X). \quad (8.2)$$

The analysis done below for the many-particle Szilard engine with a normalized interaction potential (from Eq. 8.9) suggests that there should not be a big difference between a randomly chosen force at every time step and an effective force. This means that instead of the derivative of a randomly chosen interaction potential $e_n(X)$ with respect to X we can work with the average force

$$\begin{aligned} \bar{\mathcal{F}}(X) &= \sum_{n=1}^{\infty} p(n; X) \left(-\frac{d}{dX} e_n(X) \right) \\ &= \sum_{n=1}^{\infty} p(n; X) \left(-\frac{d}{dX} \frac{\hbar^2 \pi^2 n^2}{2mX^2} \right), \end{aligned} \quad (8.3)$$

³Since the piston does not reach the right wall in this case, the free energy difference of the particle decreases: $F(h(X_0)) - F(h(X_{\max})) < F(h(X_0)) - F(h(L))$ for $X_{\max} < L$. This can be observed in Fig. 26: for $A \gtrsim 2.14 kT$, where $V_{\text{weight}}(L) > F(h(L/2)) - F(h(L))$, the total energy of the piston at the turning point is fully potential and decreases with A .

where $p(n; X)$ is the probability given by the Gibbs distribution already encountered in Section 7.1

$$p(n; X) = \frac{e^{-\frac{e_n(X)}{kT}}}{\sum_{n=1}^{\infty} e^{-\frac{e_n(X)}{kT}}} \equiv \frac{\exp\left(-\frac{\hbar^2 \pi^2 n^2}{2mX^2 kT}\right)}{\mathcal{Z}(h(X))}. \quad (8.4)$$

Using this expression for the probabilities of the Gibbs distribution we can rewrite the average force as

$$\begin{aligned} \bar{\mathcal{F}}(X) &= \sum_{n=1}^{\infty} \frac{e^{-\frac{e_n(X)}{kT}}}{\sum_{n=1}^{\infty} e^{-\frac{e_n(X)}{kT}}} \left(-\frac{d}{dX} e_n(X) \right) \\ &= kT \sum_{n=1}^{\infty} \frac{\frac{d}{dX} \left(e^{-\frac{e_n(X)}{kT}} \right)}{\sum_{n=1}^{\infty} e^{-\frac{e_n(X)}{kT}}} \\ &= kT \frac{\frac{d}{dX} \mathcal{Z}(h(X))}{\mathcal{Z}(h(X))} \\ &= kT \frac{d}{dX} \ln \mathcal{Z}(h(X)) \\ &= -\frac{d}{dX} F(h(X)). \end{aligned} \quad (8.5)$$

Here, $F(h(X)) = -kT \ln \mathcal{Z}(h(X))$ is the free energy of a quantum particle in a box of length X , as encountered in Section 5. Hence, the idea of an averaged force is equivalent to taking the free energy $F(h(X))$ as the interaction potential in the piston's classical Hamiltonian. This leads to an *effective* Hamiltonian⁴

$$\bar{H} = \frac{P^2}{2M} + V_{\text{weight}}(X) + F(h(X)). \quad (8.6)$$

With the above argumentation for the averaged force we can assume that this Hamiltonian is a good approximation for describing the classical evolution of the piston. This leads to the following conclusion: if the piston starts at $X = X_0$ with zero momentum and ends up at X , the energy gain in the momentum degree of freedom and in the form of potential energy with respect to the weight potential must be equal to $F(h(X_0)) - F(h(X))$ for any parameter setting.

The analysis shows that the piston's energy when it reaches the right wall for the first time must be equal to the change in free energy of the quantum particle. This is exactly what the simulations showed in the previous section (Section 8.1.1). Moreover, it gives a better understanding why the difference in free energy of the particle has this operational meaning and it shows that, at least in this case, the numerical simulations are stable and yield reliable results.

⁴This Hamiltonian generates the time evolution we encountered in Eq. 8.2.

We conclude this section with a remark. In the above analysis we took an average effective force $\bar{\mathcal{F}}(X)$ to approximate the evolution of the piston. This made sense because the force is what goes into the equations of the piston's evolution. This approximation is not equivalent to an average interaction potential in the piston's Hamiltonian

$$\bar{e}(X) = \sum_{n=1}^{\infty} p(n; X) e_n(X). \quad (8.7)$$

The technical reason is that the probabilities $p(n; X)$ depend on X . Thus, when calculating an average force from the effective potential by taking its derivative with respect to X it is not going to be the same as $\bar{\mathcal{F}}(X)$. It is an open question what the actual relation between these two averaging procedures is.

8.2. Long-Term Behaviour

As mentioned in the introduction to this section we are interested in whether the piston reaches a steady state in the long-term limit and what the properties of this steady state are. Fig. 27 illustrates what we mean by the term ‘steady state’. The figure shows the evolution of the piston in our model, starting from $(X, P) = (L/2, 0)$. We distinguish between a steady state and a static state. In a steady state, the behaviour of the particle is not static (it oscillates), but the main features of the state are predictable and the behaviour does not change in the future. For thermal boundary conditions it turns out that, after a transient period, an almost regular state is reached, as can be seen in Fig. 27. There is still some randomness present, but that is due to the thermal boundary conditions. We could now use the data from the plot and compute the mean steady state position, energy and fluctuations. This is what we do below for different numbers of particles with a logarithmic weight potential.

During the work on this thesis we have done countless simulations with different weight potentials, different parameter settings, different boundary conditions and different numbers of particles interacting with the piston. Instead of showing all the plots produced in that analysis we summarize the main points in words and limit the plots to the most interesting ones.

8.2.1. Many-Particle Szilard Engine

Let us start by considering N non-interacting particles in a Szilard engine. The adjustments in the procedure of our model are straight forward. Instead of choosing one number $n \in \{1, 2, \dots\}$ according to the Gibbs distribution before each time step we now choose N such numbers n_1, n_2, \dots, n_N . The interaction potential term is then the sum of the eigenenergies of all N particles:

$$e_{\mathbf{n}}(X) = \sum_{i=1}^N \frac{\hbar^2 \pi^2 n_i^2}{2mX^2}. \quad (8.8)$$

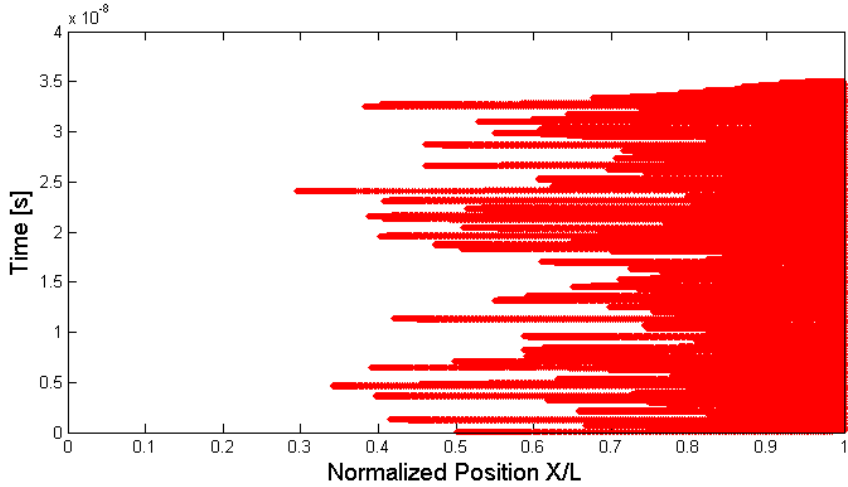


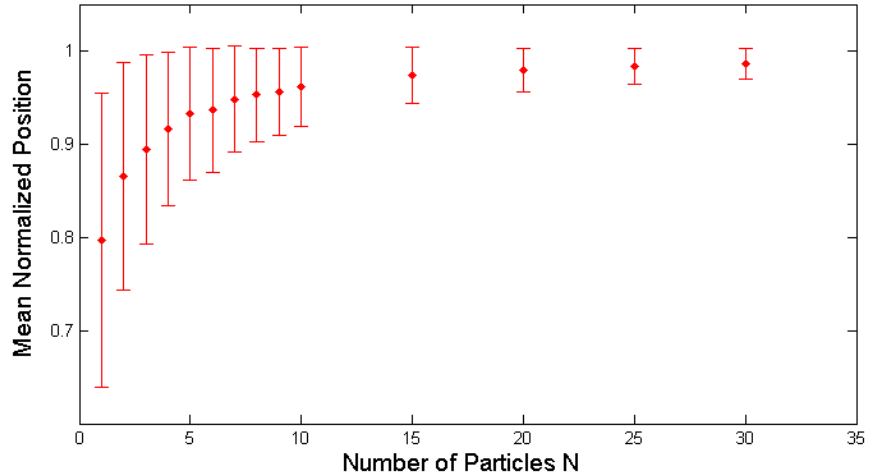
Figure 27.: Steady state of the piston for $T = 1\text{K}$, $m = 10^{-30}\text{kg}$, $M = 100m$, $L = 10^{-7}\text{m}$ and $V_{\text{weight}} \equiv 0$. We regard this as a steady state because the figures of merit of this state (mean position, mean energy, standard deviation from mean position) do not change with time if we observe the piston for long time intervals. The fluctuations that we can observe in this plot are due to the thermal boundary conditions.

It acts on the piston as a potential term due to the Born-Oppenheimer approximation. This term replaces $e_n(X)$ in the piston's classical Hamiltonian from Eq. 7.1. The rest of the procedure stays the same.

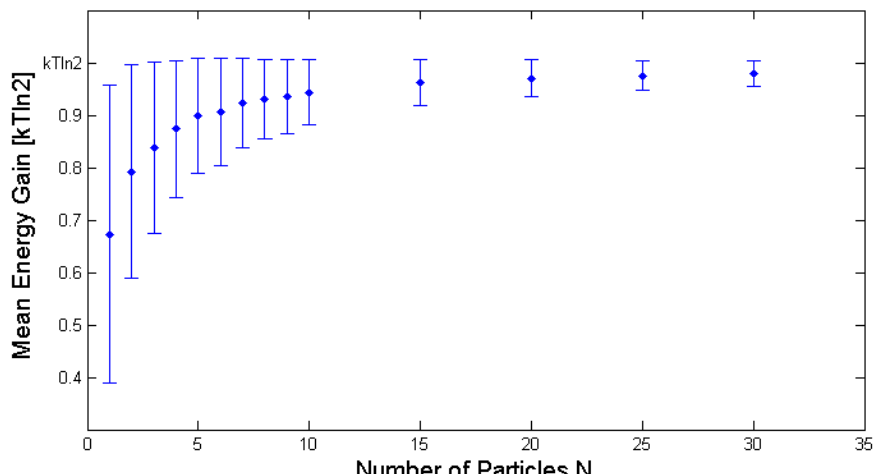
Fig. 28 shows mean position, mean energy gain, and standard deviation of normalized position of the steady state of the piston as a function of N . For these simulations the piston felt a logarithmic weight potential with $A = kT$ such that the potential energy gain at $X = L$ is exactly $kT \ln 2$ (Eq. 7.11). The boundary conditions were chosen to be thermal.

For higher numbers of particles, the steady state position of the piston approaches $X = L$ and, consequently, the mean energy gain converges to $kT \ln 2$. In addition, the standard deviation becomes smaller as N grows. However, in the one-particle case, large fluctuations can be observed and the potential energy gain is not optimal. Fig. 28 (c) leaves open whether the standard deviation reaches zero for higher particle numbers. Our guess is that it never exactly reaches zero because of the thermal boundary conditions that lead to a non-zero momentum of the piston each time it has contact to the right end of the box. But maybe this could be solved with a softer thermalization of the piston, as is discussed in the section on mixed boundary conditions in Appendix C.3. Nevertheless, the fluctuation of its position become very small for high N .

Samples of simulations of N particles interacting with a piston with other parameter



(a)



(b)

Figure 28.: (a) Mean steady state position (normalized) with the standard deviation as error bars and (b) mean steady state potential energy with error bars computed from the standard deviation from the mean position (normalized w.r.t. $kT \ln 2$). The weight potential is logarithmic and the boundary conditions are thermal. The quantities are plotted for different numbers of particles N . The other parameters are fixed to $T = 1\text{K}$, $m = 10^{-30}\text{kg}$, $M = 100m$, $A = kT$, $L = 10^{-7}\text{m}$.

settings for T (temperature), A (potential strength), ... reveal the same behaviour. Therefore the observed qualitative behaviour appears to be valid in general. Moreover, the characteristics stay the same also for different weight potentials (e.g. linear, quadratic), which is confirmed by other simulations.

Looking back at Eq. 8.8 it is quite obvious that many particles lead to a more deterministic work output of the engine than few particles. The more particles act on the piston through this potential term, the more the piston will be pushed to the right. This is clear from the $1/X^2$ -dependence of the potential $e_n(X)$. Hence, the number of particles increases the coefficient of this dependence, leading to a stronger force that pushes the piston to the right. However, it could still be that the behaviour also changes because of less statistical fluctuations. Remember, in the case of a macroscopic gas, the work output is deterministic. It could be that this is mainly due to the high number of particles ($N \sim 10^{23}$) because in this regime standard thermodynamics applies.

A way to check whether it is just an effect of the higher potential or also an effect due to less fluctuations is to normalize the potential from Eq. 8.8 to

$$\tilde{e}_n(X) = \frac{1}{N} \sum_{i=1}^N \frac{\hbar^2 \pi^2 n_i^2}{2mX^2}. \quad (8.9)$$

Now the interaction potential is a mixture of N one-particle interaction potentials. Hence the mean interaction potential that the piston feels is the same as if there was only one particle. The only difference is that in each time step the interaction potential is closer to its mean than it was before.

Simulations show that the mean position and the standard deviation of a piston interacting with N particles through the potential in Eq. 8.9 does not differ from the one-particle case. We conclude that the many-particle case with the potential from Eq. 8.9 is effectively no different from the one-particle case for all N . Therefore, the different behaviour of the piston, if it interacts with more than one particle, comes only from the higher interaction potential which causes a stronger force pushing the piston to the right. Possible statistical differences do not contribute significantly. We believe that this is due to the very small time steps after which the particle is thermalized again. Due to this, we are sampling the Gibbs distribution very often and fluctuations due to this random process vanish after a short time.

8.2.2. Single-Particle Szilard Engine

The analysis with the many-particle Szilard engine suggests a possibility to make the work output more deterministic in the one-particle case. Since the effect of many particles can be reduced to a higher interaction potential $e_n(X)$, we know that a smaller mass of one particle m has the same effect: a decreasing mass of the particle m increases the coefficient in front of $1/X^2$ in the classical Hamiltonian of the piston from Eq. 7.1. This feature of our model says that the case of many particles is the same as the case

of one particle with very small mass. Simulations of a one-particle Szilard engine within our model with different particle masses confirm this.⁵

In a classical picture, a smaller particle mass m causes softer collisions of particle and piston. This is, if they collide, the piston will feel a weaker force pushing it to the right. On the other hand, the speed of a thermalized particle with smaller mass is higher because the energy it has is of the order $kT \sim \frac{1}{2}mv^2$. Therefore it interacts with the piston more often than a heavy particle. A classical analysis using a program from Johan Åberg simulating particle and piston as two classical particles in a one-dimensional box confirm this.⁶ Also there, a smaller mass of the particle lead a more localized piston close to the right wall of the box.

What the above results tell us is that, in order to bring the piston to the right more deterministically, a higher interaction rate is more effective than stronger interactions with the particles. This feature is independent of the chosen weight potential.

⁵We omit the plots for brevity.

⁶In contrast to our simulation, this simulation is not discretized in time. The program computes the exact solution for the classical equations of motion of particle and piston between two consecutive collisions. A collision can be between particle and left wall, particle and piston, or piston and right wall. The momentum of the particle is thermalized if it bounces into the left wall of the box. The piston is reflected elastically if it bounces into the right wall. Also the collisions between particle and piston are fully elastic.

9. Conclusion

We conclude the thesis with a short review of the main points treated in Part II. Particular attention is given to open question and possible topics of further research.

9.1. General Concepts

Autonomy In the long-term analysis from Section 8.2 we found out that a Szilard engine as it is modelled here can give a deterministic work output. Work was regarded as potential energy of the piston in a steady state. With a very small mass of the particle the piston reached a steady state with very small fluctuations. Arguing in a classical picture, this is the result of many weak interactions of particle and piston that lead to a quasi-static evolution of the piston. Therefore the piston's kinetic energy never became large. Due to the small fluctuations in the steady state, one does not have to stop the piston's evolution at a specific time in order to extract an almost optimal amount of work. Since a Szilard engine is autonomous by construction, this result can be seen as a proof of principle that self-contained work extraction procedures exist also in the case of very small (quantum) systems.

Friction It remains an open question whether the fluctuations in the piston's steady state can also be small if we use elastic boundary conditions. In our model of a Szilard engine we used thermal boundary conditions, which imply friction.¹ However, we believe that in a quasi-static evolution of the piston towards the a higher potential energy the situation should not change fundamentally if we leave away friction. In this case, the kinetic energy of the piston is never very high. Thus a friction process, which only changes the kinetic part of the piston's energy, has not a big influence. Classical simulations confirm this. Using the classical simulations from the program written by Johan Åberg we were able to investigate the behaviour of a classical microscopic Szilard engine with elastic boundary conditions. There, the piston never gained much kinetic energy. Instead, it evolved quasi-statically to the right side of the box due to many weak interactions with the much smaller particle. In this light, we believe that friction is not fundamental for successful work extraction in a Szilard engine.

If we think of friction in a fully quantum analysis of a Szilard engine, this would have to be described with a dissipator for the piston, similar to the ones we encountered in Section 1.2 when we treated small thermal machines. We were not able to investigate this any further because our model is not fully quantum. However, it would be interesting

¹They mimic friction because they keep the kinetic energy of the piston in the region of the typical thermal energy kT .

to see whether it is necessary to introduce a dissipator for the piston in a fully quantum model in order to extract work optimally.

Free Energy of the Particle In Section 8.1 we found that the difference in free energy of the quantum particle in a box was converted completely into kinetic and potential energy of the piston, that determines the size of the box that the particle is in. This is an interesting relation between the free energy of a quantum particle in a box and discrete simulation technique. First of all it confirms standard thermodynamics, which predicts this behaviour. Moreover, similar results for more abstract quantum systems have been proved in [15, 14, 48]. Thus it raises the question of how generic this result is. This would have to be found out in further research.

9.2. Our Model and Simulations

Born-Oppenheimer Approximation In all of our considerations we used the Born-Oppenheimer approximation. It models the interaction between particle and piston. The energy of the particle goes into the piston's (classical or quantum) Hamiltonian as a potential term. It is based on the assumption that the influence of the particle on the piston's state is very small and can be treated within a perturbative approach. It is not clear, however, whether this assumption is fulfilled by our physical system. After all, the interaction of the particle with the piston is the main point of the model. Nevertheless, the interaction can still be weak in the sense that each time the particle interacts with the piston the change in the piston's state is only small. This is actually the case in our model of discrete time steps, where in each time step the piston evolves just a tiny little bit under the influence of the interaction potential.

However, in the case of a very fast piston this assumption is certainly no longer fulfilled. The Born-Oppenheimer approximation neglects the kinetic energy of the heavy particle (the piston) in the calculation of the energy of the small particle. Hence, the approximation breaks down if the kinetic energy of piston is too large. This emphasizes how crucial it is in our model that the kinetic energy of the piston does not grow arbitrarily. The success of our model relies on a small kinetic energy of the piston. Thus, this can be seen as another reason why friction might be important in our model.

Effective Model In Section 8.1.2 we analyzed the results from the simulation with the help of an effective model. Instead of choosing the particle's state randomly after each time step and calculating the resulting force, we took an average effective force $\bar{\mathcal{F}}(X)$. We found that the results from the simulation gave exactly the outcomes predicted by this effective model. Our explanation for this is the following: the time steps in our simulations are very small and hence the particle thermalizes very fast. Thus, fluctuations due to thermalization are suppressed. But if this is the case, we can work with average values for the force from the beginning.

In a macroscopic Szilard engine many particles lead to small statistical fluctuations

whereas in a fully quantum setting the fast thermalization process of the particle corresponds to a strong dissipator. This raises the general question under which conditions it is allowed to approximate the time evolution of a system that interacts with a thermal bath and undergoes Hamiltonian evolution with an effective model.

Numerical Simulations In our model we chose a discrete simulation of the evolution of a classical piston because it was too difficult to model the time evolution of a fully quantum Szilard engine. This caused problems. Although we found cases where the simulations were stable and generated reliable results,² the numerics lead to unphysical behaviour of the piston under some circumstances. This was the case for the long-term behaviour of the piston if we imposed elastic boundary conditions at the walls of the box. There, the violation of energy conservation lead to a wild movement of the piston until the momentum was so high that the interaction with the particle no longer mattered. Furthermore, we were not able to simulate the evolution of the piston if we increased the size of the box for the analysis done in Section 8.1.³ We believe that this indicates that our simulations may only be valid for a short time-evolution and break down in the long-term limit.

²This was the case for instance in Section 8.1, where the energy of the piston coincides in a great measure with the difference in free energy of the particle. We conclude that the numerical simulations are stable in this case.

³This is discussed in Section 8.1

Bibliography

- [1] Noah Linden, Sandu Popescu, and Paul Skrzypczyk. How small can thermal machines be? The smallest possible refrigerator. *Phys. Rev. Lett.*, 105:130401, September 2010.
- [2] Paul Skrzypczyk, Nicolas Brunner, Noah Linden, and Sandu Popescu. The smallest possible refrigerator can reach maximal efficiency. *J. Phys. A: Math. Theor.*, 44, November 2011.
- [3] Sandu Popescu. Maximally efficient quantum thermal machines: The basic principles. September 2010. [arXiv:1009.2536\[quant-ph\]](https://arxiv.org/abs/1009.2536).
- [4] Noah Linden, Sandu Popescu, and Paul Skrzypczyk. The smallest possible heat engines. October 2010. [arXiv:1010.6029\[quant-ph\]](https://arxiv.org/abs/1010.6029).
- [5] Nicolas Brunner, Noah Linden, Sandu Popescu, and Paul Skrzypczyk. Virtual qubits, virtual temperatures, and the foundations of thermodynamics. *Phys. Rev. E*, 85:051117, May 2012.
- [6] Nicolas Léonard Sadi Carnot. *Réflexions sur la puissance motrice du feu et sur les machines propres à développer cette puissance*. Gauthier-Villars, 1824.
- [7] Rudolf Clausius. Über die bewegende Kraft der Wärme und die Gesetze, welche sich daraus für die Wärmelehre ableiten lassen (Part I). *Annalen der Physik*, 79:368–397, 1850.
- [8] Rudolf Clausius. Über die bewegende Kraft der Wärme und die Gesetze, welche sich daraus für die Wärmelehre ableiten lassen (Part II). *Annalen der Physik*, 79:500–524, 1850.
- [9] William Thomson. On the dynamical theory of heat, with numerical results deduced from Mr. Joule's equivalent of a thermal unit, and Mr. Regnault's observation on steam. *Math. and Phys. Papers*, 1:175–183, 1851.
- [10] Rudolf Clausius and Thomas Archer Hirst. *The Mechanical Theory of Heat: With Its Applications to the Steam-engine and to the Physical Properties of Bodies*. J. Van Voorst, 1867.
- [11] Jochen Gemmer, M. Michel, and Günther Mahler. *Quantum Thermodynamics: Emergence of Thermodynamic Behavior Within Composite Quantum Systems*. Lecture Notes in Physics. Springer Verlag, 2004.

- [12] Baidyanaith Misra and E. C. George Sudarshan. The Zeno's paradox in quantum theory. *Journal of Mathematical Physics*, 18:756–763, April 1977.
- [13] Johan Åberg. Catalytic Coherence. April 2013. [arXiv:1304.1060\[quant-ph\]](#).
- [14] Paul Skrzypczyk, Anthony J. Short, and Sandu Popescu. Extracting Work from Quantum Systems. February 2013. [arXiv:1302.2811\[quant-ph\]](#).
- [15] Johan Åberg. Truly work-like wok extraction via a single-shot analysis. *Nat. Commun.*, 4, June 2013.
- [16] Thomas Lawson. *A Theoretical and Experimental Study into Quantum Nonlocality, the Applications of Quantum Entanglement and the Thermodynamics of Small Systems*. PhD thesis, University of Bristol, 2011.
- [17] Nicolas Brunner, Marcus Huber, Noah Linden, Sandu Popescu, Ralph Silva, and Paul Skrzypczyk. Entanglement enhances performance in microscopic quantum fridges. May 2013. [arXiv:1305.6009\[quant-ph\]](#).
- [18] James Clerk Maxwell. *Theory of Heat*. Text-books of science. Longmans, Green, and co., 1872.
- [19] Charles H. Bennett. Logical reversibility of computation. *IBM Journal of Research and Development*, 17:525–532, 1973.
- [20] Marian Smoluchowski. Experimentell nachweisbare, der üblichen Thermodynamik widersprechende Molekularphänomene. *Physikalische Zeitschrift*, 13:1069–1080, 1912.
- [21] Marian Smoluchowski. *Prisma Mariana Smoluchowskiego (Collected Works of Marian Smoluchowski)*. PAU, Krakow, 1924–1928.
- [22] Leo Szilard. Über die Entropieverminderung in einem thermodynamischen System bei Eingriffen intelligenter Wesen. *Zeitschrift für Physik*, 53:840–856, 1929.
- [23] Dennis Gabor. *A Further Paradox: A Perpetuum Mobile of the Second Kind*. Reprinted in Leff and Rex (1990), pp. 109–115, 1951.
- [24] Leon Brillouin. Maxwell's Demon Cannot Operate: Information and Entropy. *Journal of Applied Physics*, 22:334–337, 1951.
- [25] Leon Brillouin. The Negentropy Principle of Information. *Journal of Applied Physics*, 24:1152–1163, 1953.
- [26] Leon Brillouin. *Science and Information Theory*. New York: Academic Press, 1962.
- [27] Harvey S. Leff and Andrew F. Rex. *Maxwell's demon: Entropy, information, computing*. Taylor and Francis, 1990.

- [28] Charles H. Bennett. Demons, Engines and the Second Law. *Scientific American*, 257:108–116, November 1987.
- [29] Charles H. Bennett. The thermodynamics of computation—a review. *International Journal of Theoretical Physics*, 21(12):905–940, 1982.
- [30] Rolf Landauer. Irreversibility and Heat Generation in the Computing Process. *IBM J. Res. Develop.*, 5:183–191, 1961.
- [31] Charles H. Bennett. Notes on Landauer’s principle, reversible computation and Maxwell’s demon. *Studies in History and Philosophy of Modern Physics*, 34:501–510, 2003.
- [32] John Earman and John D. Norton. Exorcist XIV: The wrath of Maxwell’s demon. Part II. From Szilard to Landauer and beyond. *Studies in the History and Philosophy of Modern Physics*, 30:1–40, 1999.
- [33] John Earman and John D. Norton. Exorcist XIV: The wrath of Maxwell’s demon. Part I. From Maxwell to Szilard. *Studies in the History and Philosophy of Modern Physics*, 29:435–471, 1998.
- [34] David Reeb and Michael M. Wolf. (Im-) Proving Landauer’s Principle. June 2013. [arXiv:1306.4352\[quant-ph\]](https://arxiv.org/abs/1306.4352).
- [35] Philippe Faist, Frédéric Dupuis, Jonathan Oppenheim, and Renato Renner. A Quantitative Landauer’s Principle. November 2012. [arXiv:1211.1037v1\[quant-ph\]](https://arxiv.org/abs/1211.1037v1).
- [36] Sang Wook Kim, Takahiro Sagawa, Simone De Liberato, and Masahito Ueda. Quantum szilard engine. *Phys. Rev. Lett.*, 106:070401, February 2011.
- [37] Robert Alicki, Michał Horodecki, Paweł Horodecki, and Ryszard Horodecki. Thermodynamics of quantum information systems — Hamiltonian description. *Open Systems & Information Dynamics*, 11:205–217, 2004.
- [38] Robert Alicki. Model of quantum measurement and thermodynamical cost of accuracy and stability of information processing. May 2013. [arXiv:1305.4910\[quant-ph\]](https://arxiv.org/abs/1305.4910).
- [39] Philipp Kammerlander. Work Extraction from Pure Qubits. Semester Thesis, ETH Zurich, 2012.
- [40] Bettina Meyer. Work Extraction from Pure Qubits in Ion Traps. Master’s thesis, ETH Zurich, March 2013.
- [41] Roee Ozeri. Tutorial: The trapped-ion toolbox. June 2011. [arXiv:1106.1190v1\[quant-ph\]](https://arxiv.org/abs/1106.1190v1).

- [42] D. J. Wineland, M. Barrett, J. Britton, J. Chiaverini, B. de Marco, W. M. Itano, B. Jelenković, C. Langer, D. Leibfried, V. Meyer, T. Rosenband, and T. Schätz. Quantum information processing with trapped ions. March 2003. [arXiv:quant-ph/0212078v2](https://arxiv.org/abs/quant-ph/0212078v2).
- [43] David J. Wineland. Quantum information processing and quantum control with trapped atomic ions. *Physica Scripta*, 2009(T137):014007, 2009.
- [44] Johan Åberg. A little something about particles and a piston. April 2009.
- [45] Achim Klenke. *Wahrscheinlichkeitstheorie*. Springer London, Limited, 2008.
- [46] Torsten Fließbach. *Statistische Physik*. Lehrbuch zur Theoretischen Physik. Spektrum Akademischer Verlag GmbH, 1999.
- [47] Max Born and Robert Oppenheimer. Zur Quantentheorie der Moleküle. *Annalen der Physik*, 389.
- [48] Michał Horodecki and Jonathan Oppenheim. Fundamental limitations for quantum and nanoscale thermodynamics. *Nat. Commun.*, 4, June 2013.
- [49] Edward John Routh. *A Treatise on the Stability of a Given State of Motion: Particularly Steady Motion*. London, Macmillan, 1877.
- [50] Adolf Hurwitz. Über die Bedingungen, unter welchen eine Gleichung nur Wurzeln mit negativen reellen Teilen besitzt. *Mathematische Annalen*, 46:273–284, 1885.
- [51] George B. Arfken and Hans J. Weber. *Mathematical Methods for Physicists*. Elsevier Academic Press, 2005.
- [52] Lídia del Rio, Johan Åberg, Renato Renner, Oscar Dahlsten, and Vlatko Vedral. The thermodynamic meaning of negative entropy. *Nature*, 474:61–63, 2011.
- [53] Heinz Peter Breuer and Francesco Petruccione. *The Theory of Open Quantum Systems*. Oxford University Press on Demand, 2002.

Part III.

Appendices

A. Notation

k	Boltzmann constant, $k \approx 1.38 \cdot 10^{-23} \text{ J/K}$
\hbar	reduced Planck constant, $\hbar \approx 1.054 \cdot 10^{-34} \text{ J} \cdot \text{s}$
T_c, T_r, T_h	cold, room and hot temperature, $T_c < T_r < T_h$
β	inverse temperature $\beta = 1/kT$
Q^\uparrow, Q^\downarrow	heat brought to or taken from a thermal machine, respectively
U	internal energy of a physical system
η	efficiency of a thermal machine
τ	Gibbs state (thermal state) of a finite dimensional system (e.g. a qubit)
\mathcal{Z}	partition sum or partition function
H_{int}	interaction Hamiltonian
\mathcal{E}	completely positive trace preserving map (CPTPM)
ρ	density matrix, quantum state of a system
ρ^S	steady state of a quantum system ($\frac{\partial \rho^S}{\partial t} = 0$)
$\mathcal{D}(\rho)$	dissipator (from a master equation)
L	length of the Szilard box
V_{weight}	weight potential that the piston feels, used to define work
m	mass of the particle in the Szilard engine
x	position coordinate of the particle in the Szilard engine
p	momentum coordinate of the particle in the Szilard engine
M	mass of the piston in the Szilard engine
X	position coordinate of the piston in the Szilard engine
P	momentum coordinate of the piston in the Szilard engine
$h(X)$	Hamiltonian of the particle with the piston's position as a parameter
$F, F(h(X))$	free energy in general and in the case of a particle in a box of length X
ΔF	$F(h(L/2)) - F(h(L))$, difference in free energy of a quantum particle in a box of length $L/2$ and L
$e_n(X)$	eigenenergies of a free quantum particle in a box of length X

n	integer numbering the eigenstate of a particle in a box
$\vartheta_3(u, q)$	elliptic theta function
H_n	Hamiltonian of the piston in the Born-Oppenheimer approximation with the particle in state n
$E_{n,k}$	eigenenergy of the k^{th} eigenstate of particle and piston in the Born-Oppenheimer approximation if the particle is in the n^{th} eigenstate
J_ν, Y_ν	Bessel functions of the first and second kind, respectively
ν_n	$\nu_n = \frac{1}{2} \sqrt{1 + 4 \frac{M}{m} \pi^2 n^2}$
$z_{n,k}$	k^{th} zero of the Bessel function J_{ν_n}
$L_n^{(\alpha)}$	associated Laguerre polynomial
$U(a, b, y)$	confluent hypergeometric function U with argument y
g	$g = \sqrt{\frac{2M\alpha}{\hbar^2}}$, where α is the potential strength of a quadratic potential
$b_{n,k}$	(positive) coefficients such that $L_{b_{n,k}}^{(\nu_n)}(gL^2) = 0$
Δt	discrete time step in numerical simulations of the piston's evolution
A	potential strength of the logarithmic weight potential the piston feels in our simulations

B. Calculations for Part I

B.1. Analytical Solution for the Heat Engine

We give a complete analytical derivation of the relevant quantities arising from the master equation

$$\frac{\partial \rho}{\partial t} = -i[H_0 + H_{\text{int}}, \rho] + \sum_{i=2}^3 \mathcal{D}_i(\rho) \quad (\text{B.1})$$

where

$$\begin{aligned} H_0 &= H_1 + H_2 + H_3 = \sum_{n=-\infty}^{\infty} nE_1|n\rangle\langle n|_1 + E_2|1\rangle\langle 1|_2 + E_3|1\rangle\langle 1|_3, \\ H_{\text{int}} &= g \sum_{n=-\infty}^{\infty} \left(|n, 10\rangle\langle n+1, 01| + |n+1, 01\rangle\langle n, 10| \right), \quad \text{and} \\ \mathcal{D}_i(\rho) &= p_i (\tau_i \otimes \text{Tr}_i \rho - \rho). \end{aligned} \quad (\text{B.2})$$

System 1 consists of infinitely many equidistant energy levels $|n\rangle$, $n = -\infty, \dots, \infty$, with energy gap E_1 . Systems 2 and 3 are qubits with energy gaps E_2 and E_3 , and interact with heat baths at temperature $T_2 = T_h$ and $T_3 = T_c$, respectively, via the dissipator \mathcal{D}_i . The number p_i determine the strengths of the interaction between the qubits and the heat baths, g is the interaction strength between the qubits. By assumption it holds $T_h > T_c$. The interaction is energy conserving, because we chose the energy gaps to fulfil $E_1 + E_3 = E_2$.

In the following we introduce notation. We define for $i = 2, 3$

$$r_i = \frac{1}{1 + e^{-\frac{E_i}{T_i}}} \equiv \frac{1}{\mathcal{Z}_i}, \quad (\text{B.3})$$

\mathcal{Z}_i the partition sum if qubit i . As it turned out during the treatment of the heat engine, the relevant quantities of the model are

$$\begin{aligned} \Delta(t) &= \sum_n \left(\langle n, 10 | \rho | n+1, 01 \rangle - \langle n+1, 01 | \rho | n, 10 \rangle \right), \\ \Gamma_2(t) &= \sum_n \left(\langle n, 00 | \rho | n, 00 \rangle + \langle n, 01 | \rho | n, 01 \rangle \right), \\ \Gamma_3(t) &= \sum_n \left(\langle n, 00 | \rho | n, 00 \rangle + \langle n, 10 | \rho | n, 10 \rangle \right). \end{aligned} \quad (\text{B.4})$$

$\Delta(t)$ is related to the increase of energy in system 1 by $\frac{d}{dt}\langle H_1 \rangle = -igE_1\Delta(t)$. The other two quantities are the ground state populations of qubit i for $i = 2, 3$, which are determined by $\Gamma_i(t) = \text{Tr}(H_i\rho(t))$.

Now we use the master equation from above to find expressions for the time derivatives of the above quantities. They can be written as a linear system:

$$\frac{d}{dt} \begin{pmatrix} \Delta(t) \\ \Gamma_2(t) \\ \Gamma_3(t) \end{pmatrix} = \underbrace{\begin{pmatrix} -(p_2 + p_3) & -2ig & 2ig \\ -ig & -p_2 & 0 \\ ig & 0 & -p_3 \end{pmatrix}}_{=:A} \begin{pmatrix} \Delta(t) \\ \Gamma_2(t) \\ \Gamma_3(t) \end{pmatrix} + \underbrace{\begin{pmatrix} 0 \\ r_2 p_2 \\ r_3 p_3 \end{pmatrix}}_{=:b}. \quad (\text{B.5})$$

The general solution of such a system of equations is

$$\begin{pmatrix} \Delta(t) \\ \Gamma_2(t) \\ \Gamma_3(t) \end{pmatrix} = \sum_{j=1}^3 c_j e^{\lambda_j t} \mathbf{v}_j + \begin{pmatrix} C_1 \\ C_2 \\ C_3 \end{pmatrix}, \quad (\text{B.6})$$

where λ_j are the eigenvalues of the matrix A and \mathbf{v}_j the eigenvectors, c_j are given by the initial conditions and the C_j are determined by A and \mathbf{b} . The eigenvalues are the solutions of the characteristic equation

$$(\lambda + p_2 + p_3)(\lambda + p_2)(\lambda + p_3) + 2g^2(2\lambda + p_2 + p_3) = 0. \quad (\text{B.7})$$

Hence, the λ_j are the roots of the third-order polynomial

$$\underbrace{1}_{=:a_3} \cdot \lambda^3 + \underbrace{2(p_2 + p_3)}_{=:a_2} \lambda^2 + \underbrace{((p_2 + p_3)^2 + p_2 p_3 + 4g^2)}_{=:a_1} \lambda + \underbrace{(p_2 + p_3)(p_2 p_3 + 2g^2)}_{=:a_0}. \quad (\text{B.8})$$

From the Routh-Hurwitz criterion [49, 50] we know that all roots of a third-order polynomial have negative real part if $a_3, a_2, a_1, a_0 > 0$ and $a_2 a_1 > a_3 a_0$. The coupling constants g, p_2, p_3 are by definition positive, leading to positive coefficients of the polynomial. The second part of the criterion is also fulfilled:

$$a_1 a_2 - a_3 a_0 = (p_2 + p_3)(2(p_2 + p_3)^2 + 2p_2 p_3 + 8g^2 - 2g^2 - p_2 p_3) > 0 \quad (\text{B.9})$$

$$\forall g, p_2, p_3 > 0.$$

Now that we know that all eigenvalues have negative real part, it is easier to find the constants C_1, C_2, C_3 . In the limit $t \rightarrow \infty$ the first part of Eq. B.6 vanishes. Hence, the capital constants must fulfil

$$0 = A \begin{pmatrix} C_1 \\ C_2 \\ C_3 \end{pmatrix} + \mathbf{b}. \quad (\text{B.10})$$

From this it is straight forward to get to the long time behaviour

$$\begin{aligned}\lim_{t \rightarrow \infty} \Delta(t) &= \frac{2igp_2p_3(r_3 - r_2)}{(p_2 + p_3)(2g^2 + p_2p_3)}, \\ \lim_{t \rightarrow \infty} \Gamma_i(t) &= \frac{p_2p_3(p_3 - p_2)r_i + 2g^2(p_2r_2 + p_3r_3)}{(p_2 + p_3)(2g^2 + p_2p_3)}.\end{aligned}\tag{B.11}$$

With this it is now possible to find the long time behaviour of the time derivative of the mean internal energy and the rates of the heat flow between qubit i and its heat bath:

$$\begin{aligned}\frac{d}{dt}\langle H_1 \rangle &= \text{Tr}(H_1\rho(t)) = -igE_1\Delta(t), \\ \frac{d}{dt}Q_i &= p_i\text{Tr}(H_i(\tau_i - \rho_i(t))) = p_iE_i(\Gamma_i(t) - r_i).\end{aligned}\tag{B.12}$$

In a very similar but more complicated calculation one can find that the spread of the population in system one behaves in the long time limit as

$$\frac{d}{dt}\langle(H_1 - \langle H_1 \rangle)^2\rangle = \text{const.} > 0.\tag{B.13}$$

Hence, the standard deviation from the mean energy in system 1 grows slower than the mean energy itself, namely it grows as \sqrt{t} for long times whereas the mean energy grows as t .

B.2. Optimal Work Extraction with the Protocol by Skrzypczyk et al.

We show that in the limit $N \rightarrow \infty$ the extractable work from one degenerate pure qubit is $kT \ln 2$ with the protocol suggested by Paul Skrzypczyk *et al.* [14] The initial state of the system shall be

$$\rho_{\text{in}} = |0\rangle\langle 0|_S \otimes \left(\bigotimes_{i=1}^N \tau_{B_i} \right) \otimes |0\rangle\langle 0|_W, \quad (\text{B.14})$$

where τ_{B_i} are the thermal states of the bath qubits with Hamiltonians

$$H_{B_i} = kT \ln \left(\frac{1 - r_i}{r_i} \right) |1\rangle\langle 1|_{B_i} \equiv E_i |1\rangle\langle 1|_{B_i}, \quad \text{where } r_i = \frac{i}{2N}, \quad (\text{B.15})$$

which are such that the excitation probability of these qubits increases linearly from 0 to $\frac{1}{2}$ in steps of $\frac{1}{2N}$. By the assumptions from Section 2.4.2 w.l.o.g. the initial state of the weight is $|0\rangle_W$.

We calculate explicitly the average energy of the storage system after one step. This is, after we applied U_1 to the subsystem SB_1W , where

$$\begin{aligned} U_1 = & |01\rangle\langle 10|_{SB_1} \otimes \Gamma_{-E_1} + |10\rangle\langle 01|_{SB_1} \otimes \Gamma_{E_1} \\ & + (|00\rangle\langle 00|_{SB_1} + |11\rangle\langle 11|_{SB_1}) \otimes \mathbb{1}_W. \end{aligned} \quad (\text{B.16})$$

The global state of SB_1W after one step is then

$$\begin{aligned} \text{Tr}_{B_2 \dots B_N} (U_1 \rho_{\text{in}} U_1^\dagger) = & r_1 |1\rangle\langle 1|_S \otimes |0\rangle\langle 0|_{B_1} \otimes |E_1\rangle\langle E_1|_W \\ & + (1 - r_1) |0\rangle\langle 0|_S \otimes |0\rangle\langle 0|_{B_1} \otimes |0\rangle\langle 0|_W \end{aligned} \quad (\text{B.17})$$

where we wrote U_1 instead of $U_1 \otimes \mathbb{1}_{B_2} \otimes \dots \otimes \mathbb{1}_{B_N}$ for readability. This yields the reduced state for the weight

$$(1 - r_1) |0\rangle\langle 0|_W + r_1 |E_1\rangle\langle E_1|_W. \quad (\text{B.18})$$

Hence, the average energy in W after one step is

$$\langle E \rangle_W = \text{Tr} (H_W U_1 \rho_{\text{in}} U_1^\dagger) = r_1 E_1, \quad (\text{B.19})$$

where we assume again that we started in the state $|0\rangle_W$. By induction it is straight forward to prove that the average energy in W after N steps is

$$\langle E \rangle_W = \text{Tr} (H_W U_N \cdots U_1 \rho_{\text{in}} U_1^\dagger \cdots U_N^\dagger) = \sum_{i=1}^N (r_i - r_{i-1}) E_i, \quad (\text{B.20})$$

where $r_0 = 0$. Instead of investigating how this result actually looks we go directly to the case of arbitrary large N . There:

$$\begin{aligned}
\lim_{N \rightarrow \infty} \langle E \rangle_W &= \lim_{N \rightarrow \infty} \frac{kT}{2N} \sum_{i=1}^N \ln \left(\frac{1 - \frac{i}{2N}}{\frac{i}{2N}} \right) \\
&= \frac{kT}{2} \int_0^1 dx \ln \left(\frac{1 - \frac{x}{2}}{\frac{x}{2}} \right) \\
&= \frac{kT}{2} \left[x \ln \left(\frac{2}{x} - 1 \right) - 2 \ln(2-x) \right]_0^1 \\
&= kT \ln 2.
\end{aligned} \tag{B.21}$$

In the second line we used that any Riemann integrable function f satisfies

$$\lim_{N \rightarrow \infty} \frac{1}{N} \sum_{i=1}^N f \left(\frac{i}{N} \right) = \int_0^1 dx f(x). \tag{B.22}$$

Hence, in the limit of infinitely many bath qubits, which lead to infinitesimally small steps in the protocol, the amount of extractable work becomes maximal. This shows that the protocol is optimal.

Furthermore, by computing the final reduced state of the degenerate qubit S one finds

$$\text{Tr}_{B_1 \cdots B_N W} \left(U_N \cdots U_1 \rho_{\text{in}} U_1^\dagger \cdots U_N^\dagger \right) = (1 - r_N)|0\rangle\langle 0|_S + r_N|1\rangle\langle 1|_S = \frac{\mathbb{I}_S}{2} \tag{B.23}$$

because $r_N = \frac{1}{2}$. Thus, the final state of qubit S is the fully mixed state, as it must be, since the maximal amount of work was extracted using only this system as information resource.

C. Calculations for Part II

C.1. Classical Statistical Analysis

C.1.1. Single Particle and Piston

The analysis done here is taken from [44]. Consider two particles with masses m and M ($M \gg m$) that evolve according to the classical Hamiltonian

$$H(x, X, p, P) = \frac{p^2}{2m} + \frac{P^2}{2M} + V(x, X). \quad (\text{C.1})$$

V is some potential modelling a repulsive interaction between the particles as well as boundaries given by a box of length L . Furthermore, V will also contain a weight potential term that the piston (the heavier particle) feels.

Let k be the Boltzmann constant. To describe the thermal system we use the canonical ensemble with probability density

$$f_\beta(x, X, p, P) = \frac{e^{\beta H(x, X, p, P)}}{\mathcal{Z}(\beta)}, \quad (\text{C.2})$$

where $\beta = \frac{1}{kT}$ the inverse temperature and $\mathcal{Z}(\beta)$ the partition function,

$$\begin{aligned} \mathcal{Z}(\beta) &= \int dx \int dX \int dp \int dP e^{-\beta H(x, X, p, P)} \\ &= \int dx \int dX \int dp \int dP e^{-\beta \left(\frac{p^2}{2m} + \frac{P^2}{2M} + V(x, X) \right)} \\ &= \underbrace{\int dp e^{-\beta \frac{p^2}{2m}}}_{\mathcal{Z}_{\text{mom},p}(\beta)} \underbrace{\int dP e^{-\beta \frac{P^2}{2M}}}_{\mathcal{Z}_{\text{mom},P}(\beta)} \underbrace{\int dx \int dX e^{-\beta V(x, X)}}_{\mathcal{Z}_{\text{pos}}(\beta)}. \end{aligned} \quad (\text{C.3})$$

From that we see that we can write

$$f_\beta(x, X, p, P) = f_\beta(p)f_\beta(P)f_\beta(x, X) \quad (\text{C.4})$$

with marginal distributions¹

$$\begin{aligned} f_\beta(p) &= \frac{e^{-\beta \frac{p^2}{2m}}}{\int dp e^{-\beta \frac{p^2}{2m}}} = \sqrt{\frac{\beta}{2\pi m}} e^{-\beta \frac{p^2}{2m}} \\ f_\beta(P) &= \frac{e^{-\beta \frac{P^2}{2M}}}{\int dP e^{-\beta \frac{P^2}{2M}}} = \sqrt{\frac{\beta}{2\pi M}} e^{-\beta \frac{P^2}{2M}} \\ f_\beta(x, X) &= \frac{e^{-\beta V(x, X)}}{\mathcal{Z}_{\text{pos}}(\beta)}. \end{aligned} \quad (\text{C.5})$$

The momenta are normal distributed with standard deviation

$$\sigma_p = \sqrt{\frac{m}{\beta}} \quad \text{and} \quad \sigma_P = \sqrt{\frac{M}{\beta}}. \quad (\text{C.6})$$

When considering velocities $v = p/m$ and $V = P/M$ instead of momenta we have to transform

$$\sqrt{\frac{\beta}{2\pi m}} e^{-\beta \frac{p^2}{2m}} dp = \sqrt{\frac{\beta}{2\pi m}} e^{-\beta \frac{p^2}{2m}} mdv = \sqrt{\frac{m\beta}{2\pi}} e^{-\beta \frac{mv^2}{2}} dv, \quad (\text{C.7})$$

and the same for P and M . Hence, the standard deviation for the velocities v and V are

$$\sigma_v = \sqrt{\frac{1}{\beta m}} \quad \text{and} \quad \sigma_V = \sqrt{\frac{1}{\beta M}}, \quad (\text{C.8})$$

respectively. From now on we consider the potential

$$V(x, X) = \begin{cases} \alpha X & \text{if } 0 < x \leq X \leq L, \\ +\infty & \text{otherwise.} \end{cases} \quad (\text{C.9})$$

With this potential:

$$\begin{aligned} \mathcal{Z}_{\text{pos}}(\beta) &= \int_{-\infty}^{\infty} dx \int_{-\infty}^{\infty} dX e^{-\beta V(x, X)} \\ &= \int_0^L dX \int_0^X dx e^{-\beta \alpha X} \\ &= \int_0^L dX X e^{-\beta \alpha X} \end{aligned} \quad (\text{C.10})$$

¹Here, we used a sloppy notation for the factors in the probability density. Although the symbols for the factors stay the same (namely f_β), the three functions in Eq. C.5 are not the same. The arguments x , X , p or P determine, which function is meant. However, it should be clear from the context anyway.

and hence the marginal distribution of the piston is

$$f_\beta(X) = \frac{X e^{-\beta\alpha X}}{\int_0^L dX X e^{-\beta\alpha X}} = \frac{\tilde{X} e^{-c\tilde{X}}}{\int_0^1 d\tilde{X} \tilde{X} e^{-c\tilde{X}}}, \quad \text{for } 0 \leq \tilde{X} = \frac{X}{L} \leq 1, \quad (\text{C.11})$$

where we introduced the normalized position $\tilde{X} = X/L$ and the dimensionless parameter

$$c = \beta\alpha L = \frac{\alpha L}{kT}. \quad (\text{C.12})$$

Using the *lower incomplete gamma function* $\gamma(s, r) = \int_0^r dt t^{s-1} e^{-t}$, the marginal probability density can be written as

$$f_\beta(\tilde{X}) = \frac{c^2}{\gamma(2, c)} \tilde{X} e^{-c\tilde{X}}, \quad (\text{C.13})$$

where we used

$$\int_0^1 d\tilde{X} \tilde{X} e^{-c\tilde{X}} \stackrel{[y=c\tilde{X}]}{=} \frac{1}{c^2} \int_0^c dy ye^{-y} = \frac{\gamma(2, c)}{c^2}. \quad (\text{C.14})$$

For very high temperature (or for very small α) $c \approx 0$ and thus $e^{-c\tilde{X}} \approx 1$ on the interval $[0, 1]$. Hence, in this case $f_\beta(\tilde{X}) \approx 2\tilde{X}$.

C.1.2. Many Particles and Piston

Consider now N non-interacting particles of mass m and a piston of mass M described by the Hamiltonian

$$H(x_1, \dots, x_N, X, p_1, \dots, p_N, P) = \sum_{i=1}^N \frac{p_i^2}{2m} + \frac{P^2}{2M} + V(x_1, \dots, x_N, X). \quad (\text{C.15})$$

Suppose the position coordinates are confined to $x_1, \dots, x_N, X \in [0, \infty)$ and the potential is given by

$$V(x_1, \dots, x_N, X) = \begin{cases} \alpha X & \text{if } \max(x_1, \dots, x_N) \leq X \leq L, \\ +\infty & \text{otherwise.} \end{cases} \quad (\text{C.16})$$

The position part of the canonical partition function is then

$$\begin{aligned} \mathcal{Z}_{\text{pos}}(\beta) &= \int_0^\infty dx_1 \cdots \int_0^\infty dx_N \int_0^\infty dX e^{-\beta V(x_1, \dots, x_N, X)} \\ &= \int_0^L dX \int_0^X dx_1 \cdots \int_0^X dx_N e^{-\beta\alpha X} \\ &= \int_0^L dX X^N e^{-\beta\alpha X}. \end{aligned} \quad (\text{C.17})$$

Using again the normalized position $\tilde{X} = X/L$, the marginal distribution of the piston can be expressed as

$$f_\beta(\tilde{X}) = \frac{\tilde{X}^N e^{-c\tilde{X}}}{\int_0^1 d\tilde{X} \tilde{X}^N e^{-c\tilde{X}}} = \frac{c^{N+1} \tilde{X}^N e^{-c\tilde{X}}}{\int_0^c dy y^N e^{-y}} = \frac{c^{N+1}}{\gamma(N+1, c)} \tilde{X}^N e^{-c\tilde{X}}. \quad (\text{C.18})$$

Again we made use of the lower incomplete gamma function to express the final result. For $c \approx 0$, i.e. for high temperature compared to the maximal potential energy of the piston we find $f_\beta(\tilde{X}) \approx (N+1)\tilde{X}^N$.

C.1.3. Many Particles and Piston without Upper Bound

If there is no upper bound for the piston the potential then changes to

$$V(x_1, \dots, x_N, X) = \begin{cases} \alpha X & \text{if } \max(x_1, \dots, x_N) \leq X, \\ +\infty & \text{otherwise.} \end{cases} \quad (\text{C.19})$$

Hence, the position part of the partition function is

$$\begin{aligned} \mathcal{Z}_{\text{pos}}(\beta) &= \int_0^\infty dx_1 \cdots \int_0^\infty dx_N \int_0^\infty dX e^{-\beta V(x_1, \dots, x_N, X)} \\ &= \int_0^\infty dX \int_0^X dx_1 \cdots \int_0^X dx_N e^{-\beta \alpha X} \\ &= \int_0^\infty dX X^N e^{-\beta \alpha X} \\ &= \frac{1}{(\beta \alpha)^{N+1}} \int_0^\infty dy y^N e^{-y} = \frac{N!}{(\beta \alpha)^{N+1}}. \end{aligned} \quad (\text{C.20})$$

The marginal distribution of the piston's position is described by the *gamma distribution* $g(x; l, \theta) = \frac{x^{l-1} e^{-x/\theta}}{\theta^l \Gamma(l)}$, where in our case $\theta = \frac{1}{\beta \alpha}$ and $l = N+1$:

$$f_\beta(X) = \frac{(\beta \alpha)^{N+1}}{N!} X^N e^{-\beta \alpha X}. \quad (\text{C.21})$$

Since we deal with a gamma distribution we can use existing formulas to compute the mean position and standard deviation of the position of the piston [45]

$$\begin{aligned} \langle X \rangle &= l\theta = (N+1) \frac{kT}{\alpha} \\ \sqrt{\langle (X - \langle X \rangle)^2 \rangle} &= \sqrt{l\theta^2} = \sqrt{N+1} \frac{kT}{\alpha}. \end{aligned} \quad (\text{C.22})$$

Thus, taking the standard deviation divided by the mean position as a measure of relative fluctuations we arrive at

$$\frac{\sqrt{\langle (X - \langle X \rangle)^2 \rangle}}{\langle X \rangle} = \frac{1}{\sqrt{N+1}}. \quad (\text{C.23})$$

C.2. Static Analysis in the Born-Oppenheimer Approximation

C.2.1. No Weight

We consider first $V_{\text{weight}} = 0$. The Schrödinger equation of the piston is

$$E_{n,k} \Psi_{n,k}(X) = -\frac{\hbar^2}{2M} \Psi''_{n,k}(X) + \frac{\hbar^2 \pi^2 n^2}{2m X^2} \Psi_{n,k}(X), \quad (\text{C.24})$$

with boundary conditions $\Psi(0) = 0 = \Psi(L)$. The integer k stands for the eigenstate of the piston whereas n is (as before) the number of the eigenstate of the particle.² Substituting $\Phi(X) = \frac{\Psi(X)}{\sqrt{X}}$ and $Z = \sqrt{\frac{2ME}{\hbar^2}} X$ yields Bessel's differential equation

$$Z^2 \frac{d^2 \Phi}{dZ^2} + Z \frac{d\Phi}{dZ} + \left(Z^2 - \left(\frac{M}{m} \pi^2 n^2 + \frac{1}{4} \right) \right) \Phi = 0, \quad (\text{C.25})$$

a second-order linear ordinary differential equation. The general solution is

$$\Psi(X) = C_1 \sqrt{X} J_{\nu_n} \left(\sqrt{\frac{2ME}{\hbar^2}} X \right) + C_2 \sqrt{X} Y_{\nu_n} \left(\sqrt{\frac{2ME}{\hbar^2}} X \right), \quad (\text{C.26})$$

where we use the notation $\nu_n = \frac{1}{2} \sqrt{1 + 4 \frac{M}{m} \pi^2 n^2}$ for readability. J_ν and Y_ν are the *Bessel functions of the first and second kind*, respectively, and C_1, C_2 are constants that must be adjusted to meet the boundary conditions and to normalize the wave function.

For $0 < z \ll \sqrt{\nu + 1}$, $\nu \in \mathbb{R}$ the asymptotic behaviour of the Bessel functions is [51]

$$J_\nu(z) \sim \frac{1}{\Gamma(\nu + 1)} \left(\frac{z}{2} \right)^\nu \quad (\text{C.27})$$

$$Y_\nu(z) \sim \begin{cases} \frac{2}{\pi} (\ln(z/2) + \gamma) & \text{if } \nu = 0, \\ -\frac{\Gamma(\nu)}{\pi} \left(\frac{2}{z} \right)^\nu & \text{if } \nu > 0, \end{cases} \quad (\text{C.28})$$

where $\gamma = \lim_{l \rightarrow \infty} \left(\sum_{m=1}^l \frac{1}{m} - \ln(l) \right) \approx 0.577$ is the Euler-Mascheroni constant. From that we know that $C_2 = 0$ in order to fulfil the boundary condition $\Psi(0) = 0$, because

$$\sqrt{X} Y_{\nu_n} \left(\sqrt{\frac{2ME}{\hbar^2}} X \right) \rightarrow -\infty \quad \text{for } X \rightarrow 0, \quad (\text{C.29})$$

whereas

$$\sqrt{X} J_{\nu_n} \left(\sqrt{\frac{2ME}{\hbar^2}} X \right) \rightarrow 0 \quad \text{for } X \rightarrow 0. \quad (\text{C.30})$$

²We will omit $\{n, k\}$ from now on, unless it is necessary to write the indices explicitly.

With the second condition $\Psi(L) = 0$ we find the eigenenergies of the states. The eigenenergy $E_{n,k}$ must be such that $\sqrt{\frac{2ME_{n,k}}{\hbar^2}}L = z_{n,k}$, where $z_{n,k}$ denotes the k^{th} zero of the Bessel function J_{ν_n} . Thus, for each $n = 1, 2, \dots$ we end up with the orthonormal states:

$$\begin{aligned} \text{For } k = 1, 2, \dots \text{ we have eigenstates } \quad & \Psi_{n,k}(X) = C_{n,k} \sqrt{X} J_{\nu_n}(z_{n,k} \tilde{X}) \\ \text{with eigenenergies } \quad & E_{n,k} = \frac{\hbar^2 z_{n,k}^2}{2ML^2}, \end{aligned} \quad (\text{C.31})$$

where $\tilde{X} = \frac{X}{L}$ is the normalized position and $C_{n,k}$ is the normalization constant for the corresponding state.

The plots of the absolute square of the wave functions for different settings of $\frac{M}{m}$ and n can be found in Fig. 22.

C.2.2. Quadratic Potential

Here, we consider the potential $V_{\text{weight}}(X) = \alpha X^2$, leading to the Schrödinger equation for the piston

$$E_{n,k} \Psi_{n,k}(X) = -\frac{\hbar^2}{2M} \Psi''_{n,k}(X) + \left(\frac{\hbar^2 \pi^2 n^2}{2mX^2} + \alpha X^2 \right) \Psi_{n,k}(X). \quad (\text{C.32})$$

An example of this potential in a physical system is a spring with spring constant 2α attached to the piston leading to the energy αX^2 .

In order to arrive at a solvable differential equation we substitute

$$\Phi(X) = e^{\frac{1}{2}gX^2} \frac{\Psi(X)}{X^{\frac{1}{2}+\nu_n}} \quad \text{and} \quad Y = gX^2, \quad (\text{C.33})$$

where $g = \sqrt{\frac{2M\alpha}{\hbar^2}}$ and $\nu_n = \frac{1}{2}\sqrt{1 + 4\frac{M}{m}\pi^2 n^2}$ as before. This yields the differential equation

$$Y \frac{d^2\Phi}{dY^2} + (\nu_n + 1 - Y) \frac{d\Phi}{dY} + \left(\frac{e}{4g} - \frac{1}{2}(1 + \nu_n) \right) \Phi = 0, \quad (\text{C.34})$$

where $e = \frac{2ME}{\hbar^2}$. This is the generalized Laguerre equation which has two linearly independent solutions, the *associated Laguerre polynomial* $L_{\left(\frac{e}{4g}-\frac{1}{2}(1+\nu_n)\right)}^{(\nu_n)}(Y)$ and the *confluent hypergeometric function* $U(-\frac{e}{4g} + \frac{1}{2}(1 + \nu_n), 1 + \nu_n, Y)$.³ Hence the general

³Note that the associated Laguerre polynomial is no polynomial in the case of non-integer $\frac{e}{4g} - \frac{1}{2}(1 + \nu_n)$, but it is still well-defined.

solution of Eq. 6.6 is

$$\begin{aligned}\Psi(X) = X^{\frac{1}{2}+\nu_n} e^{-\frac{1}{2}gX^2} & \left[C_1 L_{\left(\frac{e}{4g}-\frac{1}{2}(1+\nu_n)\right)}^{(\nu_n)}(gX^2) \right. \\ & \left. + C_2 U\left(-\frac{e}{4g} + \frac{1}{2}(1+\nu_n), 1+\nu_n, gX^2\right) \right]\end{aligned}\quad (\text{C.35})$$

Similar to the solution without potential one of the functions has a singularity at $X = 0$. A calculation with Mathematica shows

$$\lim_{X \rightarrow 0^+} X^{\frac{1}{2}+\nu_n} e^{-\frac{1}{2}gX^2} U\left(-\frac{e}{4g} + \frac{1}{2}(1+\nu_n), 1+\nu_n, gX^2\right) = \infty \quad (\text{C.36})$$

for all possible settings of M, m, α, L and n . Hence, in order to satisfy the boundary condition $\Psi(0) = 0$ we need $C_2 = 0$:

$$\Psi(X) = CX^{\frac{1}{2}+\nu_n} e^{-\frac{1}{2}gX^2} L_{\left(\frac{e}{4g}-\frac{1}{2}(1+\nu_n)\right)}^{(\nu_n)}(gX^2), \quad (\text{C.37})$$

where C is the normalization constant. As before, the energy is determined by the second boundary condition, $\Psi(L) = 0$, i.e., E must be such that Ψ is zero when we input $X = L$. This time E does not show up in a multiplicative factor in front of the function's argument. Instead it is contained in the order b (as in $L_b^{(a)}$) specifying the associated Laguerre polynomial. This makes it somewhat harder to find the energies. While the zeros of the associated Laguerre polynomials for fixed orders a and b can be computed numerically, their behaviour with respect to changes in the order b is not very well-known. Nevertheless, Mathematica is able to determine them numerically for given parameters M, m, α, L and n . Suppose now we fix these parameters, then it is in principle possible to obtain parameters $b_{n,k}$ that satisfy $L_{b_{n,k}}^{(\nu_n)}(gL^2) = 0$. Notice that the $b_{n,k}$ are always positive. Choosing the energies $E_{n,k}$ such that

$$\frac{2ME_{n,k}}{4g\hbar^2} - \frac{1}{2}(1+\nu_n) = b_{n,k} \Leftrightarrow E_{n,k} = \frac{2g\hbar^2}{M} \left[b_{n,k} + \frac{1}{2}(1+\nu_n) \right], \quad (\text{C.38})$$

we end up with the analytic solution

$$\Psi_{n,k}(X) = C_{n,k} X^{\frac{1}{2}+\nu_n} e^{-\frac{1}{2}gX^2} L_{b_{n,k}}^{(\nu_n)}(gX^2). \quad (\text{C.39})$$

The plots of the squared wave function for different $\frac{M}{m}$ and n with respect to normalized position \tilde{X} can be found in see Fig. 23.

C.3. Analysis of Boundary Conditions

C.3.1. Elastic Boundary Conditions

A simple way of eliminating the problem of finding the piston outside $[0, L]$ is to check after each step whether X is inside the allowed region, and if not, to force the position of the piston to be inside $[0, L]$ again. For instance, for $L = 1$ and $(X, P) = (1.2, 0.3)$ one could reverse the momentum and set the coordinates to $(X, P) = (0.8, -0.3)$. This would correspond to an elastic reflection at the right wall. In pseudo code:

```
if X>L do                                % if X>L, reflect particle at wall
    X <- 2*L-X
    P <- -abs(P)
end

if X<0 do                                % if X<0, reflect particle at wall
    X <- abs(X)
    P <- abs(P)
end
```

But the elastic reflection bears additional problems. For sufficiently high momentum the piston may come to positions $X > 2L$ or even further to the right. A simple reflection at $X = L$, replacing X with $2L - X$ as in the above example is then no longer possible because it would lead to a negative value of X . One way to circumvent this problem is spooling the difference between X and L to the interval $[0, L]$. A pseudo code that does this is:

```
if X>L do                                % if X>L, break X down to a pos. in [0,2L]
    X <- L*mod(X/L,2)
    if X>L do                            % if now still X>L we 'reflect' again
        X <- 2L-X
        P <- -P
    end
end

if X<0 do                                % if X<0, break X down to a pos. in [0,2L]
    X <- L*mod(X/L,2)
    P <- -P                                % here we have to reverse the momentum
    if X>L do                            % if now X>L, reflect and reverse P again
        X <- 2*L-X
        P <- -P
    end
end
```

To illustrate what the above protocol does we give a few examples.

Example 1 For simplicity set $L = 1$. Suppose we arrive at $(X, P) = (-1.7, P)$ after step k . Then the above protocol changes position and momentum to $(X, P) = (0.3, P)$. This corresponds to two reflections, the first at the left wall at $X = 0$ and the second at the right wall at $X = L$. Hence the momentum is not reversed in this example.

Example 2 Suppose we arrive at $(X, P) = (3.4, P)$ after step k . Then the above protocol changes position and momentum to $(X, P) = (0.6, -P)$ corresponding to three reflections, the first and the third at right wall and the second at the left wall. The final direction of momentum is thus reversed.

The first example already indicates why this procedure of reflections might lead to problems. If the piston has a very high momentum, it will be at a position outside the box after each time step because the elastic boundary conditions do not change the momentum. This is an unphysical behaviour, because then the piston no longer interacts with the particle. Fig. 29 (a) shows how this looks in our model. In the case of zero weight potential, usually after 15'000 steps of $\Delta t = 5 \cdot 10^{-13}$ s the problem occurs. The momentum of the piston is so high that the piston leaves the box to the left at every time step. This leads to an unnatural behaviour.

We believe that this is due to numerical instabilities of our procedure. Numerical simulation are in general vulnerable to errors. In particular, the simple stepwise simulation of a differential equation is not necessarily stable. This means that small errors, which will certainly be introduced in our procedure, lead to a large deviation in the final result. What is even more difficult is the simulation of the long-term behaviour of systems as we want to do it here. In this case, small errors that happen many times have an even bigger impact. Such small errors are for instance the violation of conservation laws. While in a continuous time evolution energy is conserved in a closed system, this is not necessarily the case for discrete time evolution. Especially if the potential is very steep, one discrete time step can lead to a fatal violation of energy conservation. The interaction potential that the piston feels goes as $1/X^2$. Hence, if the piston comes close to the left wall, this potential becomes very steep. Therefore energy conservation is no longer guaranteed for this case in our model.

In contrast to this, for inelastic boundary conditions the piston does reach a steady state, as can be seen in Fig. 29 (b).

C.3.2. Inelastic Boundary Conditions

One could imagine that the wall is inelastic and slows the piston down, i.e., that if $X > L$ we reset $X = L$ and $P = 0$. On the left side resetting the piston's position to $X = 0$ is no option because the potential it feels is proportional to $\frac{1}{X^2}$ (see Eq. 5.5 and Eq. 7.1). But this can be circumvented by postulating a minimal distance ε from the origin.⁴ We

⁴This can be thought of as the ‘size’ of the particle.

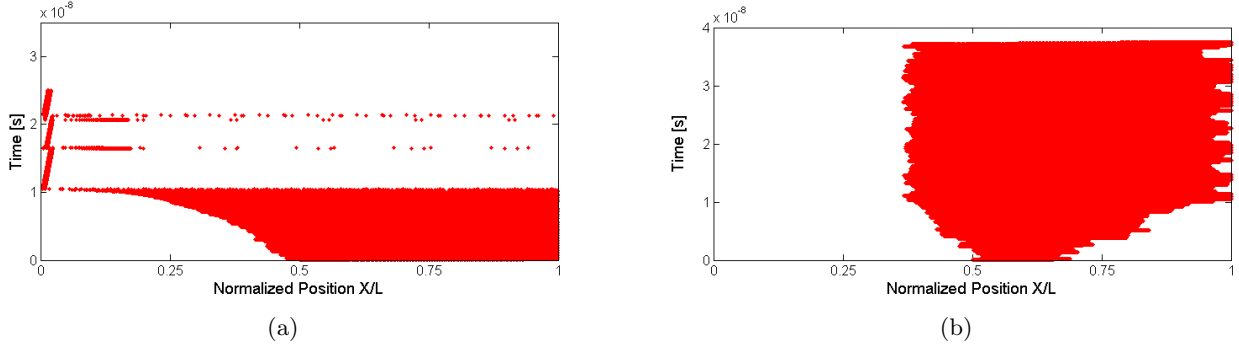


Figure 29.: (a) 50'000 steps of $\Delta t = 5 \cdot 10^{-13}\text{s}$ with $T = 1\text{K}$, $m = 10^{-30}\text{kg}$, $M = 100m$, $L = 10^{-7}\text{m}$, and $V_{\text{weight}} \equiv 0$. The boundary conditions are elastic, leading to a non-physical behaviour of the piston (after $10^{-9}\text{s} \doteq 20'000$ steps). Time is on the vertical and position on the horizontal axis. (b) 75'000 steps of $\Delta t = 5 \cdot 10^{-13}\text{s}$ with the same parameters as in (a) except that $V_{\text{weight}}(X) = \alpha X$ with $\alpha = 6 \cdot 10^{-16} \frac{\text{J}}{\text{m}^2}$. Here, the boundary conditions are inelastic, the momentum is reset to 0 each time the piston reaches $X = L$.

could then reset the piston to $X = \varepsilon$ whenever it escaped to the left side, i.e., when it had position $X < 0$ after the last step. In pseudo code:

```

if X>L do                      % if X>L, reset (X,P)=(L,0)
    X <- L
    P <- 0
end

if X<0 do                      % if X<0, reset (X,P)=(eps,0)
    X <- eps
    P <- 0
end

```

However, with ε this procedure introduces another arbitrary parameter. Furthermore, the assumption that the piston should not be thermalized when it reaches a wall is unphysical. There is no obvious reason why only the particle should be thermalized. Moreover, an inelastic boundary introduces friction which suggests the involvement of another heat bath. If the friction is totally inelastic the temperature of this heat bath would be zero. Again this is unphysical. But more important, the process would then have access to two heat baths. In the introduction of this thesis we pointed out the differences between a heat engine and work extraction. The most important point was that a heat engine needs access to two different heat baths, whereas a work extraction procedure only needs one heat bath. Hence, inelastic boundary conditions would degrade this feature of a work extraction process and are therefore unacceptable.

C.3.3. Thermal Boundary Conditions

The friction coming from the inelastic boundary conditions suggests the involvement of another heat bath of smaller temperature. A way out of this are thermal boundary conditions. The idea is to randomly choose the momentum P when the piston reaches $X = L$ according to the Gibbs distribution at temperature T , the temperature of the surrounding heat bath. This is, according to the (unnormalized) probability density function

$$f(P) = \begin{cases} \exp\left(-\frac{P^2}{2MkT}\right), & \text{for } P < 0, \\ 0, & \text{otherwise.} \end{cases} \quad (\text{C.40})$$

First of all, this introduces some randomness, which must be present in a process that mimics friction. Furthermore, the ‘temperature’ of the friction process is by definition the same as the temperature of the heat bath that thermalizes the particle after each time step Δt . This also corresponds to the classical picture of the Szilard engine, where the heat bath is surrounding the whole box. Hence, it makes sense that also the piston thermalizes when it bounces in one of the walls.

This approach brings a much faster thermalization of the piston with it. In this sense, it contradicts the idea (suggested in Section 4) that it could be helpful to prevent the piston from thermalizing and to extract the work before that happens. Nevertheless it is interesting to see how this changes the behaviour of particle and piston. It turns out that the differences in the piston’s behaviour with inelastic and thermal boundary conditions are marginal. The only difference is that with thermal boundary conditions, there are more fluctuations present in the case of very weak weight potentials. Hence, we settle for thermal boundary conditions for the simulations in Section 8.

C.3.4. Mixed Boundary Conditions

After having seen different boundary conditions we could also mix them. For instance, we could introduce an additional parameter $q \in [0, 1]$ that determines how elastic the boundary conditions are, where $q = 0$ stands for fully thermal and $q = 1$ for fully elastic boundary conditions. To do so, we would randomly choose a Gibbs distributed momentum P_{Gibbs} according to the probability density function from Eq. C.40 and reset the momentum of the piston to

$$q(-|P|) + (1 - q)P_{\text{Gibbs}} \quad (\text{C.41})$$

each time it bounces into the wall at $X = L$, where P is the momentum of the piston before its contact with the wall. Changing the elasticity parameter q would then allow to get any mixture of elastic and thermal boundary conditions. However, we did not investigate these boundary conditions any further because simulations suggested that they do not change the behaviour of the piston much compared to purely thermal boundary conditions.

C.3.5. No Boundary Condition at the Right Wall – Open Cylinder

Another possibility would be not to introduce a boundary at the right side of the piston. This would correspond to an open cylinder. Also for this case we did simulations and it turned out that the same problems occur as for elastic boundary conditions. The piston moves back and forth and comes closer to the left wall of the box with every time it comes back until it starts to jump outside the box (very similar to Fig. 29 (a)). Unfortunately, this violent behaviour prevents us from using our model in this case, which would certainly be a very interesting one.

C.3.6. Other Ideas

Another idea that could solve the problem of overshooting at $X = 0$ involves smaller time steps. Suppose the piston leaves the box to the left side in step k . Then we could split up this step into smaller time steps. Remember that the potential from the particle goes as $\frac{1}{X^2}$. This means that for small enough time steps the piston will never be able to leave the box, because a classical particle cannot tunnel through an infinitely high potential wall of any shape. This splitting of a time step in more time steps is certainly possible. The length of the time steps would then have to be adjusted such that the particle does not leave the box in step k . In principle this could lead to arbitrarily small time steps and hence the program would need much more computing time. Nevertheless, such a procedure is feasible. However, changing the length of the time steps is somehow arbitrary if the only goal is to find the maximal length such that the piston does not overshoot.

This idea is not applicable for the case of overshooting to the right. There, we have no potential with support within $[0, L]$ that prevents the piston from escaping. However, a slight modification of the box potential could have the property we need. An example of such a smooth potential with finite height is given in Fig. 30 (a). The construction uses the idea of the partition of unity. Starting with the C^∞ function

$$r(x) = \begin{cases} e^{-x^{-2}} & \text{if } x > 0, \\ 0 & \text{otherwise,} \end{cases} \quad (\text{C.42})$$

one constructs the function $s(x) = r(1+x)r(1-x)$, which is zero outside $[-1, 1]$ and non-zero in $(-1, 1)$. Using s it is possible to construct a function that is V_0 outside $(0, 1)$ and 0 in $[\delta, 1 - \delta]$ for arbitrarily small δ . Suppose $\delta = \frac{1}{n}$ for some integer n . Then the function

$$f_n(\tilde{X}) = V_0 \left(1 - \frac{\sum_{k=-n+1}^{-1} s(n \cdot \tilde{X} + k)}{\sum_{l \in \mathbb{Z}} s(n \cdot \tilde{X} + l)} \right) \quad (\text{C.43})$$

fulfils the above criterion (see Fig. 30 (a)). The height V_0 can be made arbitrarily large, while δ stays constant. Hence this smooth function approximates the finite box potential arbitrarily well. It is helpful that the potential is smooth already because then putting

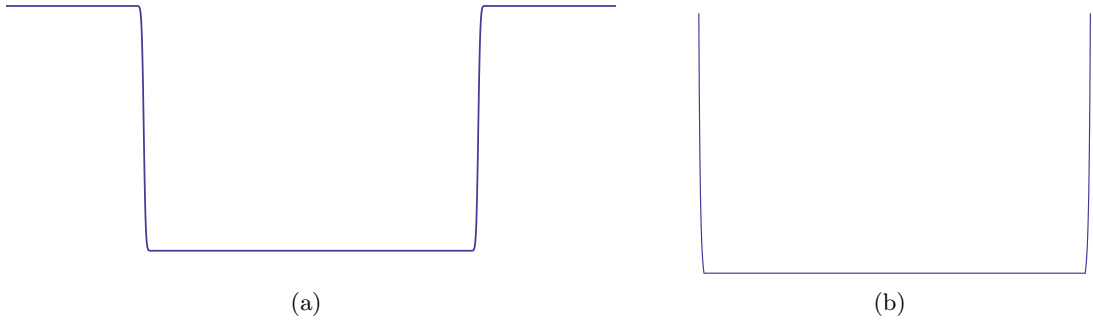


Figure 30.: (a) Shape of a smooth box potential with finite height constructed using the function f_n from Eq. C.43. (b) Shape of a continuous box potential with infinite height using the function $g_{\delta,n}$ from Eq. C.44.

it in Eq. 7.7 does not lead to further problems.

Fig. 30 (b) shows an alternative version of a box potential with infinite height:

$$g_{\delta,n}(\tilde{X}) = \begin{cases} \left(\frac{\delta}{\tilde{X}}\right)^n - 1 & \text{if } 0 < \tilde{X} < \delta, \\ 0 & \text{if } \delta < \tilde{X} < 1 - \delta, \\ \left(\frac{\delta}{1-\tilde{X}}\right)^n - 1 & \text{if } 1 - \delta < \tilde{X} < 1, \\ +\infty & \text{otherwise,} \end{cases} \quad (\text{C.44})$$

where $\delta > 0$ is again arbitrarily small and $n > 0$ is an arbitrarily high real number determining how steep the wall is. This potential is less elegant because it is not smooth. Nevertheless, it would be easy to find a smoothed version of this as well.

Of course, if the piston feels a different box potential the particle should feel it as well, at least if we stick to the classical picture of particle and piston. This would lead to a much more complicated Schrödinger equation for the particle's energy eigenstates. But as mentioned above, the region in which the proposed modified box potentials differ from the conventional discontinuous box potential (as in Eq. 7.6) can be made arbitrarily small. Hence, to a good approximation, the energies and eigenstates of the particle do not change.